



LUND UNIVERSITY

Closed-Loop Combustion Control of a Multi Cylinder HCCI Engine using Variable Compression Ratio and Fast Thermal Management

Haraldsson, Göran

2005

[Link to publication](#)

Citation for published version (APA):

Haraldsson, G. (2005). *Closed-Loop Combustion Control of a Multi Cylinder HCCI Engine using Variable Compression Ratio and Fast Thermal Management*. [Doctoral Thesis (compilation), Combustion Engines]. Division of Combustion Engines, Lund Institute of Technology.

Total number of authors:

1

General rights

Unless other specific re-use rights are stated the following general rights apply:

Copyright and moral rights for the publications made accessible in the public portal are retained by the authors and/or other copyright owners and it is a condition of accessing publications that users recognise and abide by the legal requirements associated with these rights.

- Users may download and print one copy of any publication from the public portal for the purpose of private study or research.
- You may not further distribute the material or use it for any profit-making activity or commercial gain
- You may freely distribute the URL identifying the publication in the public portal

Read more about Creative commons licenses: <https://creativecommons.org/licenses/>

Take down policy

If you believe that this document breaches copyright please contact us providing details, and we will remove access to the work immediately and investigate your claim.

LUND UNIVERSITY

PO Box 117
221 00 Lund
+46 46-222 00 00

Closed-Loop Combustion Control of a Multi Cylinder HCCI Engine using Variable Compression Ratio and Fast Thermal Management

Göran Haraldsson

**Doctoral thesis
Lund 2005**

To Fia, Julia and Anton

ISBN 91-628-6300-2
ISRN LUTMDN/TMHP--05/1028—SE
ISSN 0282-1990

Division of Combustion Engines
Department of Heat and Power Engineering
Lund Institute of Technology
P.O. Box 118, SE-221 00 LUND
Sweden

© 2005 by Göran Haraldsson. All rights reserved
Printed by Media-Tryck, Lund, January 2005

Front cover: A photo of the engine
Back cover: A screen dump of the control program

LIST OF PAPERS

Paper 1

A Turbo Charged Dual Fuel HCCI Engine

J-O. Olsson, P. Tunestål, G. Haraldsson, B. Johansson

SAE Technical paper 2001-01-1896

Presented by Jan-Ola Olsson at the International Spring Fuels & Lubricants Meeting, Orlando, May 2001

Paper 2

HCCI Combustion Phasing in a Multi Cylinder Engine Using Variable Compression Ratio

G. Haraldsson, J. Hyvönen, P. Tunestål, B. Johansson

SAE Technical paper 2002-01-2858

Presented by the author at SAE Powertrain & Fluid Systems Conference & Exhibition, San Diego, CA, October 2002

Paper 3

Operating range in a Multi Cylinder engine using Variable Compression Ratio

J. Hyvönen, G. Haraldsson, B. Johansson

JSAE Technical paper 20030178/ SAE 2003-01-1829

Presented by Jari Hyvönen at the joint JSAE/SAE Spring Fuels & Lubricants Meeting, Yokohama, May 2003

Paper 4

HCCI Combustion Phasing with Closed-Loop Combustion Control Using Variable Compression Ratio in a Multi Cylinder Engine

G. Haraldsson, J. Hyvönen, P. Tunestål, B. Johansson

JSAE Technical paper 20030126/SAE 2003-01-1830

Presented by the author at the joint JSAE/SAE Spring Fuels & Lubricants Meeting, Yokohama, May 2003

Paper 5

Super Charging HCCI to extend the operating range in a Multi Cylinder VCR-HCCI engine

J. Hyvönen, G. Haraldsson, B. Johansson

SAE Technical paper 2003-01-3214

Presented by Jari Hyvönen at SAE Powertrain & Fluid Systems Conference & Exhibition, Pittsburgh, October 2003

Paper 6

HCCI Closed-Loop Combustion Control Using Fast Thermal Management

G. Haraldsson, J. Hyvönen, P. Tunestål, B. Johansson

SAE Technical paper 2004-01-0943

Presented by the author at SAE World Congress & Exhibition, Detroit, March 2004

Paper 7

Balancing Cylinder-To-Cylinder Variations in a Multi-Cylinder VCR-HCCI Engine

J. Hyvönen, G. Haraldsson, B. Johansson

SAE Technical paper 2004-01-1897

Presented by Jari Hyvönen at SAE Fuels & Lubricants Meeting & Exhibition, Toulouse, June 2004

Paper 8

System Identification and LQG Control of Variable-Compression HCCI Engine Dynamics

R. Pfeiffer, G. Haraldsson, J-O. Olsson, P. Tunestål, R. Johansson, B. Johansson
CCA/ISIC/CACSD Technical Paper 688, Proceedings of the 2004 IEEE International Conference on Control Applications Taipei, Taiwan, pp 1442-1447, 2004
Presented by Roland Pfeiffer at Joint CCA, ISIC and CACSD, Taipei, Taiwan, September, 2004

Paper 9

Operating conditions using spark assisted HCCI combustion during combustion mode transfer to SI in a Multi-Cylinder VCR-HCCI engine

J. Hyvönen, G. Haraldsson, B. Johansson
SAE Technical paper 2005-01-0109
Accepted for publication at SAE World Congress & Exhibition, Detroit, April 2005

Paper 10

Transient Control of a Multi Cylinder HCCI Engine during a Drive Cycle

G. Haraldsson, J. Hyvönen, P. Tunestål, B. Johansson
SAE Technical paper 2005-01-0153
Accepted for publication at SAE World Congress & Exhibition, Detroit, April 2005

OTHER PUBLICATIONS

Mapping of a Honda ARC engine

G. Haraldsson, ISSN 0282-1990, ISRN/LUTMDN/TMVK – 5322 – SE
Thesis for the degree of Master of Science, Department of Heat and Power Engineering, Jan 2000

Combustion Control of the Homogeneous Charger Compression Ignition Engine

G. Haraldsson, ISSN 0282-1990, ISRN LUTMDN/TMHP--03/7010—SE
Thesis for the degree of Licentiate in Engineering, Department of Heat and Power Engineering, March 2003

ABSTRACT

The current Spark Ignited (SI) engine equipped with three-way catalyst offers low emissions, but has low efficiency at part load, which results in unnecessarily high CO₂ emissions. The Compression Ignited (CI) engines have higher efficiency and hence lower CO₂ emissions, but suffer from higher Nitrogen Oxide (NO_x) and Particulate Matter (PM) emissions, and no three-way catalyst can be used. Large efforts are made to reduce the emissions of the CI engine and raise the efficiency of the SI engine. A third internal combustion engine type, which combines the principles of the SI and CI engines, has the potential to meet demands from society in terms of current and foreseeable future emissions regulations. This engine type is called Homogeneous Charge Compression Ignition (HCCI) engine. It utilizes a homogeneous premixed air fuel mixture like the SI engine, but the mixture is compressed to auto ignition like in the CI engine. Very dilute mixtures are used to slow down the combustion rate. This results in a low combustion temperature with extremely low NO_x emissions. Due to the homogeneous charge the combustion produces no PM. The Carbon Monoxide (CO) and unburned Hydrocarbon (HC) emissions are, however, higher than for the other engine types due to the low combustion temperature, but an oxidizing catalyst can quite easily treat CO and HC emissions. Combustion control of the HCCI engine is a challenge since there is no direct means to control when combustion starts unlike the SI or CI engines. Combustion phasing in an HCCI engine can be achieved by affecting the time history of pressure and temperature in the cylinder. The most common way to do this in the lab has been to control the inlet air temperature and thereby the temperature in the cylinder at the end of the compression stroke. With an electrical heater this is a slow parameter to control. In the present study a multi cylinder engine equipped with Variable Compression Ratio (VCR) and a Fast Thermal Management (FTM) system is used to control the combustion phasing. Both the Closed-Loop Combustion Control (CLCC) using VCR and the CLCC using FTM are the first presented such systems on a multi cylinder engine in the literature. A system identification is made and a Linear Quadratic Gaussian (LQG) controller is designed for the fast thermal management instead of the standard PID controller. CLCC performance of both PID and the state feedback based LQG controllers using fast thermal management are investigated by performing step response experiments. A CLCC strategy using variable compression ratio and a cylinder individual fast thermal management is presented and investigated experimentally by running a hot drive cycle test. To this date it is the first experimental drive cycle test using inlet air preheated HCCI, i.e. FTM. It is concluded that the proposed CLCC strategy in terms of fuel consumption is good enough, but in terms of emissions there is still some room for improvement. For a scaled engine to 3.0L an improvement in fuel consumption of 16% is accomplished compared to an SI simulation using mean steady state data from the same engine, with an EC2000 drive cycle calculated for a 1.6L Opel Astra. If doing an imagined mode transfer without scaling the engine a fuel consumption of 6.8L/100km is achieved. Due to very high friction losses of this engine a simulation with lower friction losses of a modern engine is made, which result in a 15% improvement in fuel consumption compared to an "ideal" simulated HCCI drive cycle test with this engine. With an optimized controller and an optimized engine in terms of friction losses a fuel consumption of 5.8L/100km is realistic for the HCCI-SI approach.

ACKNOWLEDGEMENTS

There are many people to thank for this thesis finally being written. Professors Gunnar Lundholm and Bengt Johansson for employing me and letting me do a very interesting Master of Science project at the department and offering me this project. Bengt is full of ideas and always offers optimistic thoughts and suggestions how things can be done.

Jan-Ola Olsson and assistant professor Per Tunestål for the very nice control program, which was kindly inherited from Jan-Olas project, and all support when this program did not behave as expected. Per put a lot of hours helping me debug and improve the program when I was rewriting the program for our project. When Per and Jan-Ola could not help, Tommy Petersen our electronics man helped and rebuilt his magic devices.

Jari Hyvönen who keeps track of the money and is the project leader. He is also the inventor of both fast thermal management systems and always has very useful dreams of improved functionality in the control program and is very grateful when they are implemented. Roland Pfeiffer for helping with the advanced controllers and some programmers opinions on how to debug a program. Krister Olsson for helping me with the computers and computer upgrades and especially the logger program.

The people at Fiat-GM Powertrain Sweden, Pelle Matsson who always fix our engine when there are major disasters or only small things needed. Raymond Reinmann, who was the project leader in the beginning of the project, Eric Olofsson and Matthias Alt who are members of the steering group and gave constructive feedback throughout the project together with Tom Sloan at GM R&D.

Our technicians Tom Hademark, Kjell Jonholm and Bertil Andersson, for building new strange systems according to our needs, and keeping the engine running. Jan-Erik Everitt for placing his magic hand on the strange emission measurement systems. All other colleagues at the department who inspire with ideas during the so necessary coffee breaks.

And finally my entire family and especially Julia and Anton and my wife Fia for having some understanding during this final compilation of the thesis.

NOMENCLATURE

ABDC	After Bottom Dead Center
ATAC	Active Thermo-Atmosphere Combustion
ATDC	After Top Dead Center
AVT	Active Valve Train
A/D	Analog / Digital
BMEP	Brake Mean Effective Pressure
BBDC	Before Bottom Dead Center
BSFC	Brake Specific Fuel Consumption
BTDC	Before Top Dead Center
CAD	Crank Angle Degree
CAI	Controlled Auto Ignition
CA50	Crank Angle for 50% burned
CFR	Cooperative Fuel Research engine
CI	Compression Ignition
CLCC	Closed-Loop Combustion Control
CR	Compression Ratio
CO	Carbon Monoxide
CO₂	Carbon Dioxide
COV	Coefficient Of Variation
D/A	Digital/Analog
DISI	Direct Injected Spark Ignition
dP/dCAD	Maximum Rate of Pressure Rise per Crank Angle Degree
EC2000	European drive cycle
EGR	Exhaust Gas Recirculation
EHVA	Electro Hydraulic Valve Actuation
EVC	Exhaust Valve Closure
EVO	Exhaust Valve Opening
FMEP	Friction Mean Effective Pressure
FTM₂	Fast Thermal Management (two throttle system)
FTM₆	Fast Thermal Management (six throttle system)
FueIMEP	Fuel Mean Effective Pressure
GDI	Gasoline Direct Injection
HC	Hydrocarbon
HCCI	Homogeneous Charge Compression Ignition
HCSI	Homogeneous Charge Spark Ignition
IMEP	Indicated Mean Effective Pressure
ISFC	Indicated Specific Fuel Consumption
IVC	Inlet Valve Closure
IVO	Inlet Valve Opening
LQG	Linear Quadratic Gaussian
LTR	Low Temperature Reactions
MIMO	Multi Input Multi Output
MISO	Multi Input Single Output
MPC	Model Predictive Control
N	Nitrogen
net	Integrate over the entire engine cycle
NO_x	Nitrogen Oxides (NO and NO ₂)
O₂	Oxygen

OKP	Optimized Kinetic Process
PCI	Peripheral Component Interconnect local bus
PFI	Port Fuel Injection
PIC	Peripheral Interface Controller
PID	Controller with Proportional, Integral and Derivate gains
PM	Particulate Matter
PRBS	Pseudo Random Binary Sequence
RON	Research Octane Number
SCSI	Stratified Charge Spark Ignition
SI	Spark Ignition
SISO	Single Input Single Output
SVC	Saab Variable Compression
TDC	Top Dead Center
V	Instantaneous cylinder volume
VCR	Variable Compression Ratio
V_D	Displacement Volume
VVA	Variable Valve Actuation
VVT	Variable Valve Timing
γ	Ratio of specific heats
λ	Air/fuel ratio, relative to stoichiometric air/fuel ratio

1	INTRODUCTION	1
1.1	INTERNAL COMBUSTION ENGINES	2
1.2	THE SPARK IGNITION ENGINE	2
1.3	THE COMPRESSION IGNITION ENGINE	3
1.4	THE HOMOGENEOUS CHARGE COMPRESSION IGNITION ENGINE.....	3
2	HCCI CONCEPTS	5
3	DIFFERENT HCCI CONTROLLERS	15
4	CLOSED-LOOP COMBUSTION CONTROL FOR HCCI	21
4.1	WHY CONTROL COMBUSTION PHASING?	21
4.2	GOAL WITH THIS PROJECT	23
4.3	TEST ENGINE.....	23
4.4	CONTROL SYSTEM	26
4.5	RESULTS.....	28
4.6	DISCUSSION	52
5	CONCLUSIONS	54
6	FUTURE WORK	56
	REFERENCES	57
	SUMMARY OF PAPERS	61
	PAPER 1	61
	PAPER 2	61
	PAPER 3	62
	PAPER 4	62
	PAPER 5	63
	PAPER 6	63
	PAPER 7	64
	PAPER 8	64
	PAPER 9	65
	PAPER 10	65

1 Introduction

The internal combustion engine has evolved significantly since the first mass-produced cars. The performance of a normal car has increased by an order of magnitude even though weight has doubled, while the fuel mileage is approximately the same and emissions have been reduced by two orders of magnitude. This has been achieved by more advanced engine control strategies, exhaust gas after treatment together with computer aided design of combustion chamber, inlet manifold etc. Complete combustion of a hydrocarbon fuel results in CO₂ and water. CO₂ is a green house gas and as such it should be minimized. This can be achieved by using an engine which has higher efficiency and hence produces less CO₂. The Compression Ignited (CI) engine has higher efficiency than the Spark Ignited (SI) engine, but produces higher amounts of Nitrogen Oxides (NO_x) and Particulate Matter (PM). The NO_x emissions cause acid rain and result in over-fertilization of lakes, and PM causes cancer. The Homogeneous Charge Compression Ignition (HCCI) engine is an engine concept with high part load efficiency compared to the SI engine and extremely low NO_x emissions and no PM. The HCCI engine can be run on various different fuels and if desired renewable fuel such as ethanol.

Combustion control of the HCCI engine is a challenge since there is no direct means to control when combustion starts unlike the SI or CI engines. Combustion phasing in an HCCI engine can be achieved by affecting the time history of pressure and temperature in the cylinder.

A combustion control strategy for HCCI in a small size high-speed multi cylinder engine using Fast Thermal Management (FTM) or Variable Compression Ratio (VCR) is presented and demonstrated experimentally during transient operation and during a drive cycle. The in-cylinder pressure is measured as feedback of the combustion phasing. Cylinder-individual combustion control strategies are presented and demonstrated experimentally. A model based controller is derived by system identification and implemented in the PID based control program in an effort to systemize the controller design for the combustion phasing. The controllers are evaluated by doing step and ramp changes of various parameters and finally the entire concept is evaluated in a drive cycle test where performance of especially the Closed-Loop Combustion Control (CLCC) is crucial to meet desired results in load, speed, emissions, noise and fuel consumption.

The objectives of this thesis are to introduce a CLCC strategy for an HCCI engine using FTM and/or VCR and to experimentally demonstrate the performance of this combustion phasing control. The importance of fast and powerful combustion phasing during transients is discussed. To understand the complexity of HCCI combustion control, supplementary combustion control parameters are discussed.

Different controllers, actuators and feedback signals used in the literature are discussed, but the different HCCI concepts are limited to gasoline-like HCCI and hence no diesel HCCI is treated.

This is not intended as a school book in HCCI control and should be read as an introduction to the technical papers appended. However for the eager to learn reader there are a lot of references to the literature where to find more knowledge about this subject.

1.1 Internal combustion engines

The internal combustion engine is a heat engine with internal combustion. The internal combustion engine can be divided into SI, CI and HCCI engines, which all can be found in two- and four-stroke variants. The four strokes of a four-stroke SI engine are shown in Figure 1-1. There are differences in fuel preparation and combustion between the three internal combustion engine types, but the engine cycle principle is the same. The four strokes are (a) intake, (b) compression, (c) expansion and (d) exhaust. The work from the engine is produced by the expansion stroke.

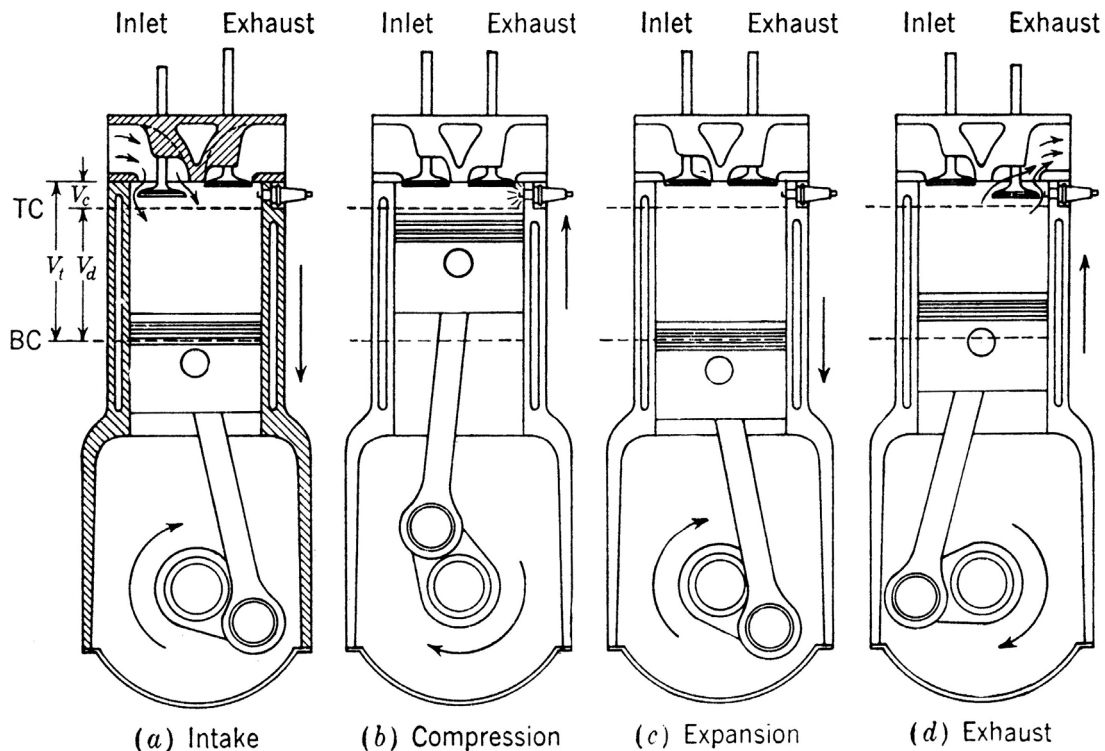


Figure 1-1 The four-strokes of an SI engine [1].

1.2 The Spark Ignition engine

In the SI engine, fuel and air are mixed homogeneously before combustion initiation. The charge is compressed and subsequently ignited by a spark plug at the most convenient time for the combustion process. To control the load of an SI engine, a throttle is used to adjust the amount of mixed air and fuel that enters the cylinder. Flame propagation from the spark gap requires an air excess ratio, λ , of approximately 1 around the spark plug. There are two strategies to inject fuel to an SI engine. Port Fuel Injection (PFI) or Direct Injection (DI). The currently most common solution is PFI, but the Gasoline Direct Injection (GDI) engines are increasing in spite of the relatively complex design. One reason to use GDI is to be able to run unthrottled lean operation by utilizing a stratified air/fuel mixture at low load. The air/fuel mixture is then rich enough around the spark plug, while it is lean in the rest of the combustion chamber. The useful work of an SI engine is shown as the enclosed area in Figure 1-2, while the pumping loss, enclosed area, is shown in the close up of the gas exchange in Figure 1-3.

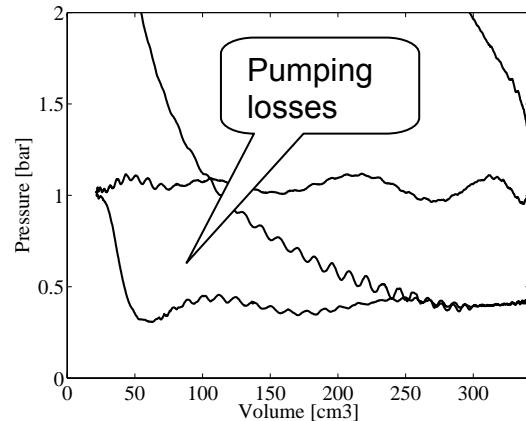
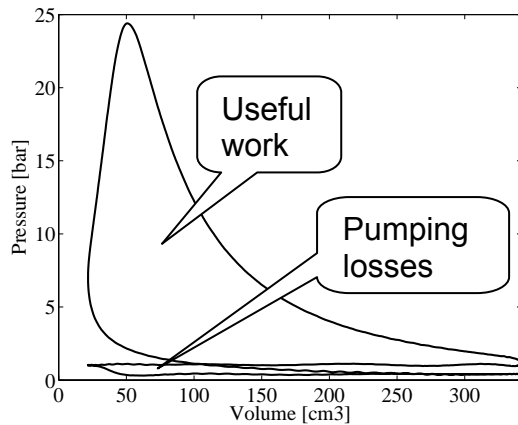


Figure 1-2 P-V plot for SVC engine in SI mode. Figure 1-3 Close-up of the gas exchange.

1.3 The Compression Ignition engine

In the CI engine, air is compressed to a higher pressure and temperature than in the SI engine, fuel is injected at high pressure into the hot compressed air and auto-ignition occurs. The diffusion flame around the fuel jet means that excess air has no negative impact on combustion. By adjusting the amount of injected fuel, the load is controlled and hence no throttling is necessary. Due to the partially fuel-rich environment with a diffusion flame there are problems with high NO_x emissions and PM. Common rail injection with very high injection pressure is applied to lower PM, and Exhaust Gas Recirculation (EGR) systems are used to lower NO_x emissions, but upcoming emission legislations are hard to meet with current technologies.

1.4 The Homogeneous Charge Compression Ignition engine

The HCCI engine can be understood as a hybrid between the SI and CI engines. HCCI engines use a premixed air and fuel mixture like the SI engine and compress this mixture to auto-ignition like the CI engine. The temperature of the charge has to be higher at the end of the compression phase, compared to the SI engine, in order to cause auto ignition with conventional SI engine fuels. The load is controlled by the injected amount of fuel, hence no throttling is necessary. HCCI works for λ between 2 and 5 so, if means of combustion control are available, load can be controlled without throttling the air. The low combustion temperature is due to very lean mixtures, which result in extremely low NO_x emissions and no PM, while the CO and HC emissions are higher than from the SI engine. Another drawback is the very high heat release rate, which leads to high maximum pressures and noise levels. To avoid too fast combustion, a diluent must be used. The diluent can be any combination of air, residual gas and EGR. The objective of using HCCI instead of SI in 4-stroke engines is to decrease fuel consumption at part load. The advantages of HCCI over CI engines are lower emissions of NO_x and PM.

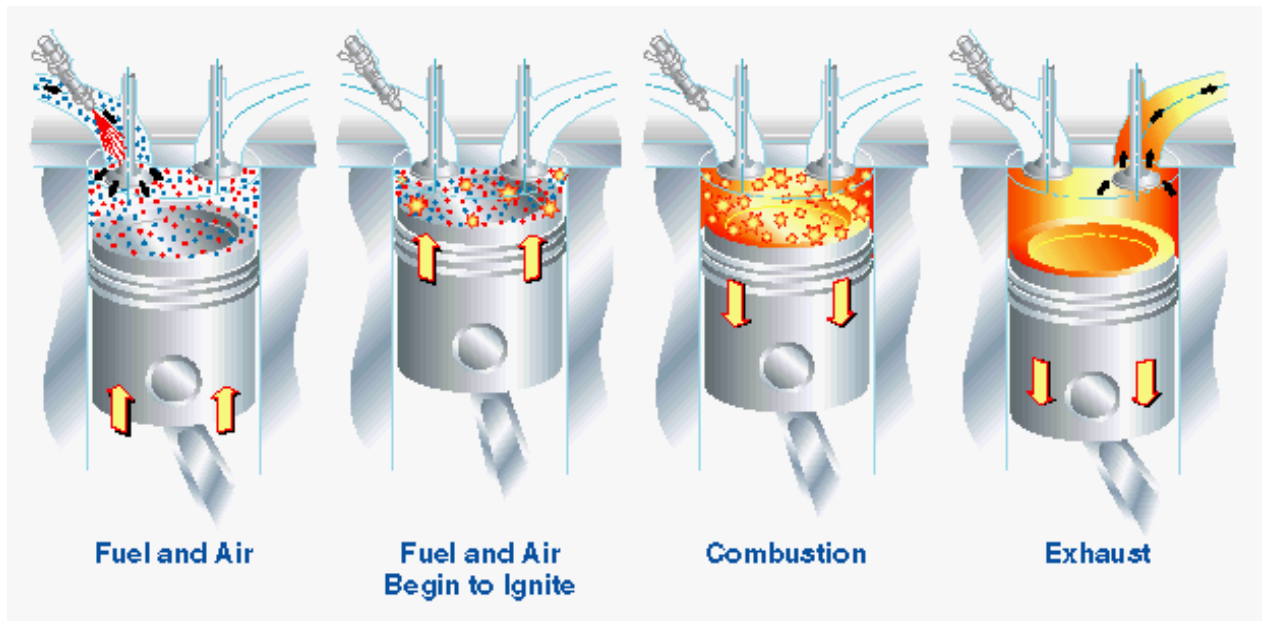


Figure 1-4 HCCI combustion process (original figure from Southwest Research Institute).

2 HCCI concepts

The first presented experiments of HCCI engines are performed on 2-stroke engines [2-3]. The primary purpose of using HCCI combustion in 2-stroke engines is to reduce HC emissions at part load operation, and to decrease fuel consumption by stabilizing the combustion of lean mixtures. Onishi et al. [2] compare Active Thermo-Atmosphere Combustion (ATAC), or HCCI which is the more common name, and SI combustion in Figure 2-1, where the left figure describes SI and the right HCCI and q is heating value per unit weight and w is mixture mass (weight).

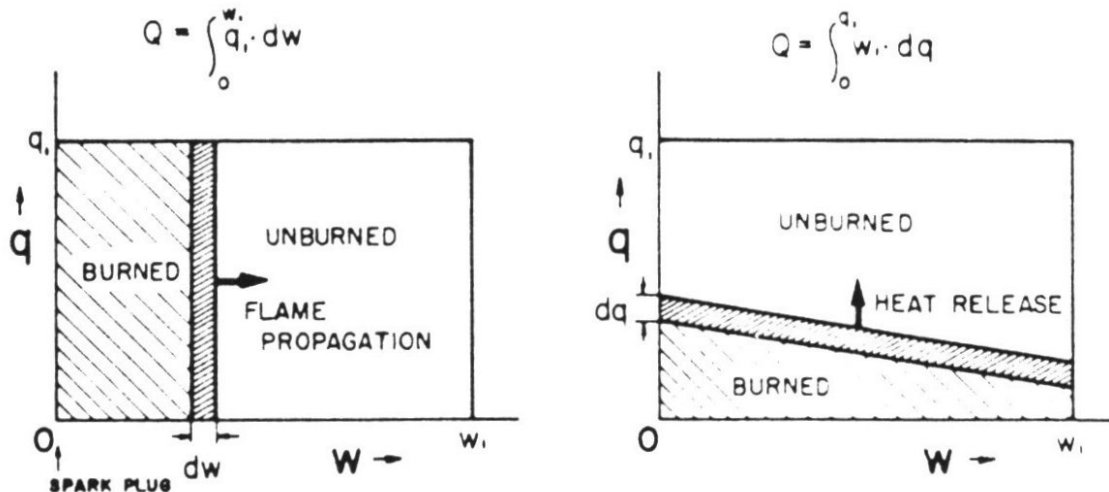


Figure 2-1 The HCCI concept by Onishi et al. [2].

SI combustion is characterized by a turbulent flame that propagates through the combustion chamber from the spark plug and creates a burned zone, which grows as the flame propagates. The zone dw is the reaction zone in which the chemistry is fast while the propagation, movement of dw to the right, is limited by the turbulent flame speed. HCCI combustion is characterized by combustion throughout the entire combustion chamber and the chemistry is the limiting factor since there is no flame propagation.

In 4-stroke engines the first presented results are by Najt et al. [4], who use a single cylinder CFR engine where EGR rate, CR and inlet air temperature can be varied. They also change between different primary reference fuels and hence octane number fuels, from RON 60 to 70. Thring et al. [5] instead use US regular gasoline with a low CR of 8:1, but very high inlet air temperatures of up to 425°C and EGR rates of 13 to 33%. They also try higher CR of 15:1, but strangely enough do not achieve HCCI combustion, but for the tested CR Indicated Specific Fuel Consumption (ISFC) values of 180 to 200g/kWh are shown, which is in the same region as for a CI engine.

Yunick et al. [6] show a probable HCCI "Hot Vapor" engine with a homogenizer similar to a turbo charger to get an extremely homogenized air/fuel mixture. The air/fuel mixture is preheated in three steps shown in Figure 2-2; with the first step from the cooling water downstream the carburetor. The second step use the exhaust heat around the homogenizer and the final step is the exhaust heated inlet manifold. With a boost level of 1.4 bar higher power than the stock engines are reported with

more than halved fuel consumption. To enable cold start hot EGR is used. The world patent [7] emphasises the need to scale cooling flows as a function of engine out power and discusses a maximum “piston dwell” of 2.5mm piston movement at TDC for 13 CAD of crank shaft movement, i.e. crank shaft stroke and piston rod length are chosen to get desired piston movement to get the entire combustion during the “piston dwell”. This will according to the patent holder increase combustion efficiency substantially between 800 and 4000 rpm. This is very much an experimental approach without combustion phasing control and no reports of noise and emissions are found. It is believed that this approach would result in very high peak cylinder pressures and maximum rate of pressure rise and hence high NO_x emissions.

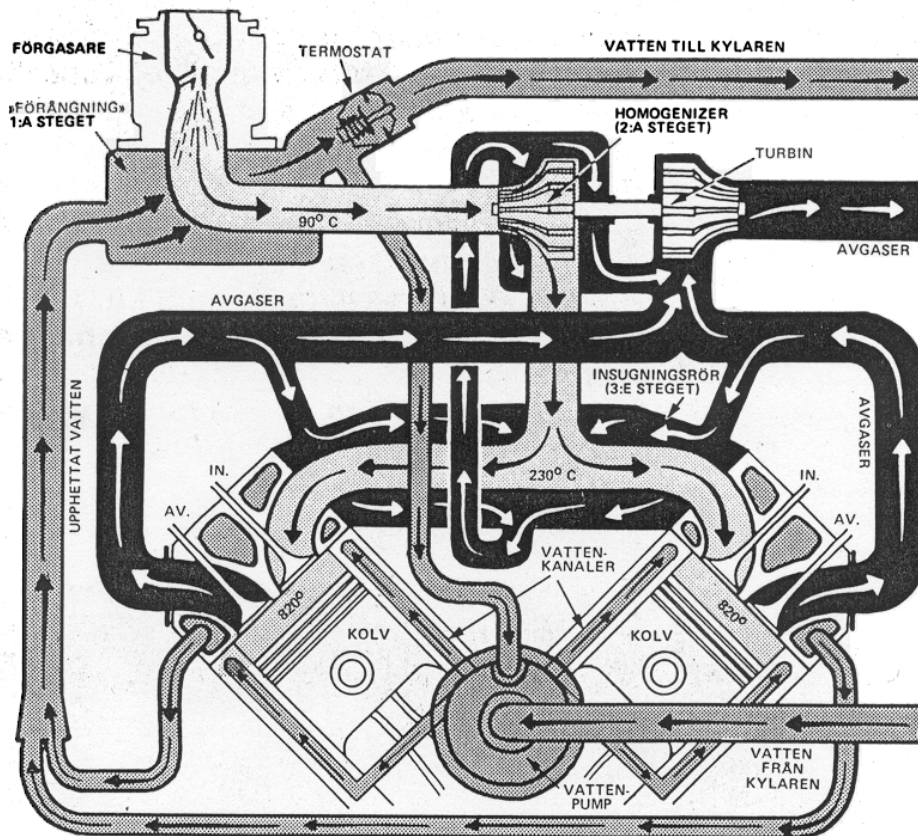


Figure 2-2 Schematic of the Hot Vapor engine [6].

Later Stockinger et al. [8] presents a self sufficient multi cylinder HCCI engine using the exhaust gas energy and coolant water to heat the inlet air. They conclude that a suitable CR needed for full load should be chosen, while inlet air preheating is used for part load operation. Brake thermal efficiency of approximately 34% (241 g/kWh) at 2 bar BMEP is shown at a CR of 18.7, which is very good compared to an SI engine. High loads are a problem though, due to instability of the combustion phasing, since no closed-loop control is applied.

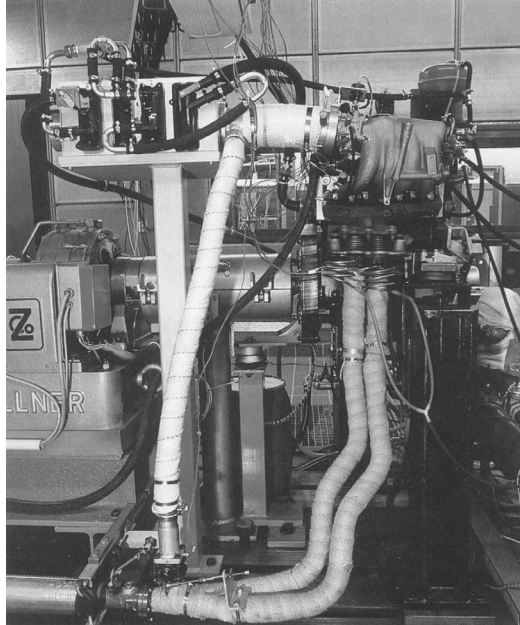


Figure 2-3 Experimental setup of the self sufficient HCCI engine using thermal management [8].

Christensen et al. [9-14] present many HCCI related performance tests on a single cylinder 1.6L engine. Relationships between octane number of different fuels and inlet air temperature with fixed CR are investigated. Supercharging using various fuels, EGR rates using different λ and inlet air temperatures are shown. Water injection is also attempted. By changing CR with a small piston in the cylinder head, Figure 2-4, various liquid fuels are investigated. In [14] it is suggested that turbulence slows down the combustion rate, which is the opposite of SI combustion where the combustion rate depends on the turbulent flame speed, which increase with turbulence. More turbulence will decrease the temperature inhomogeneity during the combustion process, which results in lower temperature in the hot zones and hence lower combustion rate. Due to the exponential dependence of combustion rate on temperature, the increased temperature in the cold zones will only partially cancel this effect. All tests are made in open-loop, i.e. inlet air temperature is manually adjusted in all tests to achieve desired combustion phasing, hence only stationary tests.

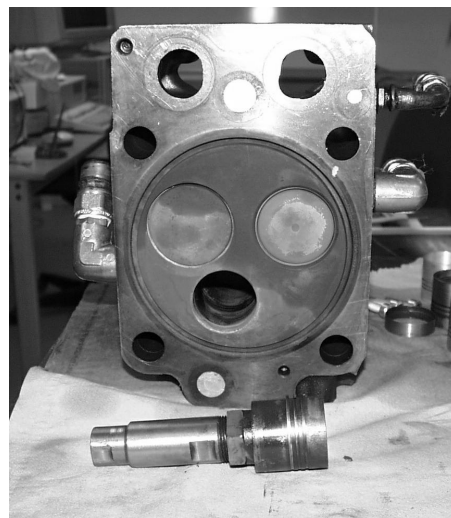


Figure 2-4 Cylinder head and auxiliary piston [13]

The first presented results of residual heated HCCI in 4-strokes using fixed camshafts and standard SI compression ratio without any inlet air heating are shown by Lavy et al. [15]. The load and speed range is very limited due to fixed valve lift profile and the need for very high residual gas rates, which limit the volumetric efficiency. However Zhao et al. [16] increase the load and speed range, but when simulating a HCCI-SI drive cycle test an improvement in fuel consumption of merely 4.7% is achieved. The load and speed range is shown in Figure 2-5, where the lower misfire limit is a result of insufficient exhaust gas temperature. The advantage with this HCCI approach is the almost standard SI engine, which can operate in SI at higher loads with standard CR, but due to the very limited load range especially at low loads there seems to be small usefulness of this approach.

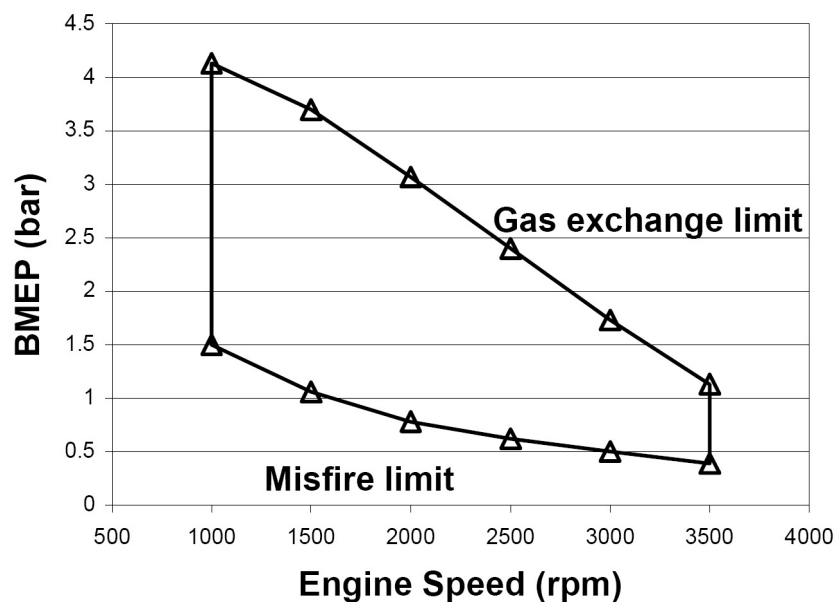


Figure 2-5 Load and speed range for residual heated HCCI achieved by restricting the gas exchange process with modified camshafts [16].

Inlet air preheating and dual fuels are used by Olsson et al. in [17,18] and Paper 1, on a Scania 12L diesel engine. The standard direct injection system is replaced by port fuel injection. Two injectors, one in each port allows two fuels to be mixed. By mixing a high octane fuel with a low octane fuel the Crank Angle of 50% heat release (CA50) can be controlled cylinder individually. CA50 then serves as a quantitative measure of the combustion phasing [17]. The heat release is calculated online from measured in-cylinder pressure. This is the first multi cylinder engine in the literature running in CLCC, which is additionally discussed in the next paragraph. The concept, however, has the disadvantage of needing two fuels, but diesel like load and efficiencies are reached in Paper 1. The maximum load and speed range is shown in Figure 2-6. To avoid the need to refuel with two fuels, a fuel reformation approach is tried in [18], where natural gas is reformed to CO and H₂ or if H₂O is available CO₂ and H₂. It is concluded that using H₂ as an ignition improver is feasible, but the control authority is not as large as for n-heptane and isooctane.

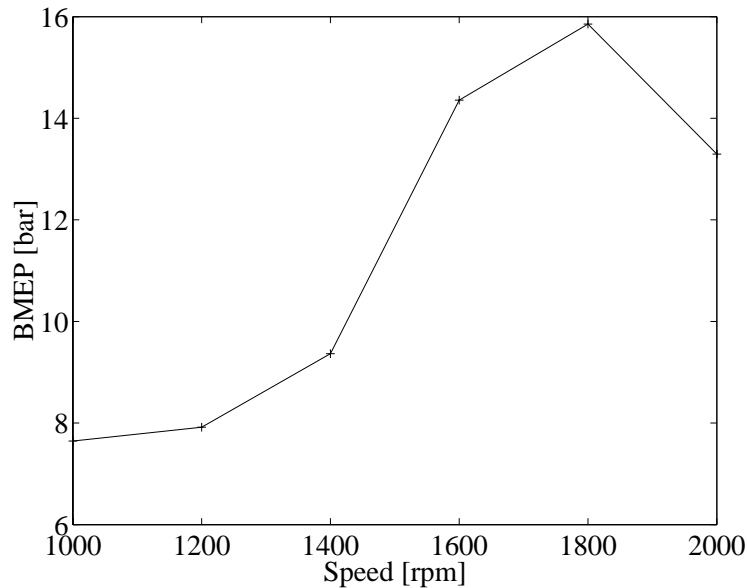


Figure 2-6 Maximum load HCCI on a Scania 12L engine using dual fuel, Paper 1.

Willand et al. [19] suggest an HCCI control strategy using early exhaust valve closing and direct injection. The fuel is injected during compression of the retained exhaust gas, which is retained by early exhaust valve closing and late inlet valve opening, i.e. negative valve overlap. The fuel changes its chemical composition and hence the ignitability is increased. The “activation injection” is shown in Figure 2-7.

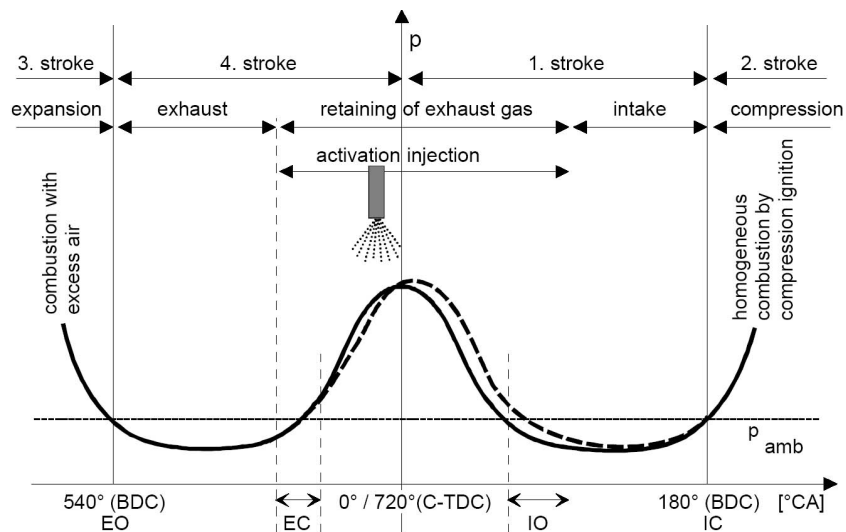


Figure 2-7 Suggested injection during negative valve overlap to control CA50 [19].

Another solution for combustion control presented by Willand et al. [19] is fuel stratification. Stratification of the fuel results in fuel rich regions where combustion starts earlier and sets off the rest of the charge. The stratification can be achieved by direct injection. However no experimental results are shown by Willand.

Another solution to achieve HCCI, without inlet air preheating, is to retain or rebreathe exhaust gas residuals by the use of Active Valve Train (AVT) presented by Law et al. [20]. Two strategies are presented, which are feasible with the totally free

electro hydraulic valve system. The first strategy is to close the exhaust valve early and hence keep the burned gas in the cylinder to the next cycle. This is by some authors called Controlled Auto Ignition (CAI), [21,22], where standard SI compression ratio without inlet air preheating is used. Instead HCCI is achieved by trapping hot burned gas residuals to heat the charge. With the second strategy the exhaust gases are expelled, but when it is time for the intake stroke both inlet and exhaust valves are opened simultaneously. This system is very nice for research and development, but is hardly a system to be put in serial production due to the complexity and hence cost per unit. Similar work with a different electro hydraulic valve system is presented by Kaahaaina et al. [21]. They use the more commonly known name, Variable Valve Actuation (VVA).

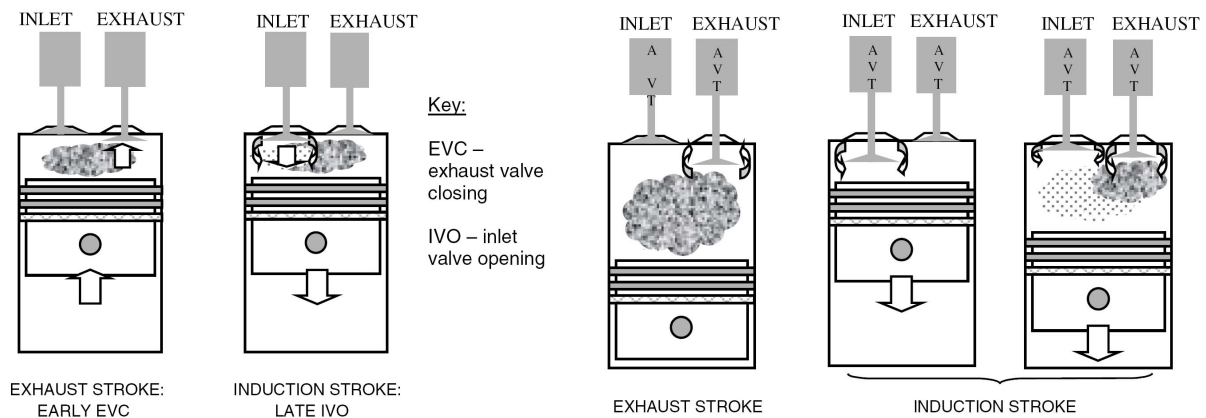


Figure 2-8 Early exhaust valve closing [20].

Figure 2-9 Rebreathing by opening both inlet valve and exhaust valve at the end of the induction stroke [20].

Mariott et al. [24] show experimental results of fuel stratification, where the combustion phasing is changed. Postponing the start of injection results in an increase in stratification with local fuel rich spots, which leads to advanced combustion phasing but also to an increase in NO_x emissions. A control range equivalent to 20°C in intake air temperature is shown. A drastic increase in PM is observed for the most advanced and retarded injections respectively. If the engine concept is equipped with direct injection this can be used to fine tune CA50 on cycle-to-cycle basis, i.e. for cylinder balancing, but for transient behavior the control authority is not enough. It is thus a fairly expensive cylinder balancing device.

An experimental study of the proposed direct injection strategy with fuel reformation during the negative valve overlap [19] combined with stratification is presented by Urushihara et al. [25]. It is found that fuel reformation does work and expands the original idea by varying the injection quantity during negative valve overlap and the injection during the inlet stroke, shown in Figure 2-10. It is found that this strategy increases combustion stability and hence the lean limit of HCCI. It is shown that the ideal fuel part injected during negative valve overlap is decreased as a function of load. By using injection during negative valve overlap and stratification, the negative valve overlap can be decreased. This is highly desirable since the negative valve overlap in this test is achieved by use of standard camshafts and hence a large overlap results in poor delivery ratio of the charge to the cylinder and hence low maximum load.

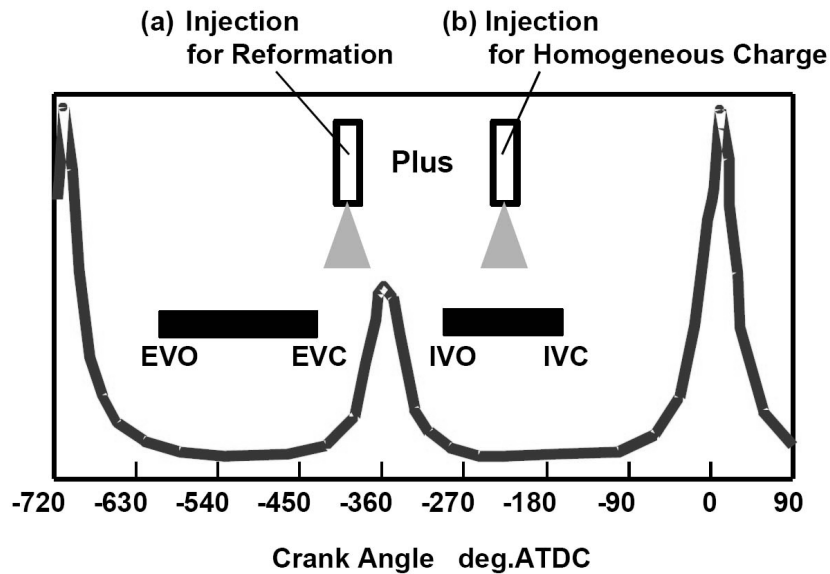


Figure 2-10 Combined injection strategy, where fuel is injected both in the negative valve overlap and in the intake stroke [25].

Onishi et al. [2] define four different combustion regions for the 2-stroke engine shown in Figure 2-11, where C is a region between HCCI and SI. In this region it is implied that spark assistance is applied. Koopmans et al. [26] are the first in the literature to show that spark assistance can affect the combustion phasing in a 4-stroke engine. Fuerhapter et al. [27] show lower COV_{IMEP} by using spark assist and Persson et al. [28] show a minor advance in CA50 and an increase in load and speed range when running the engine with negative valve overlap using fixed valve durations. Since it is very likely that the future of HCCI will be as a combustion mode in the SI engine the spark plugs are available and as such offer a low cost control parameter. Unfortunately the effect of spark assist on CA50 is small. When running inlet air preheated HCCI without EGR or negative valve overlap there exists a region between HCCI and SI, in which it is important to choose proper ignition timing. Otherwise the typical cycle-to-cycle variations from SI combustion [29] will be incorporated into HCCI, Paper 9.

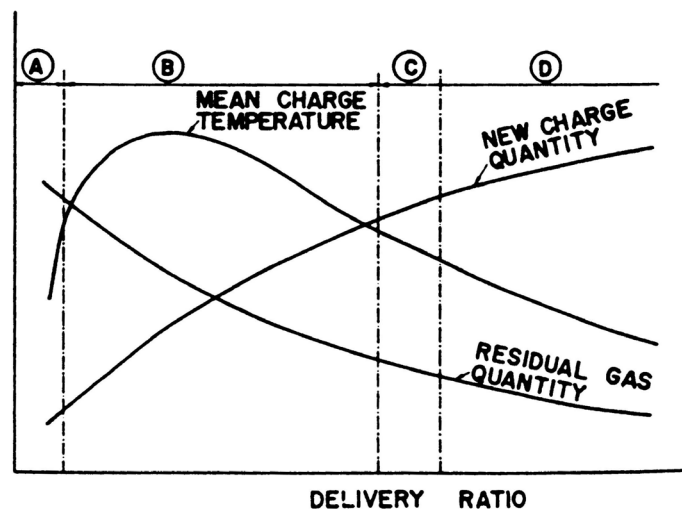


Figure 2-11 Different combustion regions as a function of delivery ratio for a 2-stroke engine [2].

Fuerhapter et al. [27,30,31,32] combine a lot of the previously discussed strategies in their Compression and Spark Ignition (CSI) engine concept, and present a fairly simple solution to achieve rebreathing, which could be used with standard camshafts even though cam phasers are used on their engine to enable the engine to be run in several different combustion modes. The system consists of Electro Hydraulic Valve Actuation (EHVA) shown in Figure 2-12, that replace the hydraulic valve lifters for one exhaust valve per cylinder. It is then possible to open this valve one extra time during the inlet stroke. This system is cylinder individual and hence a solution of cylinder individual combustion phasing control.

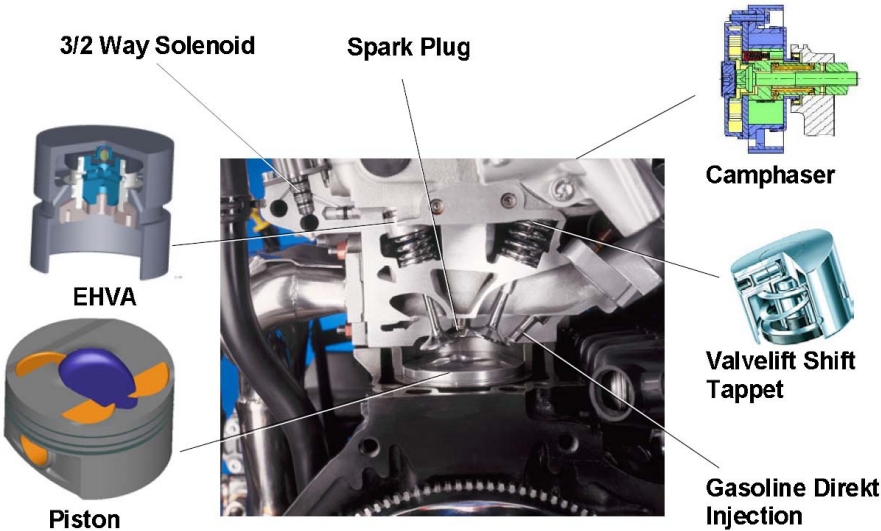


Figure 2-12 System Overview of the AVL CSI valve train with the Electro Hydraulic Valve Actuation [27]

Shown in Figure 2-12, is also the valve lift shift tappet, which enables high or low lift on the inlet valve. The engine concept is direct injected with a piston for stratified SI operation. This equipment enables four different combustion modes to cover the entire load and speed range as shown in Figure 2-13. Injection during negative valve overlap is used when the available energy in the retained exhaust is not enough for HCCI, while spark assist is used in some areas to decrease COV_{IMEP} .

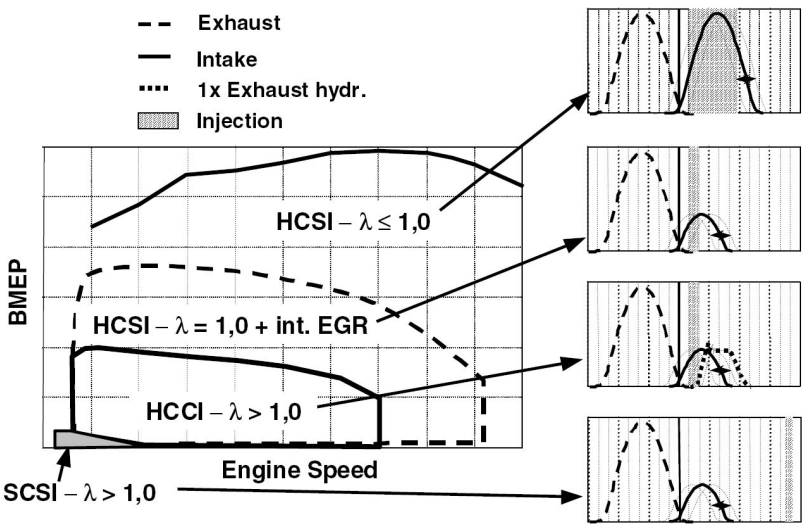


Figure 2-13 Different modes and valve lift strategies of the CSI engine [31].

The four different combustion modes are Stratified Charge Spark Ignition (SCSI), HCCI, Homogeneous Charge Spark Ignition (HCSI) using internal EGR in a Miller concept and finally HCSI using full inlet valve lift without EGR. The Miller cycle engine has different effective compression and expansion ratios [33]. The drive cycle tests include mode transfer between all modes using transition algorithms, which are shown in [31], with a reduction in fuel consumption of 12.8% [32]. This is good for this type of residual heated HCCI and this concept is very likely to be the first 4-stroke HCCI, which goes into serial production due to the small design changes compared to a standard engine with cam phasers and direct injection.

Yang et al. [34] show a single cylinder direct injected HCCI-SI Optimized Kinetic Process (OKP) engine concept. With this concept combustion phasing can be controlled by a three-way valve where hot and cold air is mixed before the cylinder. A fixed CR of 15:1 is used and by applying late inlet valve closing the effective CR is decreased and thus enabling SI Miller operation [33]. By using inlet air heating the EGR amount can be minimized, i.e. no need to heat the charge with hot residuals. This is beneficial since EGR lowers the ratio of specific heats (γ), which results in lower thermal efficiency. No transient performance is shown and since it is a single cylinder engine only indicated values are shown. Figure 2-14 shows the Indicated Specific Fuel Consumption (ISFC) of two Port Fuel Injected (PFI) engines compared to one Stratified Charge (SC) Direct Injected Spark Ignition (DISI), one CAI and the tested OKP engine. It is obvious that this type of HCCI is superior to the so called CAI HCCI concept.

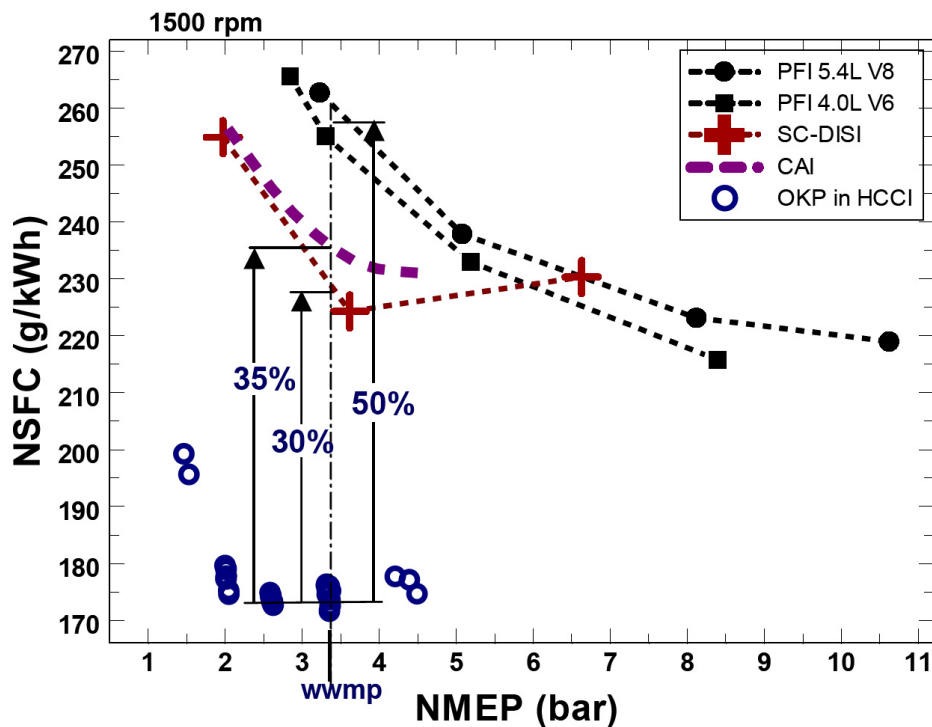


Figure 2-14 Indicated specific fuel consumption as a function of IMEP net for five different engines [34].

Instead of changing effective CR by changing inlet valve closure the geometric CR can be changed. Various VCR solutions are suggested in the literature [35-43], but none of them has yet reached serial production. The Saab Variable Compression (SVC) engine [44,45], is presented in chapter 4.3. By using its VCR feature together with inlet air pre heating, Paper 2 and Paper 3, it is possible to run in CLCC using VCR, Paper 4. This is the first CLCC using VCR on a multi cylinder engine presented in the literature. This system does not allow cylinder individual CR and hence it is necessary to balance differences in CA50 by other means. In Paper 2 to Paper 6, cylinder balancing is achieved by varying λ cylinder-individually by changing the injected amount of fuel as a function of deviation of CA50 from the mean CA50. This type of balancing is not ideal, since the load varies from cylinder-to-cylinder, however global load can still be kept constant. The largest disadvantage with the VCR concept is the rather complex and hence expensive design, a large obstacle to get this concept into serial production.

Another type of air mixing control on a multi cylinder engine is the Fast Thermal Management (FTM) presented in chapter 4.3. Thermal Management is not new in the literature [8,46], but the FTM is, or at least contemporary with Yang et al. [34] who only show steady state measurements. The first version consists of two throttles, one for hot air and one for cold air, which enable fast control of inlet air temperature and hence combustion phasing for a multi cylinder engine presented in Paper 6. It is the first CLCC FTM system on a multi cylinder engine presented in the literature. The drawback with this system is the need for an additional cylinder balancing device. The solution to this problem is to extend the FTM to consist of six throttles instead, with one cylinder individual throttle for cold air and one common for hot air, Paper 7 to Paper 10. With this system it is possible to control a multi cylinder engine with only inlet air temperature. The first drive cycle test with inlet air preheated HCCI in the literature is presented in Paper 10. This type of system consists of simple components which exist already and hence has high potential as a future HCCI engine control concept.

3 Different HCCI controllers

The first presented CLCC on a multi cylinder HCCI engine is, as discussed in the previous chapter, the one by Olsson et al. [17]. As sensors, piezoelectric pressure transducers with external charge amplifiers are used, one for each cylinder. From the pressure trace an apparent heat release is calculated to give the feedback signal, i.e. CA50, for the controller. The gain scheduled PID controller uses the error between CA50_{ref} and CA50 as input. Output from the controller is the mixing ratio between two different octane number fuels. Due to the design of the used control/measurement program, no cycle-to-cycle control is achieved in [17]. This limitation is however removed in later publications [47].

Strand et al. [48], show cycle-to-cycle control with a very similar approach using dual fuels, but for the highest loads no cycle-to-cycle control is possible. The reason is too small fuel injectors, which results in longer injection duration than the time available, i.e. longer duration than the induction stroke. The intention though is not to use dual fuel; it is used to get things up and running before taking on other control strategies with other actuators. PID and Linear Quadratic Gaussian (LQG) controllers are shown in [48], with both pressure transducers and ion current as feedback sensors. However the ion current can only be utilized at a λ less than 2.6 for this particular setup otherwise the signal to noise ratio is too low. An LQG controller is a model based state feedback controller. The model can be either physical or a black box model. They use a black box model which is derived through exciting the system and then identifying the model using system identification commands in Matlab. The engine model is chosen to be a Multi Input Single Output (MISO) type, i.e. it uses total fuel energy, fuel ratio, inlet air temperature, inlet pressure and engine speed as input, while CA50 is the single output. In [49] Bengtsson shows step changes in CA50 and disturbance of the system as step changes in fuel heat, i.e. load, when applying a Model Predictive Controller (MPC) [50], shown in Figure 3-1. Inlet valve closure, i.e. effective CR, is used for actuation and is represented by the lower plot. This is a cylinder individual VVA CA50 control.

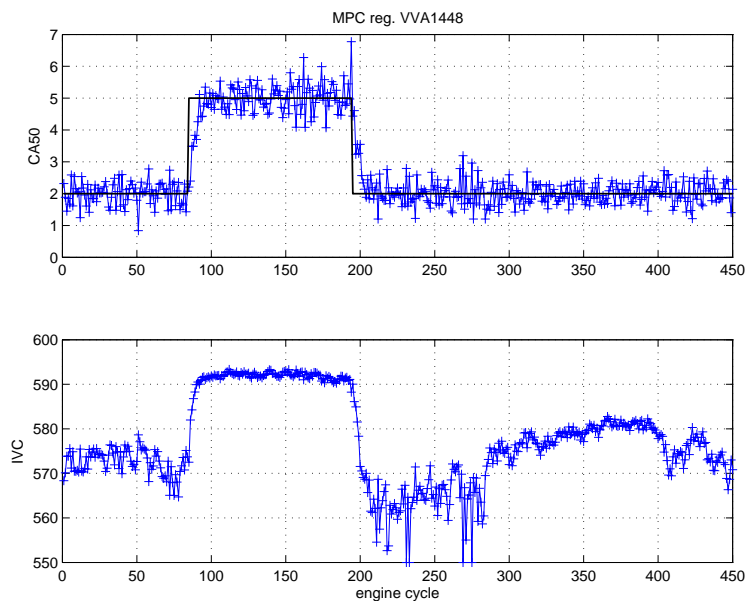


Figure 3-1 Step change in CA50 and response to step change in load using a MISO MPC controller with IVC as actuator on a multi cylinder engine [49].

The identified engine model for the MPC controller uses the same inputs as the LQG controller, but IMEP net and dp/dCAD are added as outputs together with CA50. The MPC controller has a very nice feature of taking constraints of the actuators into account, but suffers from large online calculation time. However Bengtsson et al. prove it to handle cycle-to-cycle control on a truck size engine, i.e. engine speeds up to approximately 1200 rpm, but calculation time could be a problem when trying to apply the MPC controller in current engine control modules. By advancing CA50_{ref} HC and CO emissions are minimized until the chosen constraint of dp/dCAD is reached and then CA50_{ref} is retarded to fulfill the constraint. With this solution it is possible to run the engine without a CA50 map, but other constraints like maximum brake efficiency are not considered.

Souder et al. [51] designed a physical engine model, which is used for simulations, but for the controller design the 41 differential equations, i.e. 41-state model, is found too extensive. Instead the engine is modeled as a Single Input Single Output (SISO) black box system of seventh order, i.e. seven states. The SISO model is developed using subspace system identification and an LQG controller is created from the engine model. Input to the engine model is throttle position and output is CA50. The throttles, one in each exhaust port, of the 4-cylinder passenger car engine are used as actuators and control the amount of EGR cylinder individually by throttling in the exhaust ports. This is not an optimal actuator since it results in high pumping losses, but it is used to emulate a more practical VVT system. Ion current sensors, knock sensors, microphones or regular pressure transducers are used for the combustion sensing. Step changes in CA50 are shown in Figure 3-2 with both microphone and pressure transducer as feedback sensors.

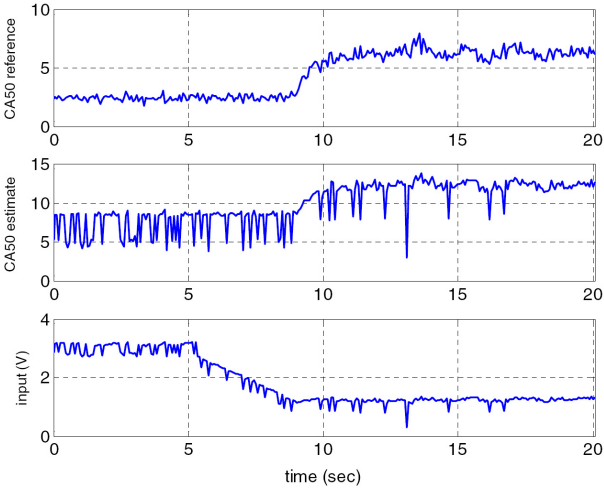


Figure 3-2 Step change in CA50 reference from 2 to 7 CAD ATDC using both a pressure transducer, “CA50 reference” and a microphone, “CA50 estimate”, when throttle control voltage “input” is lowered [51].

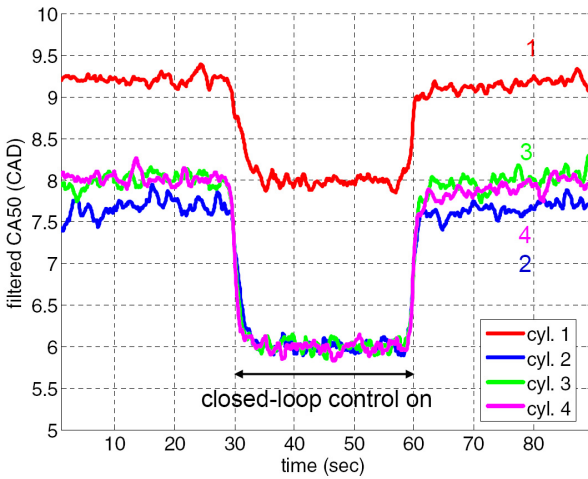


Figure 3-3 CLCC turned on at 30 to 60s with CA50 reference of [8,6,6,6] due to cylinder-to-cylinder differences, which saturate the controller [51].

The cylinder pressure measurement is crank angle based and due to the dynamometer design, the engine is only run at 1800 rpm. The step change in Figure 3-3 indicates that the controller is fairly fast, but also that there exist cylinder-to-cylinder variations for which the throttle control authority is not enough and hence the variation in reference value for cylinder 1 in Figure 3-3. However the retarded CA50 of cylinder 1, even though filtered, seems as stable as the more advanced CA50 of the other three cylinders, which is an indication of a good controller.

Fuerhapter et al. [30,31,32] use a combination of steady state maps together with physical and semi empirical models for their CLCC. In-cylinder pressure is used for feedback and the electro-hydraulic valves serve as main actuators for cylinder individual rebreathing. Since the approach of this engine concept is to be able to run in four different modes, transition algorithms between SI-HCCI and HCCI-SI are developed and tested experimentally. In Figure 3-4 a block diagram of the transition algorithm is shown, where different maps are used depending on which direction the transfer is going. The maps consist of steady state values and are compensated by the transition function depending on cycle number. A model based correction of the first cycle as a function of exhaust gas temperature and load is applied.

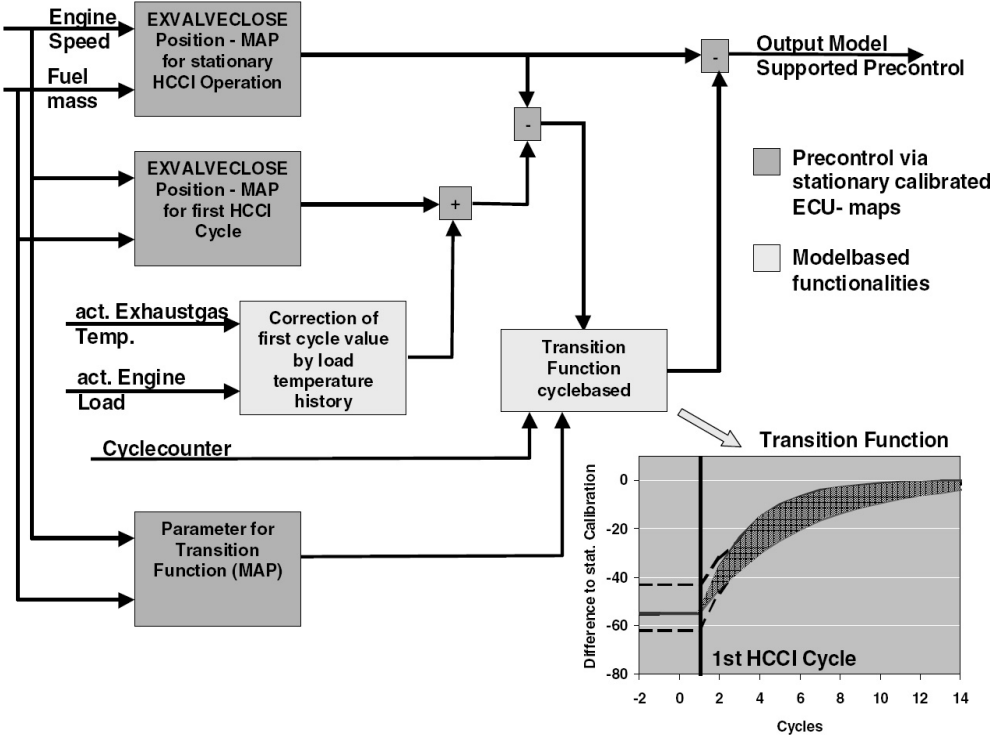


Figure 3-4 Block diagram of the transition algorithm for closing time of the hydraulic exhaust valve lift [31].

A transition between operating modes is shown in Figure 3-5, where the actual transition algorithm is active for less than 0.7s at 2000 rpm, represented by a vertical line. When λ reaches 1.2 the combustion process is defined as HCCI combustion and the CLCC takes care of combustion phasing. Since the transition is very fast the mapping approach has the possibility to work even for an old worn engine, but it could result in harsh transitions.

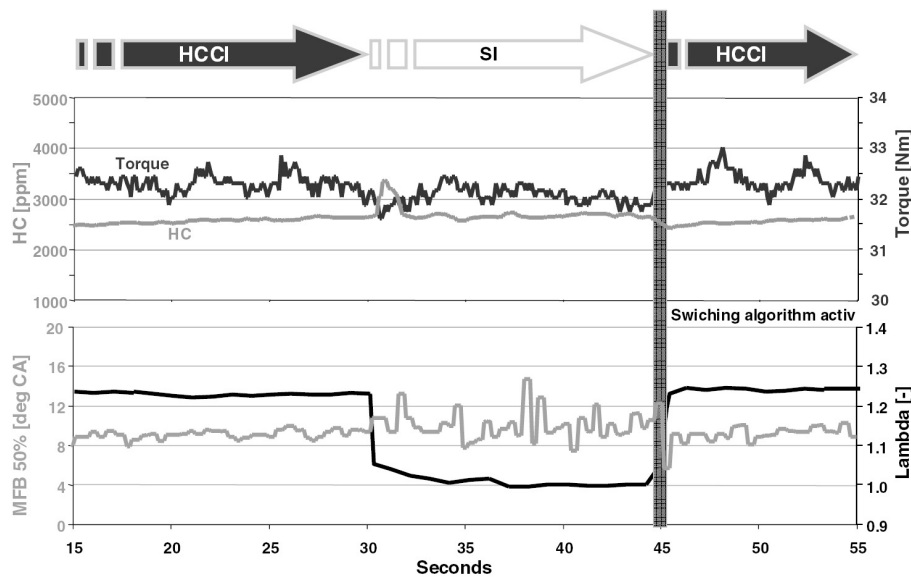


Figure 3-5 Transition from HCCI-SI-HCCI with Torque, HC, CA50 and λ as functions of time [31].

Agrell et al. [52] use two separate valve strategies on a single cylinder engine equipped with a Lotus Active Valve Train System. One is the inlet valve closing to change effective CR and the other is the negative valve overlap, i.e. coordinated change of inlet valve opening and exhaust valve closing. A voltage signal representing the Rassweiler and Withrow mass fraction burned function [53] is produced by a PIC controller based on measured in-cylinder pressure. A nice feature of this design is that “CA50” is available as feedback signal very fast, but due to stability concerns for the PI controllers used, the input to the controller is an average of five engine cycles, which makes cycle-to-cycle control impossible. In [54] the two separate valve strategies are incorporated to an automated control, which changes between inlet valve closing and the overlap method depending on different conditions in inlet pressure, inlet air temperature, volumetric efficiency, best fuel consumption and saturation of the other actuator. This is an expensive system useful for laboratory experiments to find new valve lift strategies, but not feasible for any serial production.

Sun et al. [55] present a power plant for a hybrid vehicle based on a VW TDI engine, which start in SI if the coolant and oil temperature are below 50°C. A supercharger is added upstream of the turbocharger and used to heat the inlet air and to some extent increase inlet air pressure. The standard coolant pump is exchanged for a variable speed electrical pump. Two air-to-air intercoolers and an EGR system with cooler are added. A rapid prototyping electronic control system from Southwest Research Institute control fuel amount, air and boost control valves, water pump and intercooler fan to adjust combustion phasing. All these actuators are adjusted simultaneously as a function of load and speed according to predefined optimized maps. For transients the control system moves in the steady state map. Dp/dCA is used as feedback for the CLCC. A transient from 3.5kW to 30kW is made in 5s and mode transfer is shown both to and from HCCI, but no transition algorithms are used. The system consists of mostly standard parts, however all extra parts make it rather expensive. The mapping approach is acceptable for a new engine, but some considerations must be taken to have some kind of remapping as the engine and all surrounding systems are worn. The CLCC might be able to handle even a worn engine.

Shaver et al. use physical models to control the reinduction/rebreathing of exhaust gases with a VVA system in [56,57]. A physical nonlinear model is derived with the molar ratio, α , of reinducted products and reactants used as input and peak cylinder pressure as the output. From this nonlinear model a linear model is created at one operating point at design time and a second order LQG controller is designed [56]. The LQG controller has the output α' which corresponds to a certain combination of IVO and EVC according to a predefined map. The most important concept in this physical model approach simulation is the coupling between the present cycle and the previous cycle in terms of residual gas energy.

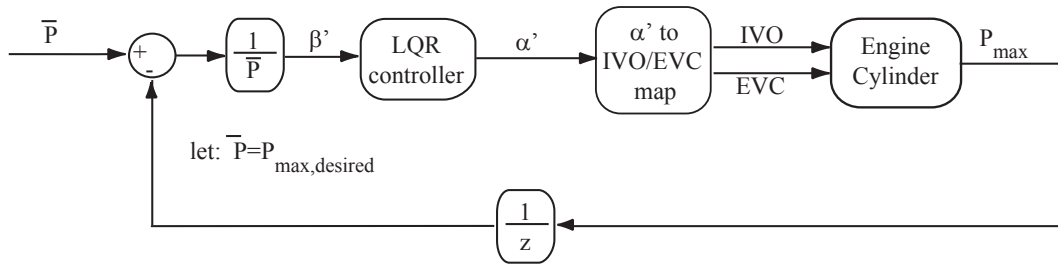


Figure 3-6 Schematic of the peak cylinder pressure controller [56].

In [57] experimental results on a single cylinder engine are shown with the CLCC using peak cylinder pressure as feedback with cycle-to-cycle control, but no CA50 control is applied. However later tests using the decoupled CLCC controller in Figure 3-7 combustion phasing control is added on a slower timescale than the peak cylinder pressure controller [58]. Results using this controller are shown in Figure 3-8, where IVC is used as actuator to change effective CR and hence CA50. Sampling is time based, while control is done on cycle-to-cycle basis. The engine is only run at one engine speed and more work is required to get a controller that handles speed transients.

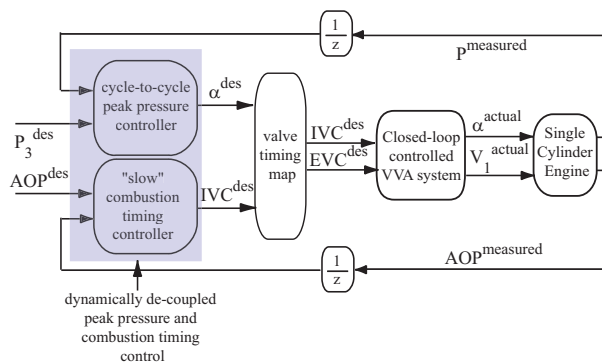


Figure 3-7 CLCC of CA50 and peak cylinder pressure [58].

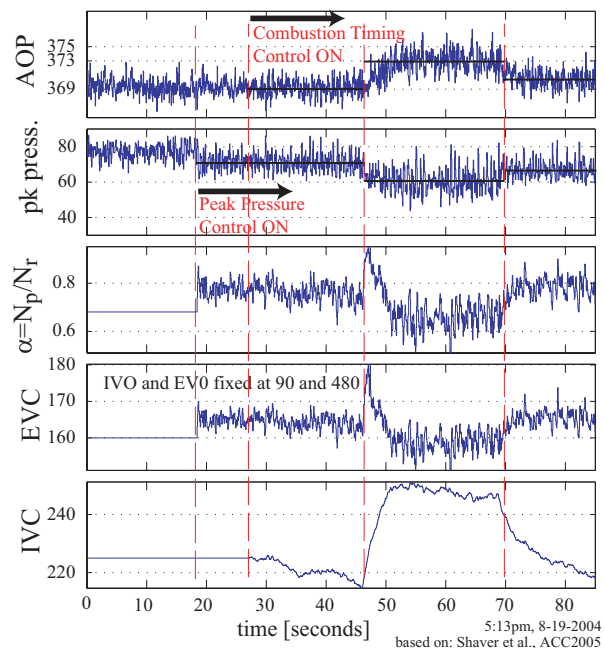


Figure 3-8 CLCC of peak cylinder pressure and CA50 as a function of time [58].

Koopmans et al. [59] show the first multi cylinder mode change in the literature. The Volvo Rapid Prototyping System (VRPS) uses an electronic valve control, which is a VVA system, as actuator to control CA50. In-cylinder pressure is used as feedback. No explicit mode transfer routines are used and it is not revealed what type of controllers that are used in the VRPS. Most likely it is a time based system, while data for saving and post processing are saved crank angle based. The system seems production-near in its design, but probably far too expensive to get into serial production.

In Paper 2 to Paper 7 the author and co-authors use PID controllers with either CR or throttle position as actuators to control CA50. When adjusting CR the real actuator is a hydraulic valve that sets CR and CR_{ref} is set by another PID controller, i.e. it is a cascade coupled CLCC using CR. The combustion feedback signal is CA50 computed from measured in-cylinder pressure. When using the throttles as actuators in Paper 5, Paper 6, Paper 7 and Paper 9 the same type of PID controller is used with CA50 as input and throttle position as output. No closed-loop control is applied on the actual throttle position, i.e. only a reference value is set and a primitive controller sets the actual valve position. In Paper 8 and Paper 10, a state feedback based LQG controller is used with the throttles as actuators and CA50 error as the main feedback signal. The LQG controller is a MISO controller, which has three additional input signals used for feed forward action. These are: CR_{ref} , Fuel Heat and engine speed. The LQG controller is synthesized from a black box model, which is identified by simultaneously adding Pseudo Random Binary Sequences (PRBS) signals on the throttles, CR_{ref} , Fuel Heat and engine speed while measuring resulting CA50, Paper 8. All sampling is CAD based, which is somewhat troublesome, when adjusting CR, since this is changed on a time base. With the rather high CR used the angular movement on the feedback sensor for calculating CR on the engine is very small. Some play in the mechanical connection of this sensor results in a sometimes unstable CR control at high CRs.

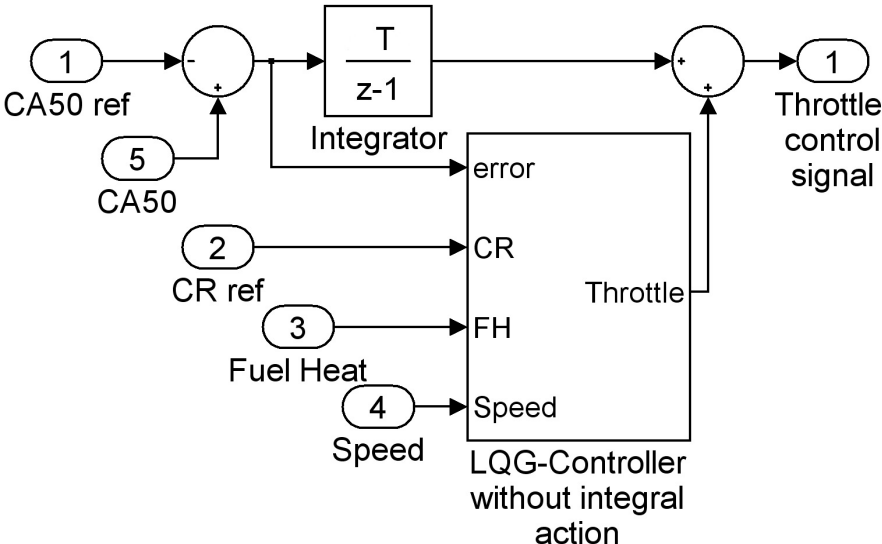


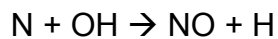
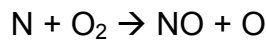
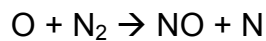
Figure 3-9 LQG controller used for CLCC with an integrator in parallel for one cylinder.

4 Closed-Loop Combustion Control for HCCI

4.1 Why control combustion phasing?

One of the main difficulties with the HCCI engine is combustion control since the onset of combustion depends on temperature, pressure, and mixture formation in each cylinder and there is no direct means to get combustion started. If the combustion control is not fast enough excessively advanced or retarded combustion can appear. If worse comes to worst, the retarded combustion phasing can result in misfire or high HC and CO emissions. The advanced combustion results in a high peak cylinder pressure, $dp/dCAD$, and hence noise.

Another problem with an early combustion is a high combustion temperature and hence a drastic increase in NO_x emissions will appear. The mechanism of thermal NO formation is governed by the following three reactions:



This is often called the extended Zeldovich mechanism [1]. The initial NO formation rate can be expressed as:

$$\frac{d[NO]}{dt} = 6 \times 10^{16} T^{-\frac{1}{2}} e^{\left(\frac{-69090}{T}\right)} [O_2]_e^{\frac{1}{2}} [N_2]_e \quad (\text{Eq. 4.1})$$

Where $[O_2]$ and $[N_2]$ are the equilibrium concentrations of oxygen and nitrogen, respectively [1].

In Figure 4-1 NO_x emissions are shown as a function of maximum combustion temperature [60]. There is an exponential behavior of the formation rate and significant NO_x emissions are found at above 1800-1900K. These combustion temperatures are reached if CA50 is too early or the combustion is excessively fuel rich. The increase of NO_x emissions as a function of CAD for peak of heat release rate is shown in Figure 4-2 [60]. The CAD for peak of heat release rate is approximately equivalent to CA50. It is also shown that HC and CO increase with later CA50.

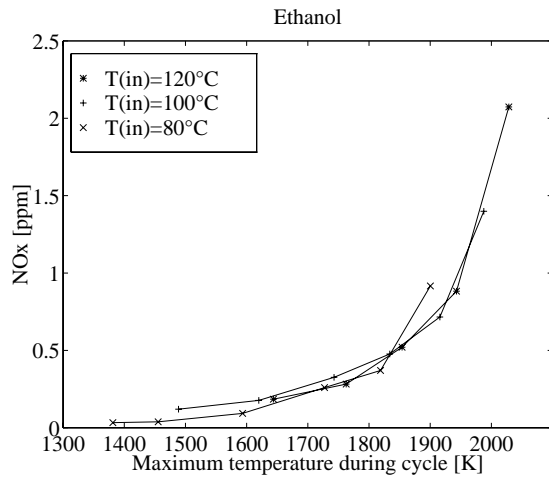


Figure 4-1 NO_x emissions as a function of maximum combustion temperature [60].

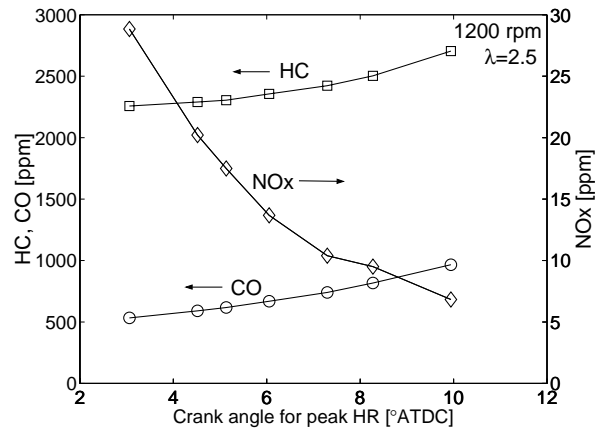


Figure 4-2 Emissions as a function of CAD for peak heat release rate [60].

Another driver to have an effective closed-loop combustion control is the fact that COV_{IMEP} increases drastically as a function of retarded CA50, shown in Figure 4-3, where λ and engine speed are kept constant. Combustion phasing is achieved by manually adjusting inlet air temperature.

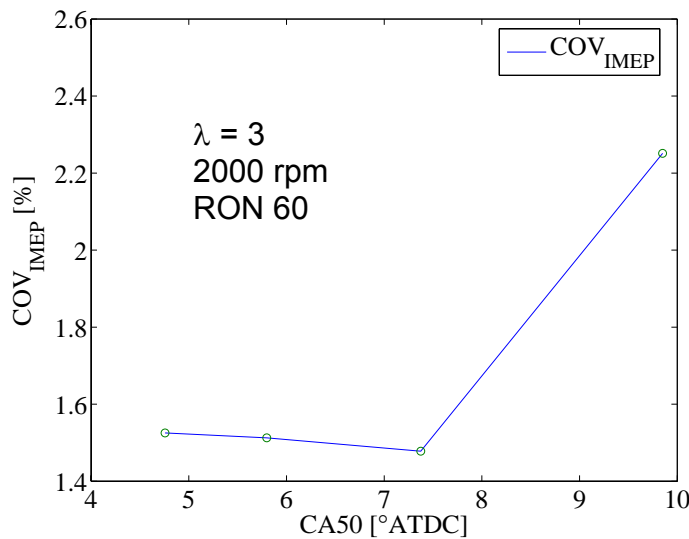


Figure 4-3 Mean of COV_{IMEP} for all five cylinders as a function of mean CA50 at 2000 rpm for a constant λ of 3 and a mixture of isooctane and n-heptane corresponding to RON 60.

An advanced combustion results in higher in cylinder temperature where the charge is guaranteed to auto ignite at an earlier CAD. This of course results in a higher maximum rate of pressure raise ($dp/dCAD$) and higher NO_x emissions. It is therefore very important to maintain an optimal CA50, which depends on load, speed and given limitations in emissions and noise. CA50 for optimum brake thermal efficiency is approximately 7 CAD ATDC for this particular engine, which depends on heat losses compared to expansion work.

4.2 Goal with this project

The goal with this project is to find if the SVC engine with its variable compression ratio feature can be used to control HCCI, since CR is a very powerful actuator for closed-loop combustion control. In the first papers this solution is used to control combustion phasing, Paper 2 to Paper 4, but cheaper solutions are desirable. The two-throttle FTM shows possibility of equally fast CLCC, Paper 6. Neither the VCR nor the two-throttle FTM system allow cylinder-individual CLCC and cylinder balancing with λ is not desirable. A new FTM system is shown in Paper 7, where the cylinder balancing issue is addressed. With this final system the goal is to control HCCI during transients and in a drive cycle which is addressed in Paper 10.

4.3 Test engine

The engine used for all tests except the high load dual fuel test is a five-cylinder 1.6L Saab Variable Compression prototype engine with the main geometric specifications given in Table 4.1. This engine is the base for a downsized highly boosted SI engine concept [44]. The VCR mechanism is schematically shown in Figure 4-4.

Table 4.1 Geometric specifications of the engine.

Displacement	1598 cm ³ (320 cm ³ /cyl)
Number of cylinders	5
Bore x Stroke	68mm x 88mm
Exhaust valve open	45°BBDC at 0.15mm lift
Exhaust valve close	7°ATDC at 0.15mm lift
Inlet valve open	7°BTDC at 0.15mm lift
Inlet valve close	34-49°ABDC at 0.15mm lift
Combustion chamber	Pent roof

The principle is to change the compression volume by raising or lowering the upper part of the engine. This is achieved by tilting the upper part of the engine around a pivot point. The distance between the crankshaft and the cylinder head and hence piston and cylinder head is then adjustable. A main advantage of this design is the unchanged combustion chamber, which is important for efficiency, emissions etc. With the SVC engine, the cylinder head and cylinder liner is a single part called a monohead. The advantages are: no head gasket, better cooling, and no deformation of the cylinder due to cylinder head bolts [44,45].

The engine is run naturally aspirated with wide-open throttle, or very close to, during the tests presented in this thesis. In Figure 4-5 the SVC engine concept is shown in its SI configuration where a supercharger, charge air cooler and VCR allow a boost pressure of 3 bar abs. The engine is then comparable to a 3.0L engine in terms of maximum power and torque. The supercharger with its parasitic losses is not engaged at part load. This results in higher brake thermal efficiency than the larger 3.0L engine, while having the same power and torque when the super charger is engaged at higher load [44]. However friction losses are high due to the robust design to withstand high peak cylinder pressures, which is thoroughly discussed in chapter 4.5.

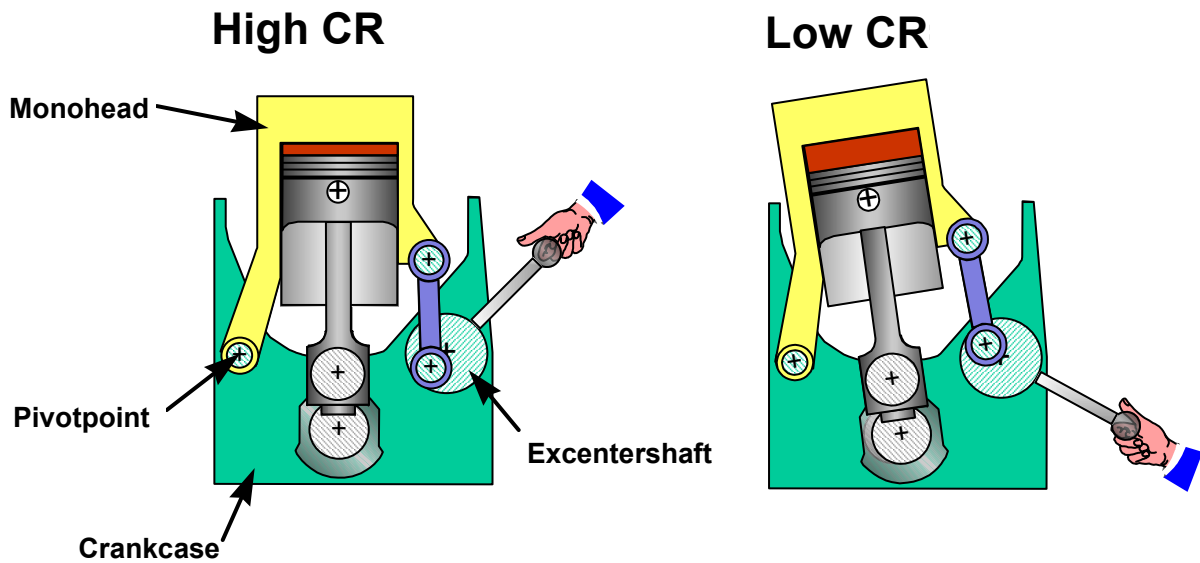


Figure 4-4 Saab Variable Compression engine [44].

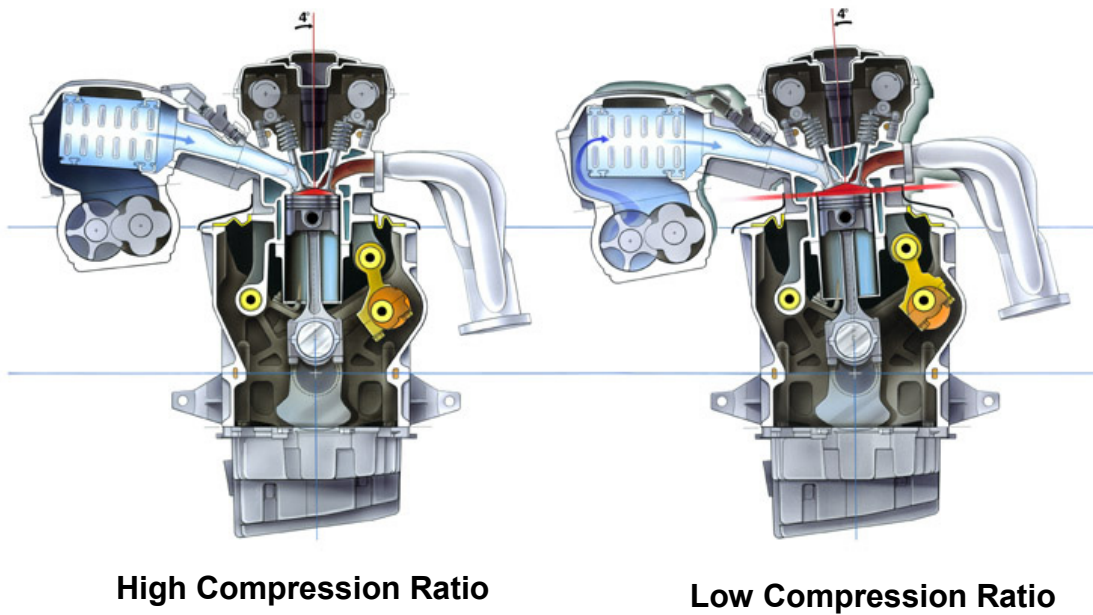


Figure 4-5 Schematic picture of the SVC engine concept with a Lysholm type of supercharger and charge air cooler [44]

The main configuration changes during this project are listed here below, but for detailed data the reader should turn to the technical papers. The different hardware phases during the project are:

1. Defined as the first test configuration, where CR is variable from 9-17:1 and an electrical heater of 11kW is used for inlet air preheating. The standard SI camshafts are used and the entire mechanical supercharger and intercooler system as shown in Figure 4-5 are still fitted on the engine, Paper 2.

2. The maximum CR is increased to 21:1 to allow a broader operating range. The electrical heater is still used but only for startup, since a heat recovery system is fitted, which enables heat to be recovered from the exhaust gases. This allows inlet air temperature control and is called two-throttle fast thermal management (FTM₂). It is however the first version, which does not allow cylinder individual control. To enable accurate CLCC using VCR the hydraulic valve from the SI concept is exchanged to a more suitable valve, Paper 3 to Paper 6.
3. The standard SI inlet camshaft is replaced with one with shorter duration, 236 to 221° to enable higher effective CR, Paper 5
4. The two-throttle FTM₂ system is replaced by a cylinder individual six-throttle system FTM₆ allowing cylinder individual CLCC, Paper 7.
5. The CR is increased to range from 10 to 30:1, which enable cold start and hence the electrical heater is removed due to many failures. In addition a spark ignition system is added to enable mode transfer to and from SI. In Figure 4-6 the engine is shown in hardware phase 5, Paper 8 and Paper 10.
6. The cylinder individual six-throttle system, FTM₆, is replaced by the two-throttle system for better SI performance in Paper 9.

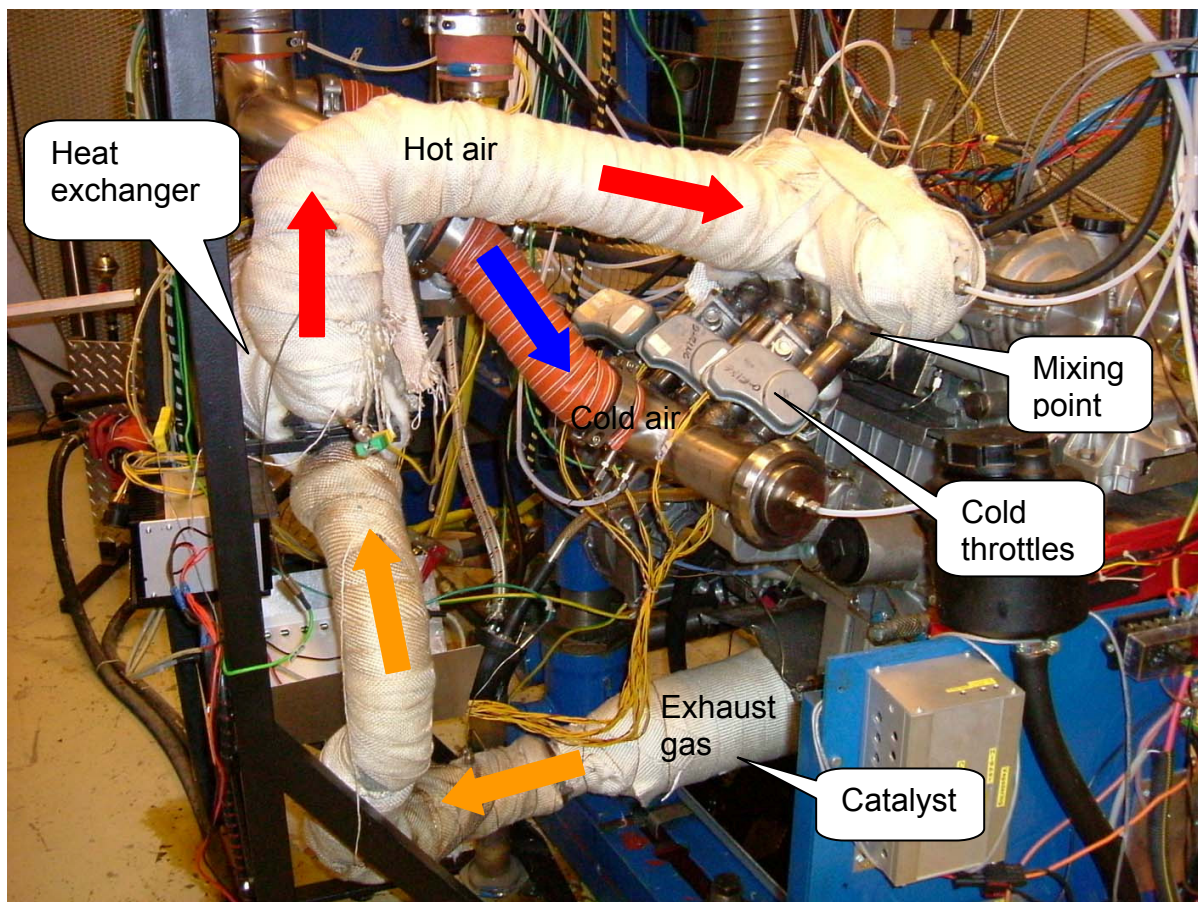


Figure 4-6 SVC engine equipped with six-throttle FTM₆ system as in hardware phase 5.

4.4 Control system

The control system and especially the software code are under continuous evolution, but some major changes in the structure are defined below:

1. Closed-Loop control of CR and electrical heater, but no closed-loop control of CA50. Cylinder balancing is achieved by varying λ cylinder-individually. CA50 is adjusted manually by changing CR_{ref} , inlet air temperature or injected amount of fuel from the graphical user interface. All controllers are PID or PI. A 667MHz Pentium III PC using Windows 98 as operating system is used. A Wave Book 516 and a Multi function PCI card NI6052E are used for A/D and D/A conversion, Paper 2.
2. Implemented Closed-Loop Combustion Control using VCR ($CLCC_{CR/PID}$) as actuator and mean CA50 as feedback signal. Upgraded to a 1.0GHz Pentium III PC, Paper 3 to Paper 5.
3. Implemented Closed-Loop Combustion Control using the FTM_2 throttles ($CLCC_{FTM2/PID}$) as actuators and mean CA50 as feedback signal. A counter board NI6602 is added for throttle actuation and IMEP control is added, Paper 6.
4. Closed-Loop Combustion Control using Cylinder-individual FTM_6 is implemented ($CLCC_{FTM6/PID}$), Paper 7.
5. Upgraded to a Pentium 4 2.8GHz hyper threading PC using Windows XP as operating system and exchanged the Wave Book for a DAP 5400a, from Microstar Laboratories capable of sampling 5 samples per CAD and cylinder over the entire speed range of the engine during continuous operation. A system identification is made and a state feedback LQG controller ($CLCC_{FTM6/LQG}$) is implemented as an alternative to the $CLCC_{FTM6/PID}$ controller. BMEP and Speed control is added, Paper 8 and Paper 9.
6. Combined $CLCC_{CR/PID}$ and $CLCC_{FTM6/LQG}$ as function of engine speed together with cylinder balancing using the FTM_6 when the $CLCC_{CR/PID}$ is applied, Paper 10.

The reason for the relatively high resolution of 5 samples per CAD is that the system is used both as a control system during the tests and as a measurement system for post analysis of e.g. heat release. The initial Wave book based system featured full resolution up to 3000 rpm. Above this speed limit the control program discarded old cycles of data if a new cycle was available before the old ones had been processed. This approach is satisfactory for the PID controllers, but not good at all for the state feedback controller which needs continuous data to update the states. For 3000 rpm a sampling interval of maximum 40ms for one cylinder is allowed, i.e. 200ms for five cylinders, defined in Figure 4-7, and this is very closely achieved by the DAP, as shown in Figure 4-8.

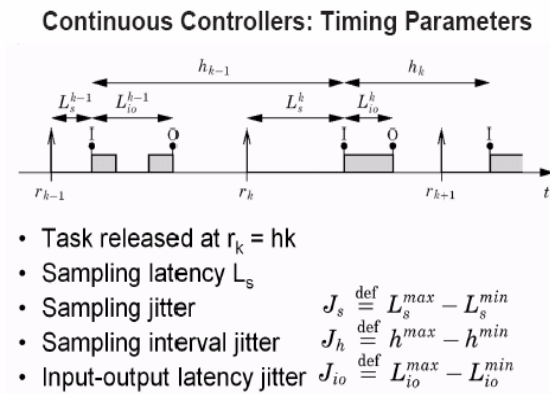


Figure 4-7 Timing parameters [61]

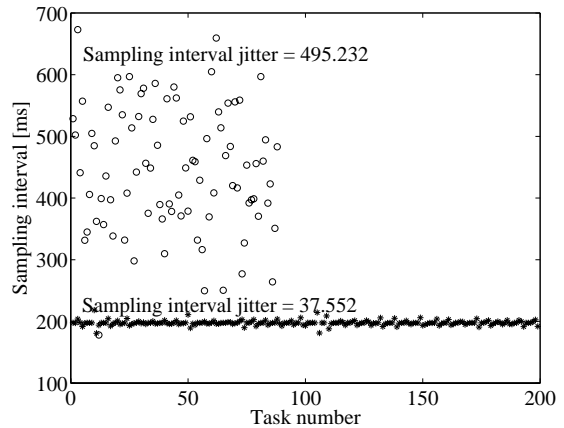


Figure 4-8 Sampling interval and sampling interval jitter for Wave Book (o) and DAP (*) at 3000rpm for one cylinder.

When using the wave book system a check is made how much data is available in the driver buffer and then that amount of data is transferred to the control program circular buffer. Due to a 20ms delay in the wave book driver no real time performance is achieved. For the DAP it is possible to get a fixed number of samples, which is the preferred method. The number of samples chosen is 3600 samples, which results in one cylinder cycle of data is completed each time data are transferred to the control program buffer. One engine cycle consists of five combustion events, i.e. five cylinder cycles. With an update of feedback data each cylinder cycle it is possible to have cycle-to-cycle control if the actuators are fast enough. However the main combustion phasing actuators like VCR and FTM are not that fast. Note that the x-label “Cycles” in the results section always stands for engine cycles.

4.5 Results

The main combustion phasing parameters used for the SVC engine are the CR and inlet air temperature, but variable λ are also used in combination with the VCR and the two-throttle FTM system.

With two almost similar control knobs it is possible to run at constant CA50 with high CR and low inlet air temperature or at low CR and high inlet air temperature. The optimum choice is not quite obvious and depends on different criteria. Considerations have to be taken into account as to whether highest brake thermal efficiency and low NO_x emissions are desirable or if low CO emissions are more important.

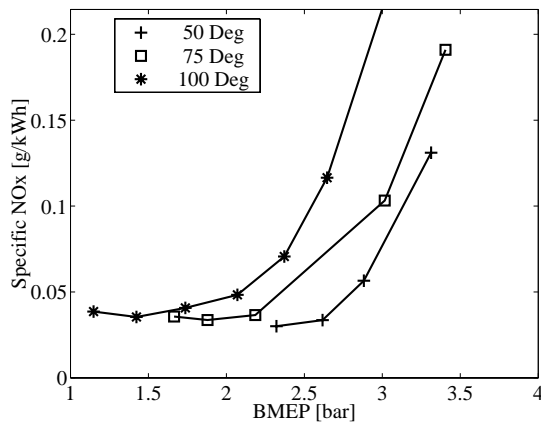


Figure 4-9 Specific NO_x emissions as function of load for three different inlet air temperatures on the SVC engine, Paper 2.

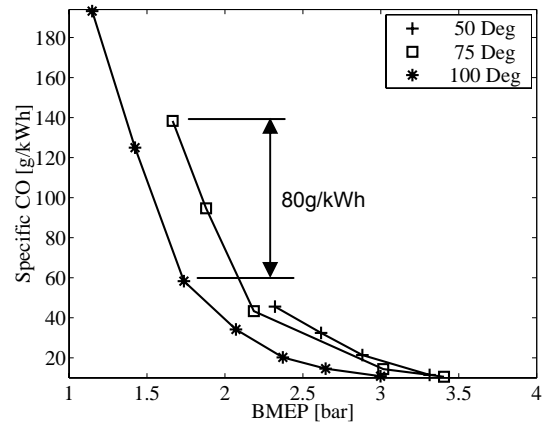


Figure 4-10 Specific CO emissions as function of load for three different inlet air temperatures on the SVC engine, Paper 2.

The specific NO_x emissions in Figure 4-9 rise with inlet air temperature, but are still very low. The specific CO emissions in Figure 4-10 are not low at the lower loads though. The largest effect of inlet air temperature is for a load of 1.7 bar BMEP, where CO is reduced by 80 g/kWh through an increase of the inlet air temperature by 25°C. If the CO emissions can be effectively reduced by an oxidizing catalyst, a high CR should be used at all times. If the aim is to minimize both CO and NO_x, the strategy is to use a high inlet air temperature at a load lower than 2 bar BMEP and for higher load use a low inlet air temperature and high CR.

A case of high inlet air temperature and transient operation using CLCC_{CR/PID} to change the CA50 with a step in set point from 1 to 9 and back to 1 CAD ATDC is shown in Figure 4-11. The time it takes for the CLCC_{CR/PID} to retard the CA50, represented by a thick line in the middle plot, to 63% of the set point, represented by a thin line in the middle plot, is defined as the time constant of the CLCC_{CR/PID}. The time constant for the positive step in Figure 4-11 is 14 engine cycles, which is equivalent to 0.84s at 2000 rpm. It is interesting to know that the time constant for the CR controller is merely 3 engine cycles, which is equivalent to 180ms at 2000 rpm. It might be possible to get a somewhat faster CLCC_{CR/PID} if no cascade coupling were used, i.e. use valve position of the hydraulic valve that sets CR as output from the CLCC_{CR/PID} instead of CR_{ref} as used here.

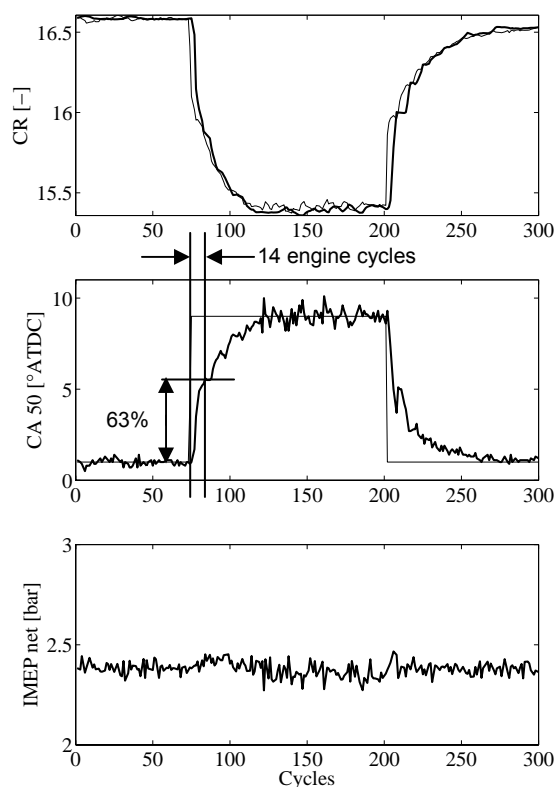


Figure 4-11 Step change in set point of CA50 from 1 to 9 to 1 CAD at 2000 rpm and 1.5 bar BMEP using CLCC_{CR/PID}, Paper 4.

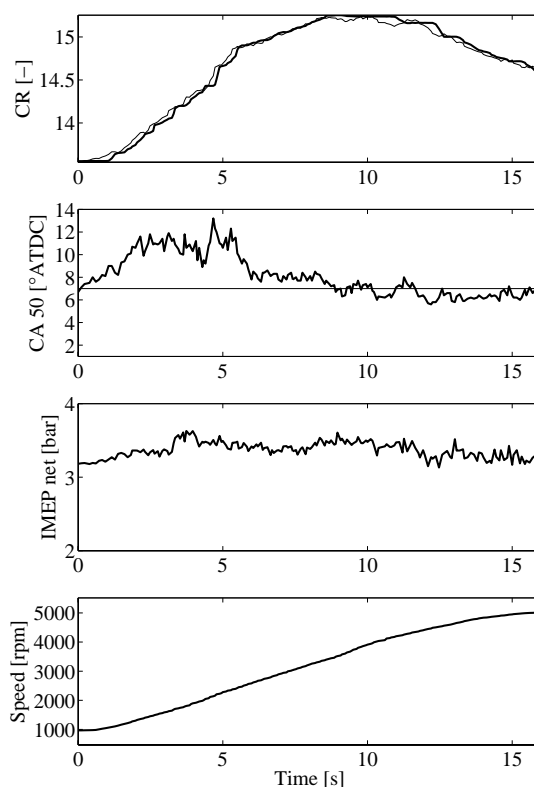


Figure 4-12 Positive ramp on engine speed, using CLCC_{CR/PID}, from 1000 to 5000 rpm at a load equivalent to 2.5 bar BMEP at a constant speed of 2000 rpm, Paper 4.

The upper plot in Figure 4-11 shows measured CR, represented by a thick line, and CR_{ref}, represented by a thin line. For a step in CA50 of 8 CAD the CR is changed from 16.6 down to 15.4. Mean IMEP net of all five cylinders in the lower plot does not change in magnitude with the step, but COV_{IMEP} for cylinder 1 rises from 2.5% for the first 70 cycles up to 14% from engine cycles 71 to 200. This is due to the fact that advanced combustion is more stable than retarded combustion.

If the HCCI engine is to be used in a passenger car, the transient performance has to be comparable to the SI and CI engines of similar size. A transient in speed using the CLCC_{CR/PID} is shown in Figure 4-12. The load is set with a constant injected fuel amount, which is equivalent to 2.5 bar BMEP when running the engine at 2000 rpm. The speed of the dynamometer is then raised manually, while trying to keep a constant output from the engine of 1 bar BMEP. This is of course not the same as the manner in which it would have been done in an SI or CI transient, where the load would be raised as speed rose, but with this test the response of the CLCC_{CR/PID} to a ramp in speed is demonstrated. More realistic load and speed ramps are shown during the drive cycle test in Paper 10.

The total amount of time for the positive speed ramp in Figure 4-12 is 16s, and it is completed in 412 engine cycles. This is too slow for a car and more control authority or a faster controller is needed for a passenger car application. The five-cylinder mean COV_{IMEP} is 10%. During the speed ramp, CA50 is retarded by a maximum of 6

CAD at 4.6s from start, when the rate of speed change (dN/dt) is at its maximum of 15.7 rps^2 . This is due to a decreased time to initiate combustion. Increasing CR, which is done by the $CLCC_{CR/PID}$, then compensates for the retarded combustion. The upper plot in Figure 4-12 shows the applied CR, thick line, and CR_{ref} , thin line, which starts at 13.5 and ends at 14.6. There is a maximum CR of 15.2 at approximately 10s. From there on, the CR decreases due to increased wall temperature, which is the result of increased heat losses at higher engine speeds. Note the heat loss per cycle decrease due to shorter time.

The response to a ramp in inlet air temperature is shown in Figure 4-13. The CA50 advances severely and the speed change of the temperature is in fact faster than for the $CLCC_{CR/PID}$. The CA50 deviation is however decreased to a minimum at engine cycle 300 where the control variable saturates and the deviation of CA50 increases again. During this transient, CR is changed from 16 to 21 and the drop in inlet air temperature is 60°C . This implies that a 12°C change is equivalent to a change of 1 CR unit. This is less than the estimated 25°C for the static test in Paper 2. This can be explained by a large time constant of the thermocouple used and hence it is not the actual inlet air temperature that is shown in Figure 4-13. IMEP net drops considerably during the temperature transient due to excessively retarded combustion. COV for mean IMEP net goes from 1.5% for engine cycles 1 to 60, to 11% for engine cycles 61 to 250.

The highest rate of temperature change (dT/dt) is located at approximately cycles 140-160, where the largest deviation in CA50 from the set point appears. This means that dT/dt is faster than the $CLCC_{CR/PID}$, which does not keep up with the pace here. The maximum dT/dt of the system is however not used, since it in this test was limited by the speed of the $CLCC_{CR/PID}$. With more aggressive PID parameters for the $CLCC_{CR/PID}$ it has potential of an even faster control, but with the current setup it becomes unstable. The reason is believed to be the large sample time jitter of the system in hardware phases 1 to 4. By using a $CLCC_{CR/PID}$ with the hydraulic valve as output in hardware phase 5 the $CLCC_{CR/PID}$ is believed to have time constants equivalent to the CR control, i.e. 180ms.

The temperature transient in Figure 4-13, made by manually using the FTM_2 , is the transient most difficult to control for the $CLCC_{CR/PID}$ and the cylinder balancing. The inlet air temperature distribution changes substantially when mixing cold air into the hot air flow to the engine. With only hot air cylinder one, for example, can have a 10°C higher temperature than the mean in Figure 4-13, but when the cold air stream is opened, this cylinder can have a 10°C lower inlet temperature than the mean, i.e. a 20°C difference. This together with the global change strains the system to its limits.

In Figure 4-14 the engine is run at a constant load of 2.5 bar BMEP and 2000 rpm with a constant inlet air temperature. The difference in CA50 is shown in the upper plot, where no cylinder balancing is used for the first 112 engine cycles. The difference in CA50 is mainly due to large differences in inlet air temperature caused by very poor mixing of cold and warm air from the FTM_2 heat recovery system, but it is also due to small deviations between the individual cylinders' CR shown in Paper 3, Paper 4 and Paper 7. The cylinder balancing using variable λ is turned on at engine cycle 112 and the deviation reaches a minimum steady state value 28 engine cycles later, which is equivalent to 1.7s at 2000 rpm.

The maximum allowed fuel offset is chosen to be 30%. Without this limit, IMEP net would deviate excessively between the cylinders resulting in fluctuating noise intensity between the different cylinders, discussed in Paper 9.

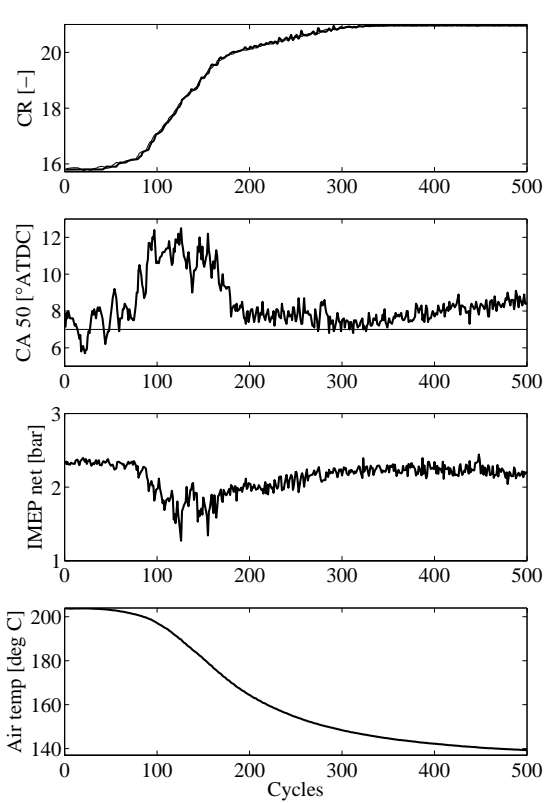


Figure 4-13 Negative ramp on inlet air temperature from 200 to 140°C at 2000 rpm and 1.5 bar BMEP using CLCC_{CR/PID}, Paper 4.

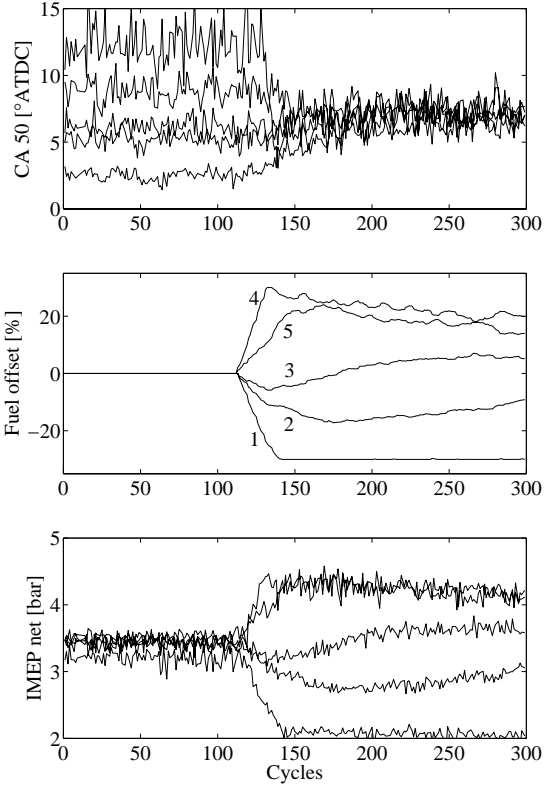


Figure 4-14 Cylinder balancing using variable λ , Paper 4.

The plot of fuel offsets shows that, at first, the offset has to be higher than the final value. This is due to the inertia in wall temperature. The IMEP net difference goes from 0.5 to 3 bar. This results in differences in emissions, noise etc between the cylinders as well. For this case, it would be beneficial to set an offset on CA50 between the cylinders. No offsets are set here though in order to clearly show the performance of the cylinder-balancing controller. This kind of cylinder balancing control is useful for fine-tuning CA50, but other measures should be taken to equilibrate cylinder individual CR and inlet air temperature variations to minimize the need for cylinder individual λ -control. This is discussed further in paragraph 4.6.

With the FTM₂ a step from the expensive prototype VCR solution is made and by having the throttle signal as output from the PID controller a CLCC_{FTM2/PID} is designed. The drawback is, as shown before when using the CLCC_{CR/PID}, that cylinder balancing using variable λ is necessary since the CLCC_{FTM2/PID} is engine global in the same manner as CLCC_{CR/PID}. Step changes in CA₅₀ with the CLCC_{FTM2/PID} shows a time constant of 8 engine cycles, Figure 4-15, which can be compared to the 14 engine cycles of the CLCC_{CR/PID} in Figure 4-11 at the same engine speed. Initial speed ramps however indicate that the CLCC_{FTM2/PID} is not fast enough to manage the speed ramp that the dynamometer can manage, shown in Figure 4-16.

Note the difference in ramp time between this and the one in Figure 4-12. Here the dynamometer reference speed is set from the control PC, which enables repeatable ramps. It is actually set as a step change from the control PC, but step changes on the engine speed is physically impossible and hence the ramp is the result of the dynamometer inertia and analogue controller delays. The error in CA₅₀, which leads to retarded CA₅₀ for some cylinders can partly be explained by Low Temperature Reactions (LTR) [62,63,64,65], but mostly by the limited effect of throttle position on the air mixing at low air flows, i.e. low engine speed. This is discussed further below.

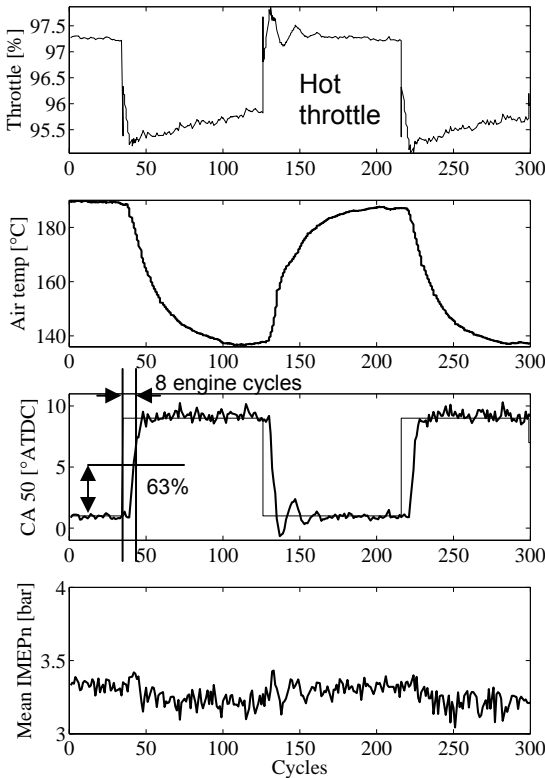


Figure 4-15 Step change in CA₅₀ at 2 bar BMEP and 2000 rpm using CLCC_{FTM2/PID}, Paper 6.

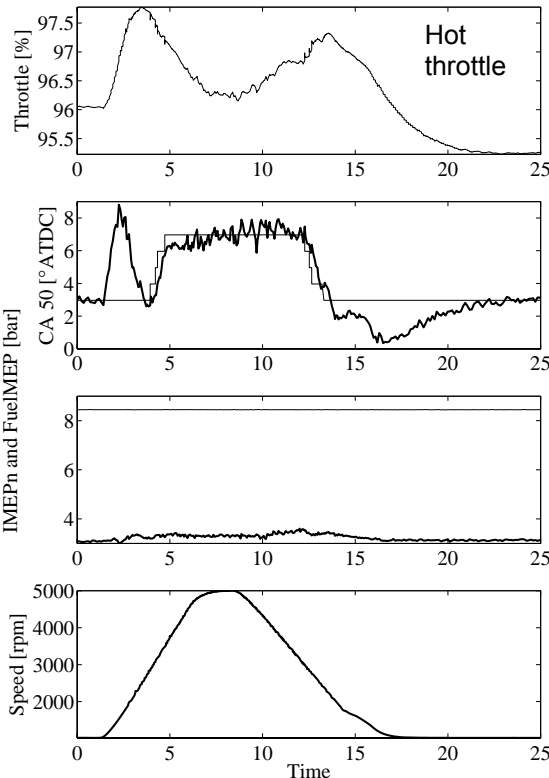


Figure 4-16 Speed transient using CLCC_{FTM2/PID} from 1000 to 5000rpm and back with CA_{50_ref} changed as a function of speed to manage effect of low temperature reactions and low air flow past throttles, Paper 6.

A thin type K thermocouple with a diameter of 0.5mm is used to measure the inlet air temperature and since nothing else is changed during the step change in Figure 4-15, the inlet air temperature should be almost an exact inverse of CA50. This is not the case and calculation from the step response gives a time constant of 1.2s or 21 engine cycles at 2000 rpm for the thermocouple. This is by far too slow to resolve the actual inlet air temperature and for that reason the inlet air temperature is not shown in subsequent plots. Even thinner thermocouples have been tested, but then durability becomes an important issue.

With the FTM₆ the need for additional cylinder balancing is minimized, however manually fine tuning CR between the different cylinders is shown effective in Paper 7. Already for the FTM₂ an alternative to the gain scheduled [66] PID controller is investigated, but never implemented [67]. However in Paper 8 the first experimental results with CLCC_{FTM6/LQG} are shown. The main driver to adopt other controllers is to get a systematic method of controller design. For the PID controller, the Ziegler-Nichols method [68] is used to provide a starting point for the control parameter optimisation. Trial and error type iteration is then used to fine-tune the controller. If gain scheduling is used it requires a lot of calibration work .e.g. in the case of the CR controller, which has parameters that are functions of the actual CR. Note it is only the CR controller that is gain scheduled and not the CLCC_{CR/PID}, Paper 4.

When comparing results from both CLCC_{FTM6/PID} and CLCC_{FTM6/LQG} in Figure 4-17 and Figure 4-18 it seems like similar performance is achieved, however the CLCC_{FTM6/LQG} is more robust and handles disturbances in CR, load and speed better. This is logical since the LQG controller has knowledge about these variables and uses them for feed forward compensation. The PID controller only sees the CA50 error and corrects throttle position in correspondence with that, in this case without any gain scheduling. The synthesized LQG controller is a second order model extended to fifth due to a time delay on the throttles, i.e. air flow, Paper 8. This can be compared to a PID controller, which is of second order as well, i.e. two states, one in the integrator and one in the derivative part. A PID controller written in continuous time is shown in Eq. 4.2:

$$u(t) = K \left(e(t) + \frac{1}{T_i} \int e(s) ds + T_d \frac{de(t)}{dt} \right) \quad (\text{Eq. 4.2})$$

where K is the proportional parameter, T_i the integral parameter and T_d the derivate parameter, i.e. three design parameters. To this it is standard procedure to implement a filter for the derivate part, which results in an additional parameter.

The identified engine model is a second-order discrete stat space model, which is extended to a fifth-order due to time delay on the throttle response. The engine model has the following structure:

$$\begin{aligned} x(k+1) &= Ax(k) + Bu(k) + w(k) \\ y(k) &= Cx(k) + Du(k) + v(k) \end{aligned} \quad (\text{Eq. 4.3})$$

In Eq. 4.3, w(k) and v(k) are white process and measurement noise respectively at cycle k. y(k) is CA50 and u(k) is a vector consisting of throttle, CR, fuel heat and engine speed.

The matrices in Eq. 4.3 are as follows:

$$A = \begin{pmatrix} 0.79732 & 0.50455 & 0 & 0 & 0.083843 \\ -0.93326 & 0.61003 & 0 & 0 & -0.035222 \\ 0 & 0 & 0 & 0 & 0 \\ 0 & 0 & 1 & 0 & 0 \\ 0 & 0 & 0 & 1 & 0 \end{pmatrix}$$

$$B = \begin{pmatrix} 0 & -0.0031596 & -2.4059 \cdot 10^{-5} & 2.1599 \cdot 10^{-5} \\ 0 & -0.0059634 & 6.4163 \cdot 10^{-8} & -1.35 \cdot 10^{-5} \\ 1 & 0 & 0 & 0 \\ 0 & 0 & 0 & 0 \\ 0 & 0 & 0 & 0 \end{pmatrix}$$

$$C = (358.14 \quad -76.753 \quad 0 \quad 0 \quad 0)$$

$$D = (0 \quad 0 \quad -0.00026456 \quad -0.008621)$$

Matlab functions *kalman*, *dlqr* and *lqgreg* are used to create a Linear Quadratic Gaussian controller using the matrices above. For the model based LQG controller there are two design parameters plus one for the integrator added in parallel, Paper 8 and Paper 10, since integral action is not inherent in LQG controllers.

The optimal LQG controller is designed by minimizing the cost function Eq. 4.4:

$$J(u) = \sum_{k=1}^{\infty} (x(k)^T Q x(k) + u(k)^T R u(k) + 2x(k)^T N u(k)) \quad (\text{Eq. 4.4})$$

where Q punishes the states, x, and R punishes the output, u, while N is set to zero here. This results in the designed LQG controller with a control structure according to:

$$\begin{aligned} z(k+1) &= A_c z(k) + B_c e(k) \\ u(k) &= C_c z(k) + D_c e(k) \end{aligned} \quad (\text{Eq. 4.5})$$

Here e(k) is the difference between CA50_{ref} and CA50 at cycle k and u(k) is a scalar containing the throttle command. The z-vector contains the controller states. After adding the integrator the matrices have the following values:

$$A_c = \begin{pmatrix} 0.25492 & 0.62079 & 0 & 0 & 0.083843 & 0 \\ 0.22269 & 0.5423 & 0 & 0 & -0.035222 & 0 \\ -2.0931 & -5.0974 & -0.37489 & -0.22558 & -0.12414 & 0 \\ -2.177910^{14} & 4.667510^{15} & 1 & 0 & 0 & 0 \\ -2.764310^{15} & 5.924110^{16} & 0 & 1 & 0 & 0 \\ 0 & 0 & 0 & 0 & 0 & 1 \end{pmatrix}$$

$$B_c = \begin{pmatrix} -0.0031596 & -2.3659 \cdot 10^{-5} & 3.4656 \cdot 10^{-5} & 0.0015145 \\ -0.0059634 & -1.6928 \cdot 10^{-7} & -2.1107 \cdot 10^{-5} & -0.00088237 \\ 0 & -5.2598 \cdot 10^{-7} & -1.7139 \cdot 10^{-5} & -0.0019881 \\ 0 & 1.6088 \cdot 10^{-20} & 5.2426 \cdot 10^{-19} & 6.0811 \cdot 10^{-17} \\ 0 & 2.042 \cdot 10^{-21} & 6.6541 \cdot 10^{-20} & 7.7185 \cdot 10^{-18} \\ 0 & 0 & 0 & 1 \end{pmatrix}$$

$$C_c = (-2.0931 \quad -5.0974 \quad -0.37489 \quad -0.22558 \quad -0.12414 \quad 1.0264 \cdot 10^{-3})$$

$$D_c = (0 \quad 0 \quad -0.00026456 \quad -0.008621)$$

The states in the state feedback controller can be said to know everything worth knowing of the system's earlier history to be able to tell how the system will behave in the future [69]. Note the index c, which shows that it is not the same A, B, C and D as found from the identification in Eq. 4.3, however those are used to create the new matrices in Eq. 4.5.

When the integrator is added to the LQG controller one additional design parameter is added, hence a total of three design parameters. This is the same number of design parameters, or one less depending on implementation strategy, as a PID controller without feed forward and gain scheduling. It is believed that a well tuned gain scheduled PID controller equipped with feed forward action would perform as well as the state feedback based LQG controller. The drawback is the extensive work of fine tuning it at many operating points, i.e. gain schedule. It can be concluded that the LQG controller handles a much broader operating range with approximately the same number of design parameters due to the control synthesis from an identified model, which holds information of how different disturbances affect CA50.

The FTM₆ system is the first prototype of that type of control shown in the literature and in-house found throttles are used in the design, Paper 7. The smaller cold throttles are used on SVC engines for boost pressure control and are not optimized for this system. This results in a much larger total throttle area than optimal, which results in less pressure difference especially at lower engine speeds compared to the FTM₂ system. During step changes in Figure 4-17 and Figure 4-18, where a PID controller is compared to an LQG controller, inlet air pressure control is added to increase the pressure difference over the throttles by closing the hot throttle by applying an offset from the cold throttle inverse. The inlet pressure control results in the time constant for a CA50 step decrease from 35 engine cycles to 8 engine cycles at 2000 rpm, i.e. comparable to the FTM₂ system.

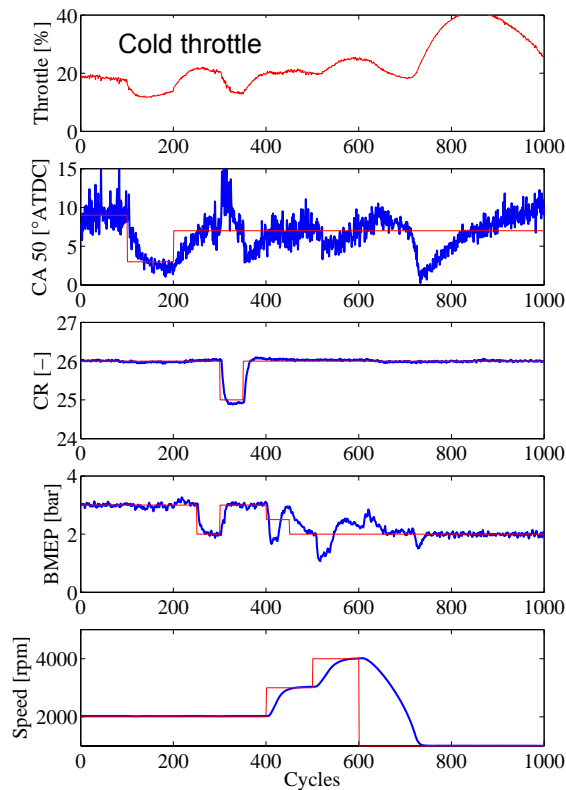


Figure 4-17 Step in CA50 and disturbance on CA50 using the CLCC_{FTM6/PID} for one cylinder, Paper 8.

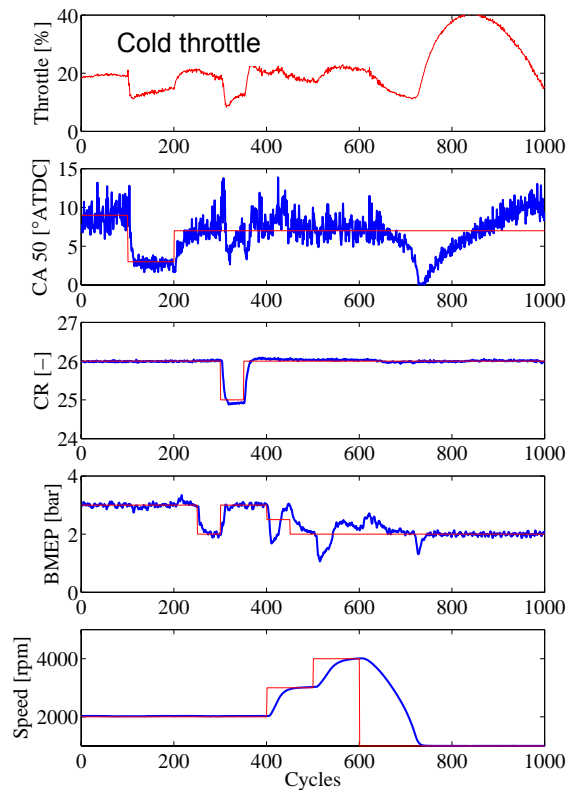


Figure 4-18 Step in CA50 and disturbance on CA50 using the CLCC_{FTM6/LQG} for one cylinder, Paper 8.

By adding spark plugs and ignition coils to the engine it is possible to do mode transfer. In Paper 9, manual mode transfers are made with the two-throttle system and the transfer area between HCCI and SI is investigated. No mode transfers are shown in the literature for inlet air preheated high compression ratio HCCI before.

Some initial tests to do controlled mode transfer are shown in Figure 4-19, where λ control is added to the control program while CLCC_{FTM6/LQG} is applied during HCCI combustion. The λ control is applied, for simplicity, by controlling an additional throttle to decrease inlet pressure. The injected fuel amount controls load independent of λ , i.e. a PID based control loop use the BMEP error and sets injected fuel amount. A map for one load and speed point is derived by trial and error iteration and empirical knowledge. In this case the map is made for 3 bar BMEP and 1500 rpm, but similar performance is achieved at 2000 rpm in Figure 4-19 as for tests at 1500 rpm.

The CLCC_{FTM6/LQG} is applied from the start and until engine cycle 47 where the cold throttles are fully opened to avoid any inlet air heating and hence knock. λ and CR are decreased almost simultaneously from 2.5 and 26 respectively to 1.2 and 10 respectively. However the λ control is very poor due to a somewhat slow update frequency of the λ measurement from the ETAS λ meter and the fact that the cold throttles are switched from fully closed to fully opened. This probably induce some pressure wave in the inlet responsible for the increase in measured λ around engine cycle 55. The drop in BMEP can as Koopmans et al. [59] suggests, be like a cold

start for the SI operation, with the very cold cylinder wall temperature from HCCI operation compared to normal SI conditions, which results in some partial burn and perhaps even misfires. This is indicated in the load plot in Figure 4-19, where FuelMEP [70], represented by the upper lines, is shown to increase to compensate for the decrease in BMEP, represented by the lower thick line. Koopmans et al. [59] do not use any transition algorithm, while Fuerhapter et al. [31] show large improvement in the transitions between different modes, Figure 3-5, with their transition algorithm in Figure 3-4.

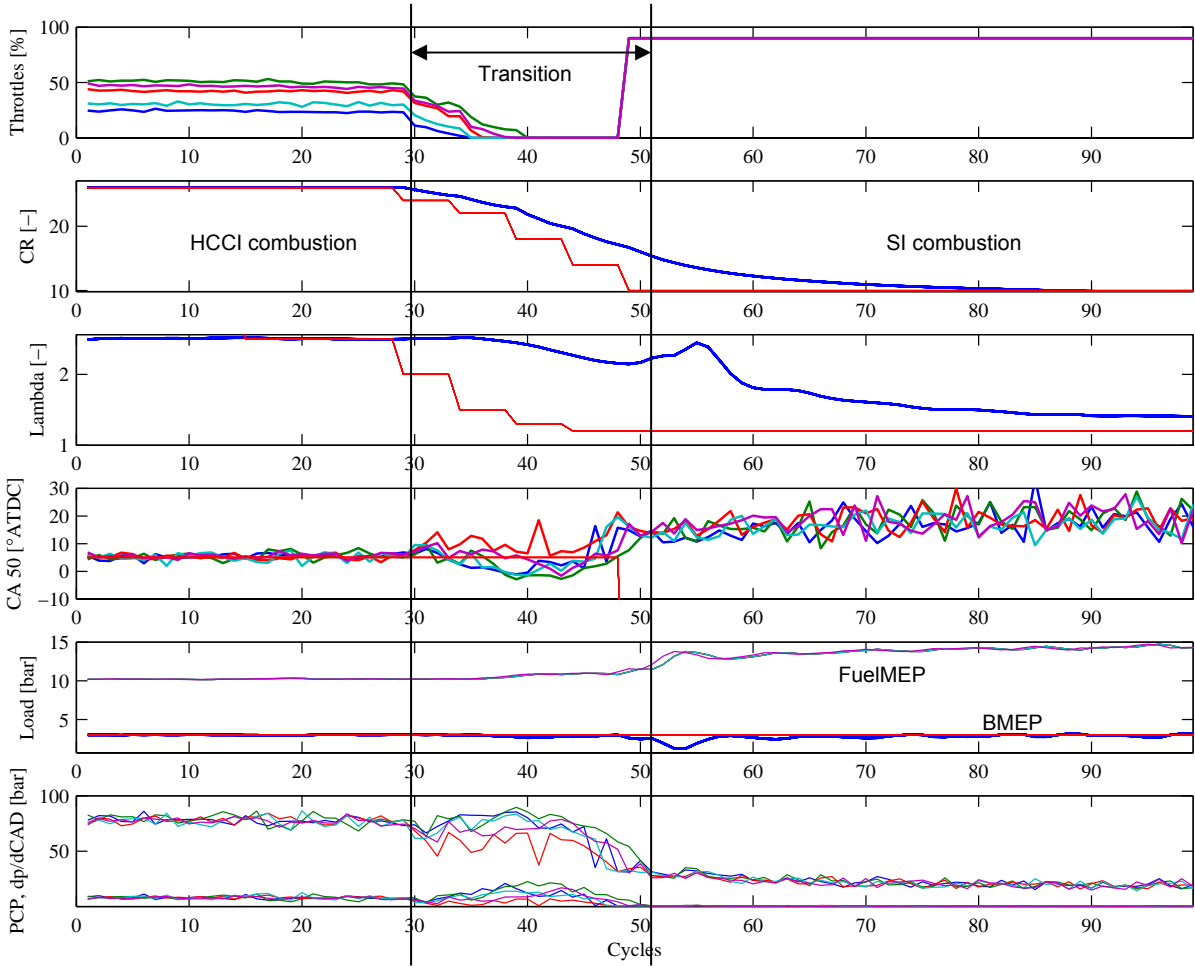


Figure 4-19 Mode transfer from HCCI to SI using CLCC_{FTM6/LQG} and a transition map at 2000rpm and 3 bar BMEP.

When looking at the CA50 variations for the SI combustion it is clear that the current engine configuration with the FTM₆ throttle and inlet manifold system is far from optimal for SI operation. Due to the unfavorable volume to area ratio for this particular engine, a goal to improve HCCI performance has been to decrease all turbulence by, e.g. removing squish areas in the combustion chamber when replacing pistons for higher CR.

The lower turbulence levels results in lower lean limit of this engine in terms of λ . With an engine with larger volume to area ratio it is believed that necessary turbulence levels for SI can be retained without excessive heat losses for optimal HCCI performance. The turbulence level is also affected by the FTM₆ inlet manifold, which is designed to be able to mix hot and cold air cylinder-individually whereas no

design effort has been put into the flow field or turbulence. In Paper 9 where the engine is operated both in SI and HCCI the FTM₂ inlet manifold system is used and the turbulence level is increased by putting a plug in one inlet port per cylinder.

A mode transfer can be done, but needs a fully functional transition algorithm, which is believed to consist of maps and some models of wall temperature and exhaust gas temperature to get an acceptable transition between the two operating modes. The wall temperature affects the HCCI combustion directly, while the exhaust gas temperature affects the available inlet air temperature. An acceptable transition from the driver's point of view is when no deviations in load or noise occurs, but for the environment the emissions need to be kept at a low level during the transition as well.

Instead of trying to improve the SI performance with the FTM₆ system, focus is set to evaluate the CLCC and especially the CLCC_{FTM6/LQG} during a drive cycle, Paper 10. Two main approaches to cover the EC2000 [71] drive cycle are experimentally tested. The first approach is to cover the entire drive cycle in HCCI mode. This requires scaling of the engine size to 3.0L. Load is calculated for a 3.0L engine, with all other variables held constant, e.g. car size and weight. The same scaling factor is used for fuel flow, which also affects the emissions.

Acceptable performance requires that the engine manages to keep load and speed according to the drive cycle and hence accelerate and decelerate properly. This is not shown here but it is shown in Paper 10. Note that no cold start is made and the engine is run hot before starting the drive cycle tests. The scaling approach could be questioned, but the main issue here is the state feedback controller performance. With the scaling of the engine the load range is from -1.1 bar BMEP at deceleration to 4.1 bar BMEP as maximum load needed within the test cycle for the Opel Astra used.

The scaling approach is shown in Figure 4-20, where the mean steady state maximum and minimum load curves as functions of speed are represented by thick lines and the calculated load and speed needed to keep a desired vehicle speed according to the EC2000 drive cycle is represented by circles. The maximum load is chosen as this engine's approximate maximum load in steady state tests, naturally aspirated, without having too high maximum rate of pressure rise or producing higher NO_x emissions than 15 ppm. This happens to coincide with an engine size of 3.0L and hence the reason to scale the engine to this size i.e. drive cycle scaled for a 3.0L engine.

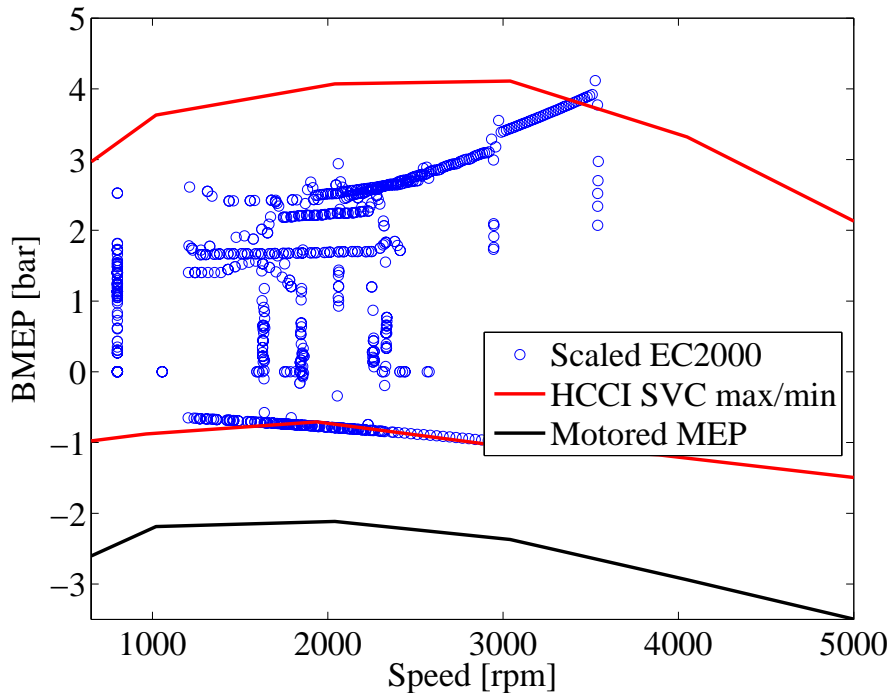


Figure 4-20 Scaled engine to 3.0L for HCCI operation during the entire EC2000 drive cycle with speed and load points where each point represents 0.5s in time together with the maximum, minimum and motored load curve, Paper 10.

The second and more realistic approach consists of a mix of experimental transient HCCI operation as long as the load is below 3.0 bar BMEP and steady state SI operation above, i.e. no scaling is made here and no actual mode transfer. The load and engine speed for this approach is shown in Figure 4-21, where the grey represents the SI operating region, the circles represent the drive cycle load as a function of speed and the thick curve represents the mean steady state HCCI maximum and minimum load as a function of speed.

The EC2000 drive cycle- load and engine speed points are calculated for an Opel Astra 1.6 in a Lotus vehicle simulation software, represented by circles. Each circle is separated by 0.5s and hence the density of the circles is proportional to the time spent at that specific load and speed. The maximum, minimum and motored load curves are derived from mean steady state data, and it is not obvious that the maximum points can be reached during a transient. However for the 1.6L a choice of a 3 bar limit is used during the drive cycle test even though a lot of points would be covered by HCCI mode if increasing the load limit some tenths of bars in Figure 4-21. The minimum load curve coincide with the drive cycle load in Figure 4-20, but for the 1.6L in Figure 4-21 a lot of drive cycle points are below the minimum load curve. This will limit the drivability since there is a deviation between the motored and minimum load curve and other measures should be applied to overcome this deviation.

No actual mode transfer to SI operation is made in the drive cycle test, but all HCCI and SI data is experimental and the simulated results for SI operation is interpolated from mean steady state data from the same engine in the same test cell taken before it was rebuilt for HCCI operation. It should be noted though that the HCCI part of the 1.6L test is from an actual drive cycle test as well as the entire 3.0L HCCI test.

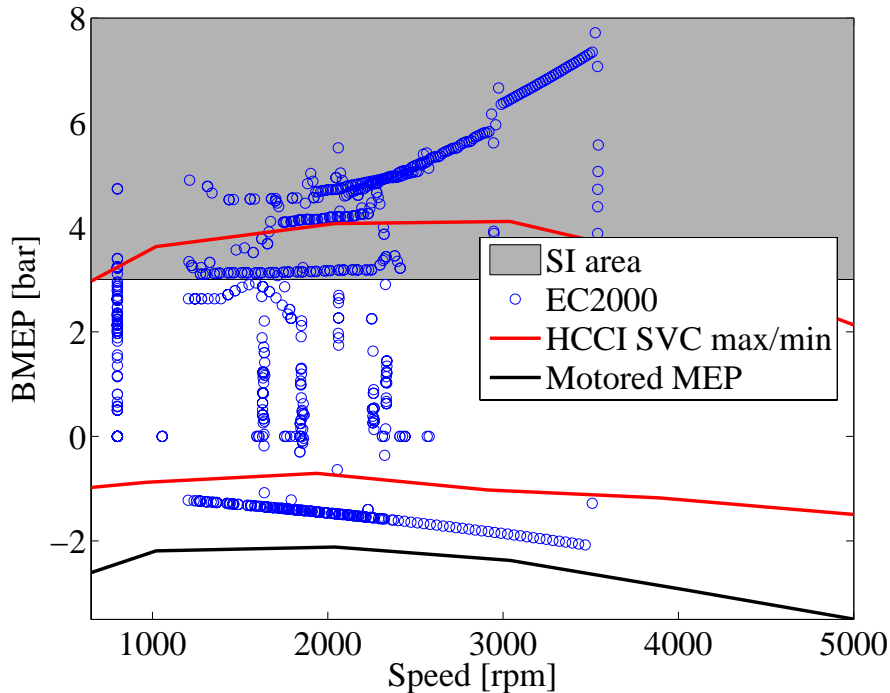


Figure 4-21 Speed and load points during the 1.6L EC2000 drive cycle where each point represents 0.5s in time with two combustion modes together with the maximum, minimum and motored HCCI load curve for the SVC engine, Paper 10.

When using the FTM at low engine speeds the control authority is significantly lower than at higher engine speeds. To improve performance during the drive cycle test the $CLCC_{CR/PID}$ is used below 1500 rpm while the FTM_6 system is used to do slow cylinder balancing. At speeds above 1500 rpm the $CLCC_{FTM_6/LQG}$ is used and a large difference in control authority for the throttles is shown in Figure 4-22, where the deviations between the different cylinders increase at low engine speeds. The grey area in Figure 4-22 represents the time spent in SI and the white represents the time spent in HCCI. 81% of the total time is spent in HCCI, where 51% of the fuel is consumed and 45% of the total work is produced.

When investigating the total number of misfires according to the control program [17] (defined here as CA50 larger than 20 CAD ATDC) and comparing those to the number of misfires for loads above 0 bar BMEP. The number of misfires above zero load is 407 for the 1.6L HCCI-SI, which is only 11% of the total number of misfires and 0.5% of the total elapsed engine cycles during the drive cycle. Even 0.5% misfires is of course unacceptable, though.

There are mainly three reasons for retarded combustion phasing or misfire:

1. Low load below the minimum load curve in Figure 4-20 and Figure 4-21.
2. Oscillations on the throttles when slow cylinder balancing is applied by the cold throttles.
3. Speed and load increase.

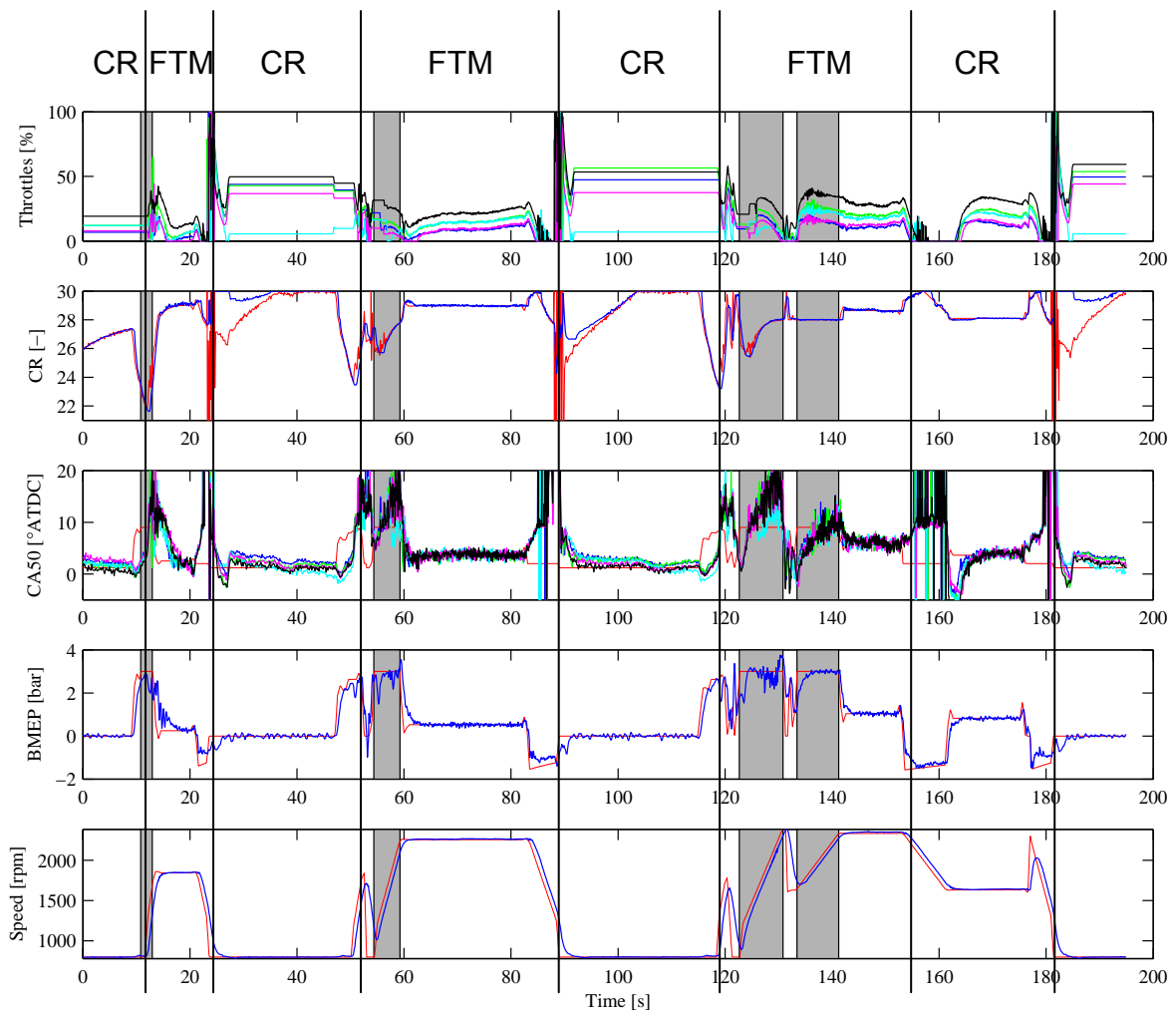


Figure 4-22 Actuator positions and feedback signals for all five cylinders together with load and speed where the approximate usage of CLCC controller is marked by vertical lines for the first 200s of the HCCI-SI 1.6 drive cycle test and the SI areas are marked grey.

The first kind occurs when the speed is decreased and negative load is applied and the $CLCC_{FTM6/LQG}$ tries to compensate this, which will result in some smaller oscillations on the throttles, but only with an amplitude of 5 to 10% opening. These are “desired” misfires, since lower load than the minimum load is desired. No fuel cut-off is applied due to a somewhat coarse load controller and hence every actual misfire results in some minor increase in fuel consumption and HC emissions. Fuel cut-off should be applied at least below the minimum load curve defined in Figure 4-20 and Figure 4-21. It can however be difficult to implement this due to the deviation between minimum load and motored load.

The second kind of retarded CA50 or misfires occurs when the $CLCC_{CR/PID}$ takes care of CA50 control and the $CLCC_{FTM6/LQG}$ is turned off. Then the throttles only perform slow cylinder balancing. At this time the throttles start to oscillate between 0 and 100% opening, which results in some disturbance to the $CLCC_{CR/PID}$ and on CA50. The phenomenon of the oscillating cylinder balancing throttles are unfortunately due to a minor bug in the control program, which creates these heavy oscillations every time the simple throttle cylinder balancing is applied, i.e. every time the $CLCC_{CR/PID}$ is turned on. It should be noted that the cylinder balancing does work as intended after 2s or approximately 20 engine cycles. One typical example is shown at the first vertical line to the left in Figure 4-22, where $CLCC_{CR/PID}$ is turned on

and the oscillations on the throttles cause the CR_{ref} to drop down to 20:1. However the PID based cascade coupled CR controller does not change CR as fast as the $CLCC_{CR/PID}$ changes CR_{ref} and hence it does not automatically result in misfires.

The third reason for retarded CA50 or misfires is speed and load increase, which results in retarded $CA50_{ref}$ and with the limited performance of the $CLCC_{FTM6/LQG}$ at retarded CA50s this results in some overshoot and in worst case some misfires. The reason for the slow control at retarded CA50s is that there actually are 2 state feedback controllers for each cylinder. One is used when the mean of CA50 and $CA50_{ref}$ is later than 9 CAD ATDC and the other when it is earlier than 5 CAD ATDC. Between 5 and 9 the controller outputs are weighted together linearly. This solution is chosen since it was difficult to identify the system at retarded CA50s and hence no acceptable model was found for retarded CA50s. However, there are no misfires above 2500 rpm, which indicates that the controller manages CA50 control without any additional misfires when not disturbed by too low load or oscillating throttles as described above.

There are some very advanced combustion phasings in Figure 4-22 at low load. This is the result of the high CR used and the apparent heat release, which is utilized in the control program. Since heat losses are not taken into account, the control program finds an excessively advanced CA50 that is not correct.

In Figure 4-23 a Simulink simulation of CA50, upper plot, is made with a square wave applied on $CA50_{ref}$. Corresponding control output, i.e. inlet air temperature, is shown in the lower plot. The simulation model based on an identified black box engine model is designed by Pfeiffer [67]. In Figure 4-24 an unstable system is shown.

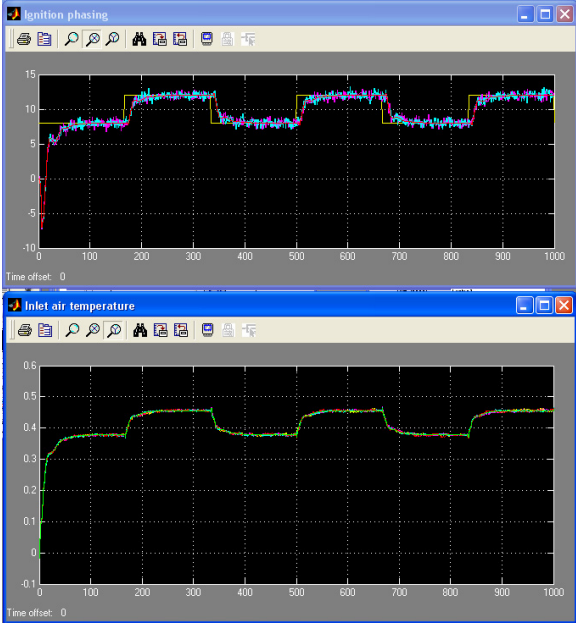


Figure 4-23 Simulink simulation using identified merged engine model and designed LQG controller.

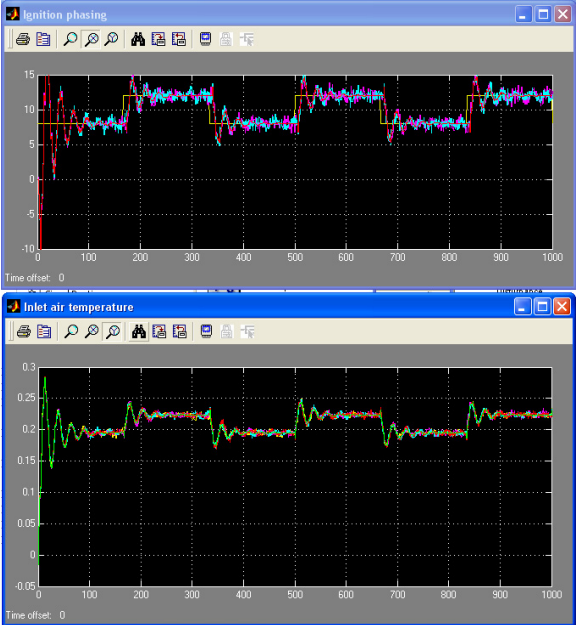


Figure 4-24 Simulink simulation using an engine model from four points with retarded CA50s, but with the same LQG controller as before.

It is the same LQG controller in both plots, but the engine model used in the simulation in Simulink is not. For Figure 4-23 a merged engine model of all test points is used, which is the same engine model from which the controller is designed. When using the LQG controller on an engine model identified from retarded CA50s it becomes unstable as shown in Figure 4-24 exactly as when running it on the engine. The solution to this problem is discussed additionally in paragraph 4.6. It should however be noted that the engine model based on retarded CA50s only consist of four operating points compared to 15 for the used model, which in general makes the controller more precise and aggressive.

By doing a drive cycle simulation with mean steady state data for both HCCI and SI the improvement potential in terms of fuel economy and emissions can be estimated. It is also of interest, which improvement the transient HCCI show compared to the same engine in SI based on mean steady state SI data. It should be noted though, that the SI SVC is optimized for high loads resulting in low fuel consumption by engine downsizing.

In Figure 4-25 to Figure 4-30 the emissions are given in g/km both engine out, Figure 4-25 to Figure 4-27 and after the catalyst, Figure 4-28 to Figure 4-30. The contributions of the two operating modes are shown as different parts of the total bars. Those bars labeled with only SI represent simulated SI from mean steady state SI data, while the 3.0L HCCI consists of transient HCCI during an actual drive cycle test and the one labeled HCCIs consists of mean steady state data for HCCI. The one labeled 1.6L HCCI consists of both HCCI data during an actual entire truncated drive cycle together with mean steady state SI data.

The highest engine out emissions of HC and CO are obtained for the scaled 3.0L engine, shown in the left part of these figures. This is due to the scaling, which results in very low load and combustion temperature during the major part of the drive cycle, resulting in low combustion efficiency.

The lowest HC emissions are achieved for the 1.6L SI. There are two major effects which counteract each other. For the 1.6L engine the higher mean load results in more HC into the crevices, which would result in higher HC emissions for the 1.6L SI, but the scaling effect for the 3.0L engine is more dominating and hence higher HC emissions for the 3.0L engine. The HCCIs with its "ideal" HCCI shows slightly less HC emissions than the transient 3.0L HCCI and this can be explained by some actual misfires during transients, which are not present in the steady state HCCI data.

The CO engine out emissions in Figure 4-26 show very much the same trends as the HC emissions in Figure 4-25. Here on the other hand there is a larger difference between transient 3.0L HCCI and HCCIs. With ideal HCCI there is no need to have a lot of control authority of the $CLCC_{FTM6/LQG}$, i.e. increased bandwidth by adjusting CR. This results in a lower CR used in the ideal HCCI case, which results in lower CO emissions shown in Paper 2. Even though the CO emissions of the SI SVC engine are relatively high, they are small when compared to the HCCI SVC engine. It should be noted though that the maximum CR is increased from 14 for the SI SVC to 30 for the HCCI SVC engine.

Almost all NO_x derive, as expected, from the very much hotter combustion process of the SI SVC engine. Figure 4-27 shows that it is very advantageous to run in HCCI operation as much as possible if low NO_x emissions are desirable. Note that during the transient 1.6L HCCI test the engine operates with SI combustion during 19% of the time, but the SI combustion produces 99% of the total NO_x .

A standard three-way catalyst from a Saab 9-5 3.0 V6 is used during the drive cycle test, but no emissions are measured after catalyst, since it would require dual emission systems to be used or running the drive cycle twice, which would be a repeatability issue. Instead HC and CO is calculated from the engine out emissions with a conversion efficiency of approximately 95% for HC and 99% for CO as a function of engine speed, Paper 5. The NO_x emissions are engine out emissions, i.e. no reduction of NO_x for HCCI, but for SI a conversion efficiency of 99% is used. Differences in conversion efficiency during mode transfer are not accounted for.

In Figure 4-28 the Euro IV gasoline limit of HC is plotted on top of the bars. The transient 1.6L HCCI is 3.8% above the limit while the 3.0L SI is 13% below the limit. It should be noted though, that no cold start is made here and almost all HC during a drive cycle derive from the cold start until the catalyst has light-off [72].

The CO emissions in Figure 4-29 are all well below the limit of 1.0 g/km. The same holds for the NO_x emissions in Figure 4-30, which are below the limit of 0.08 g/km. However there is quite a big improvement potential from transient 3.0L HCCI to the HCCIs. The difference between ideal HCCI and the transient HCCI is that there are no advanced combustion phasings as shown in Figure 4-22 for the HCCIs. It might seem strange that the NO_x emissions are higher for the 3.0L SI simulation than for the 1.6L SI simulation. This is explained by the fact that lower load for the scaled 3.0L engine does not produce that much lower NO_x emissions compared to the higher NO_x levels at higher load for the 1.6L SI.

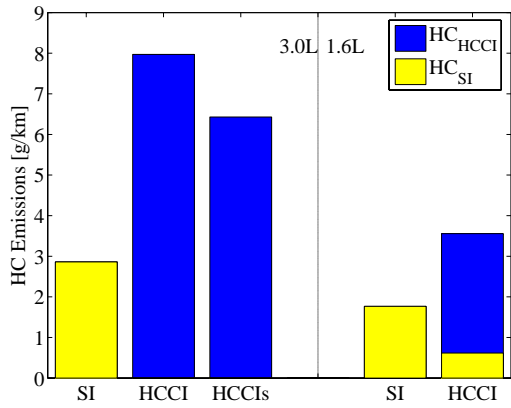


Figure 4-25 Engine out HC emissions for five test cases.

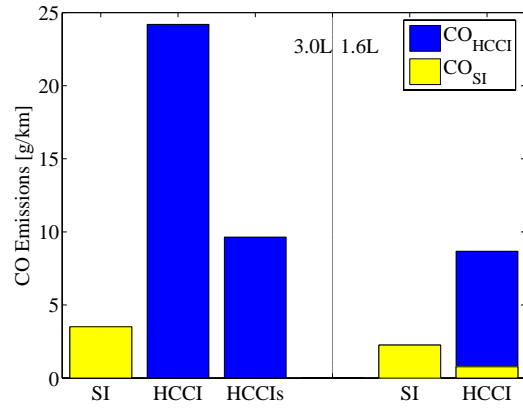


Figure 4-26 Engine out CO emissions for five test cases.

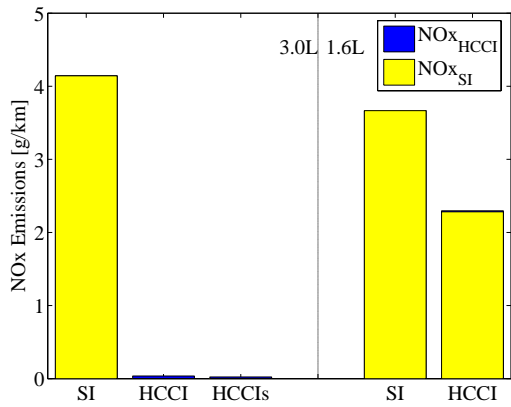


Figure 4-27 Engine out NO_x emissions for five test cases.

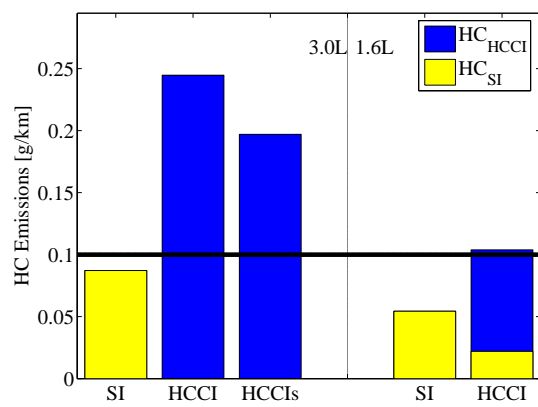


Figure 4-28 HC emissions after catalyst for five test cases.

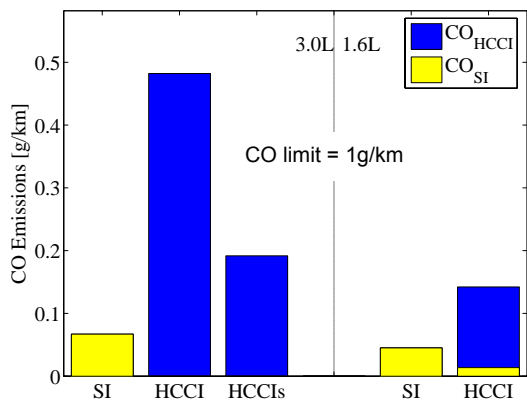


Figure 4-29 CO emissions after catalyst for five test cases.

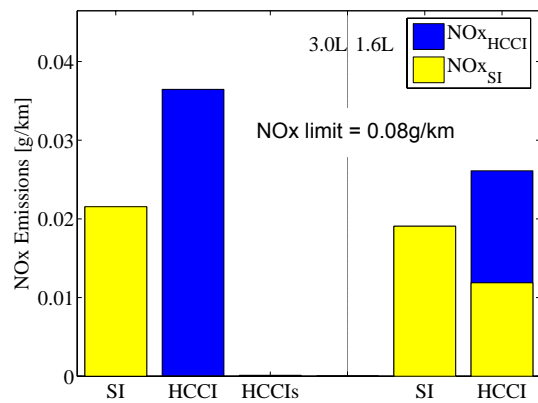


Figure 4-30 NO_x emissions after catalyst for five test cases.

In Figure 4-31, a fuel consumption of 11.7L/100km is shown for the scaled SI simulation, while a fuel consumption of 9.8L/100km is achieved for the transient scaled 3.0L and 9.2L/100km for the simulated HCCIs. The gain in running in HCCI mode the entire drive cycle, i.e. scale to 3.0L, is 16% compared to the 3.0L SI simulation. The gain by having a perfect CLCC controller for this engine is quantified by the difference between the 3.0L transient HCCI and the simulated HCCIs, which is merely 6%.

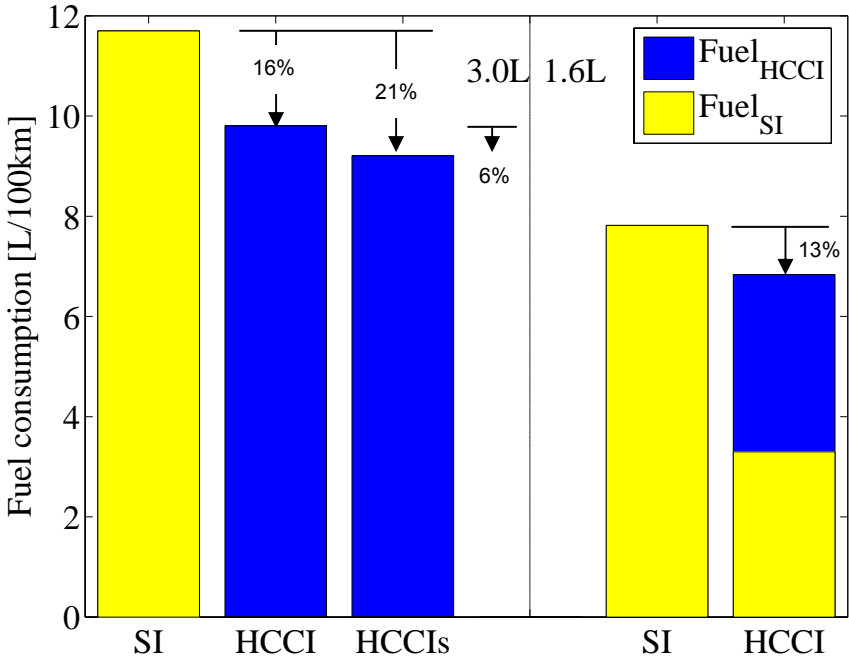


Figure 4-31 Fuel consumption given in L/100km for both the scaled 3.0L engine and the 1.6L.

For the simulated 1.6L SI simulation taken from mean steady state SI data a fuel consumption of 7.8L/100km is accomplished, which can be compared to the 6.8L/100km when running in combined transient HCCI and simulated SI operation. The gain with combined HCCI-SI is 13% compared to the 1.6L SI simulation.

The possible Brake Specific Fuel Consumption (BSFC) or fuel consumption gain with the current 1.6L HCCI engine compared to the same engine in SI mode is shown in Figure 4-32. This can be compared to the BSFC gain by Zhao et al. [22] in Figure 4-33 or the gain achieved by Fuerhapter et al. [31] in Figure 4-34.

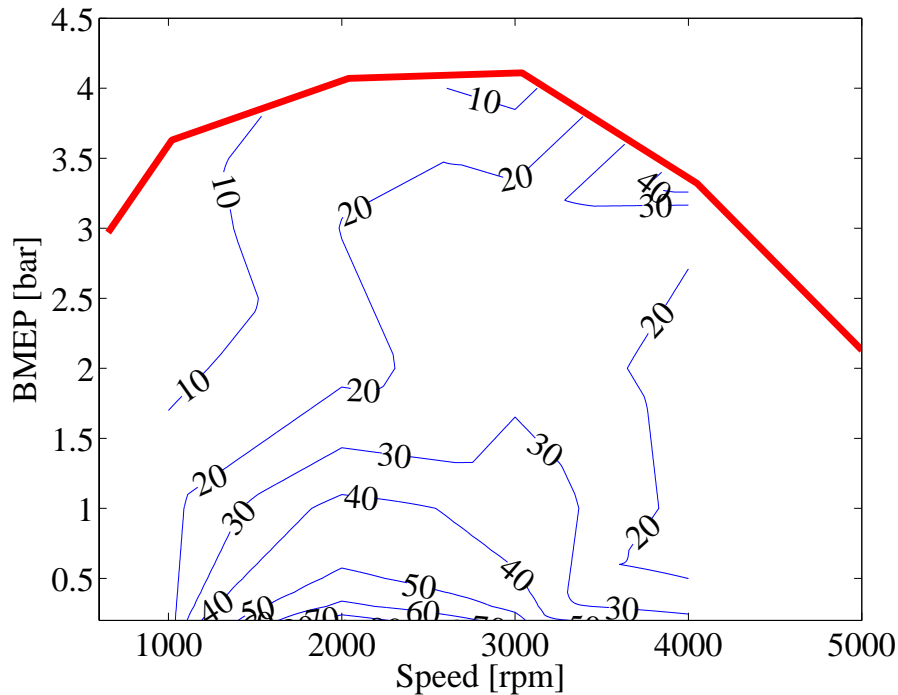


Figure 4-32 Ideal fuel or BSFC gain in percent for inlet air preheated HCCI compared to SI on the SVC engine.

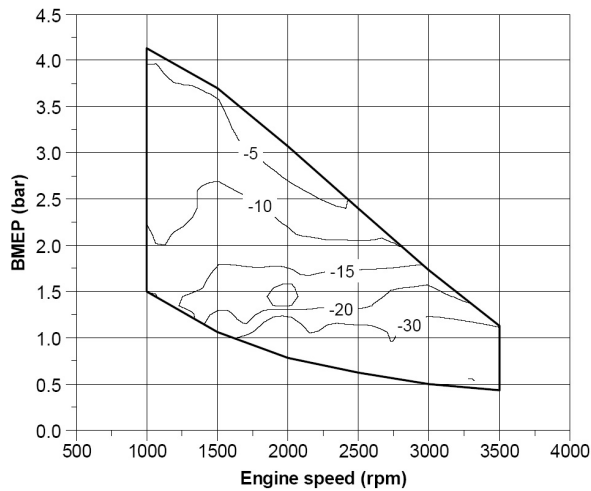


Figure 4-33 BSFC gain by running in residual heated HCCI compared to SI [22]

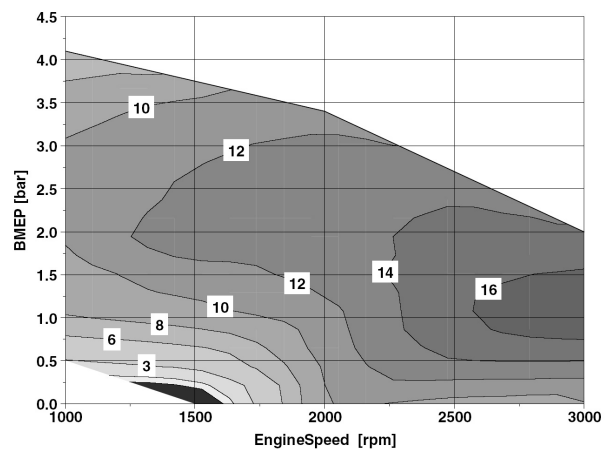


Figure 4-34 Fuel consumption gain by running in residual heated HCCI compared to SI [31]

It is clear that inlet air preheated HCCI has a larger fuel reduction potential than the residual heated HCCI achieved by camshaft throttling or rebreathing. Note the much larger operating range in terms of engine speed for the SVC engine. The limit at 4000 rpm for the fuel consumption gain in Figure 4-32 is due to the lack of data for 5000 rpm from the SI reference tests and not a limit in HCCI operation. During a simulated drive cycle Zhao et al. [16] achieved a total gain of 4.7% compared to SI operation, while Fuerhapter et al. [32] show a total gain of 12.8% during an actual hot drive cycle test.

It is shown in the fuel consumption figures in Figure 4-31, that the approach to cover the entire drive cycle by scaling the engine to 3.0L is not a good idea with this engine. By scaling the engine a lower BMEP is needed for the same torque, which results in higher BSFC for the same torque. In other words, by scaling, the drive cycle point is moved towards lower BMEP, where BSFC is higher. The BSFC for mean steady state HCCI data are shown for the scaled 3.0L engine in Figure 4-35, while mean steady state SI and HCCI data are combined for the standard 1.6L HCCI-SI in Figure 4-36.

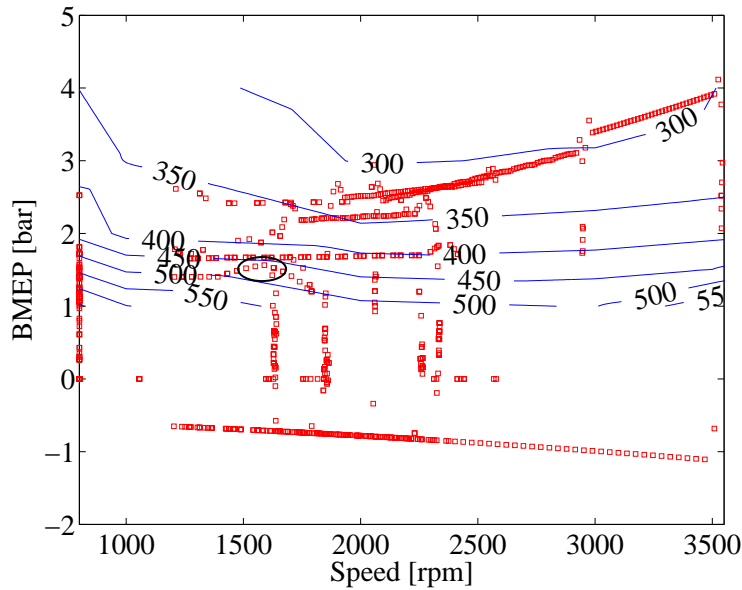


Figure 4-35 BSFC for the ideal HCCI scaled to 3.0L engine together with load points for the drive cycle, Paper 10.

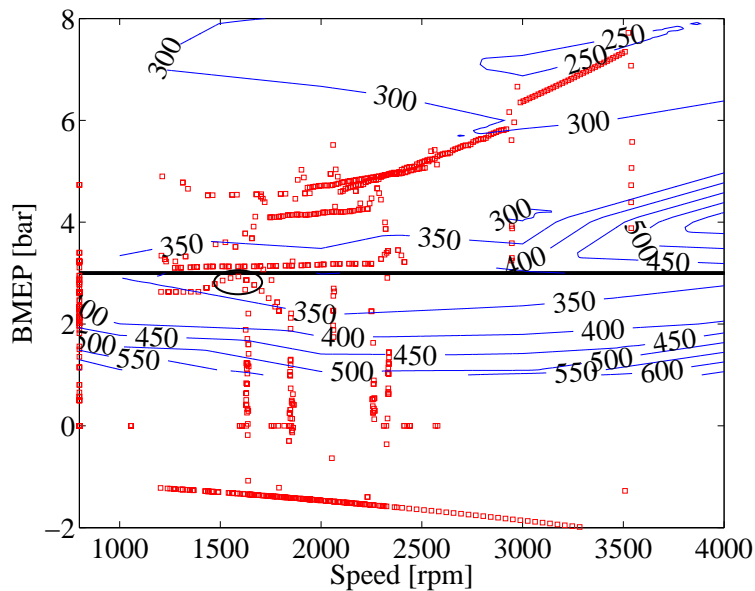


Figure 4-36 BSFC for the simulated HCCI-SI as a function of load and speed together with load points for the drive cycle and a 3 bar BMEP limit between HCCI and SI.

Below 1 bar BMEP BSFC increases to infinity at 0 bar BMEP, and hence is not plotted below 1 bar BMEP. Each square represents one point in the drive cycle map with a time of 0.5s between. This means that the density of the squares is proportional to the time spent at that specific load and speed and hence BSFC. If comparing BSFC for the same drive cycle speed and load points marked with small ellipses in Figure 4-35 and Figure 4-36, it is clear that there is an approximate difference of at least 100g/kWh between the two. In Figure 4-36 the mean load is higher, which results in the lower fuel consumption figures for the transient 1.6L HCCI.

A drawback of the SVC engine is the high Friction Mean Effective Pressure (FMEP) of this engine, shown in Figure 4-37, which severely penalizes the fuel economy when running the urban parts of the drive cycle where BMEP is very low. As a comparison, FMEP for a 6L Audi W12 is shown in Figure 4-38 together with a scatter band of FMEPs for other engines in gray. The difference between these two engines is significant and one reason for the very high FMEP of the SVC engine is the friction between the piston rings and the cylinder liner, which is high due to the design for very high IMEPs of the downsized highly supercharged SI SVC prototype.

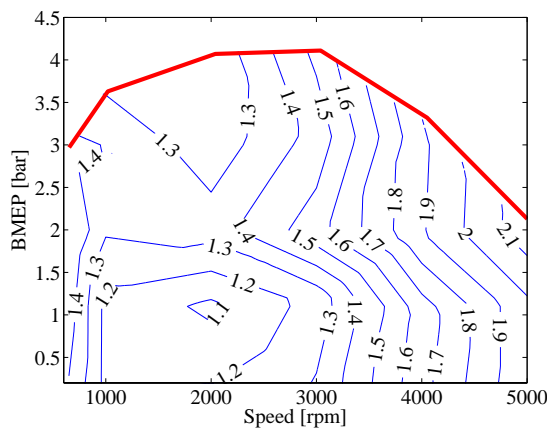


Figure 4-37 Iso-lines of FMEP in bar for the HCCI SVC engine as a function of load and speed.

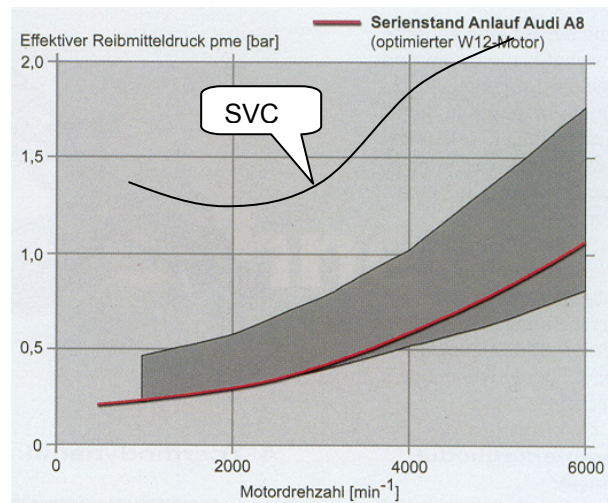


Figure 4-38 FMEP as a function of speed for an Audi W12 engine [73].

By simulating a drive cycle with the same conditions as the “ideal” 3.0L HCIs and use the FMEP in Figure 4-38, i.e. keep BMEP constant and decrease the needed $IMEP_{net}$ a fuel consumption of 7.8L/100km is achieved, which can be compared to the 9.2L/100km for the HCIs. This is a 15% improvement for the HCIs FMEP compared to the same “ideal” HCIs shown in Figure 4-39.

If anticipating the same improvement potential with a low friction engine for the 1.6L test a fair guess would be a fuel consumption of 5.8L/100km. The possible BSFC gain, in percent, for the HCCI SVC 1.6L engine using the low FMEP in Figure 4-38 compared to the standard 1.6L SI SVC is shown in Figure 4-40 together with the improved maximum load curve.

Not that in this comparison it is only the HCCI SVC that has low FMEP and not the SI SVC i.e. the gain is both due to low FMEP and HCCI operation. This gain can be compared to the possible BSFC gain in Figure 4-32, which is much lower. The limit at

4000 rpm for the fuel consumption gain in Figure 4-40 is due to the lack of data for 5000 rpm from the SI reference tests and not a limit in HCCI operation.

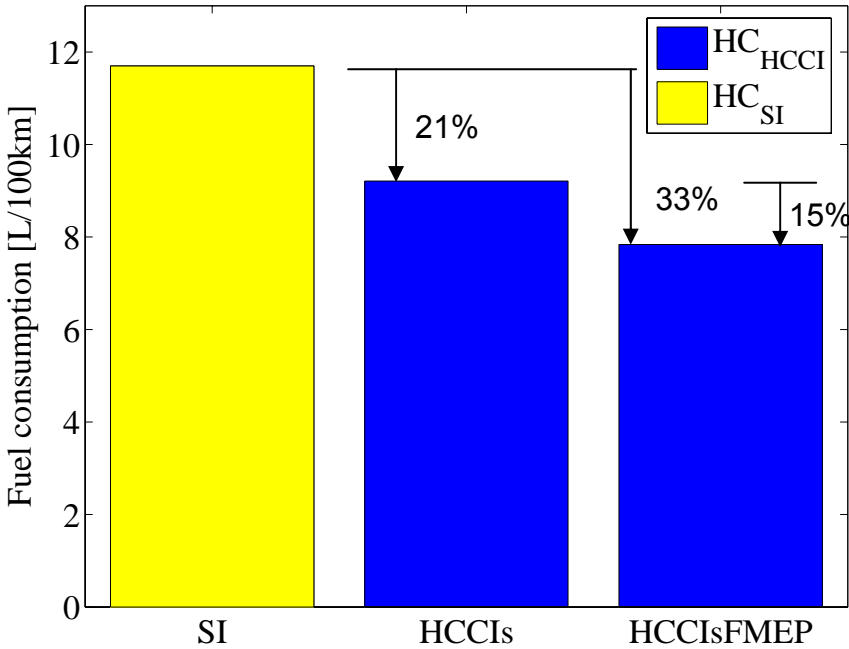


Figure 4-39 Drive cycle fuel consumption for the scaled 3.0L engine for SI, “ideal” HCCI and “ideal” HCCI with low FMEP using mean steady state data.

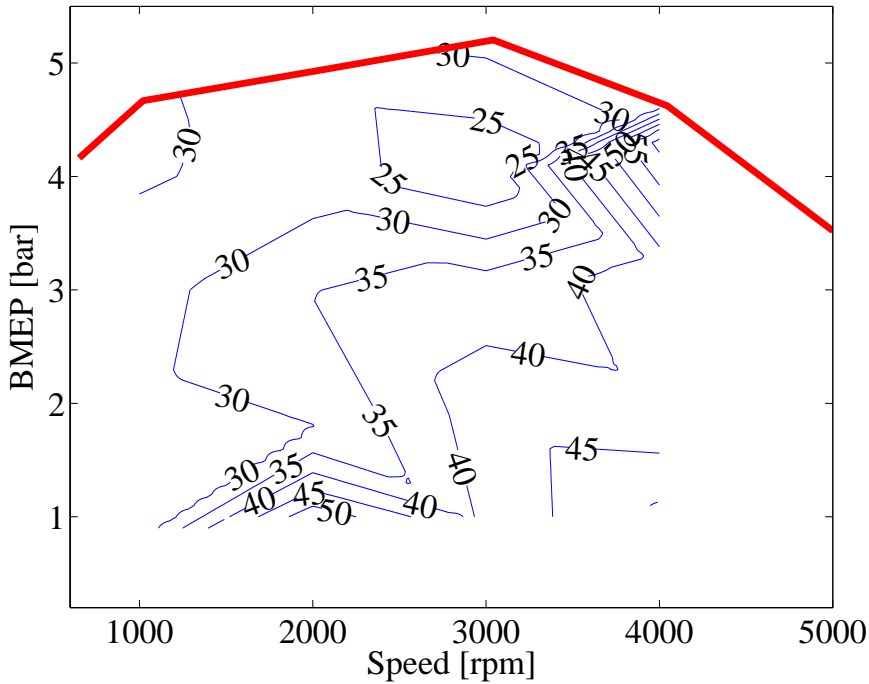


Figure 4-40 Maximum load curve together with the possible BSFC gain with a low friction HCCI engine compared to the standard SI SVC 1.6L engine.

With the low FMEP a much larger part of the drive cycle points will be covered in HCCI as shown in Figure 4-41, but a lower FMEP also result in a somewhat higher minimum load where some points are below this limit. When splitting the drive cycle in the urban part and the highway part it can be seen that almost the entire urban part is covered by the low FMEP 1.6L HCCI engine, while most of the highway part needs to be run in SI mode. There is a gained area between the maximum load curves and a lost area between the minimum load curves and the gained number of points is clearly larger than the lost.

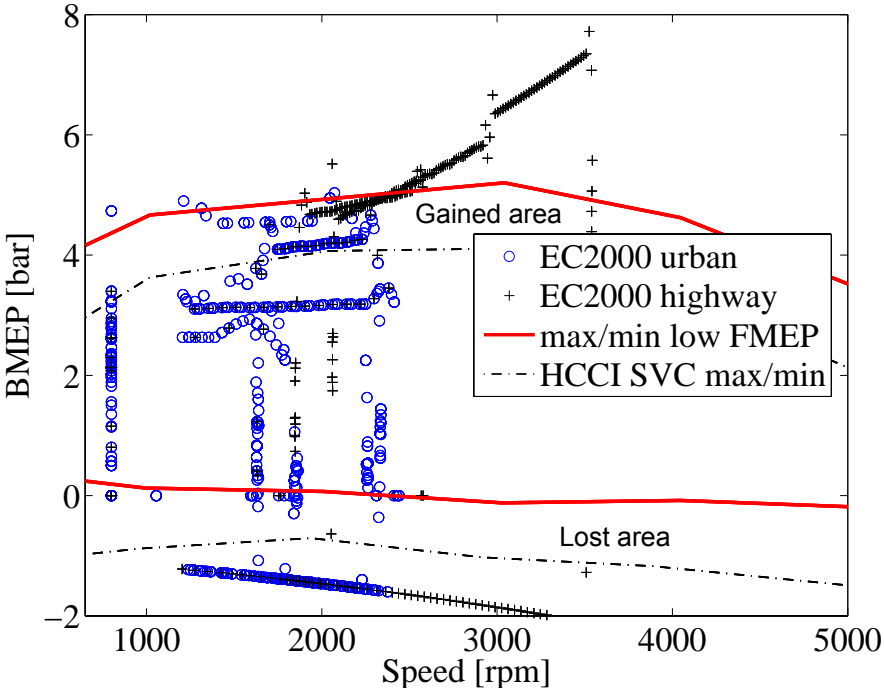


Figure 4-41 Improved load range with a low FMEP HCCI SVC 1.6L engine compared to the standard HCCI SVC load range together with drive cycle load and speed points divided into urban part and highway part.

4.6 Discussion

Tests with the state feedback based LQG controller show a stable and efficient controller at all engine speeds. The drawback still to be solved is the lack of a fast and stable controller at retarded CA50s. Bengtsson [49] do not have these problems and it could be due to the difference in speed range between the SVC and the 12L Volvo Truck engine. Shaver et al. [56,57,58] and Souder et al. [51] run at a constant speed of 1800 rpm. At speeds below 2000 rpm it is easier to run the SVC in open loop, which results in more favorable conditions to identify a suitable engine model. The drawback below 2000 rpm though, is the lack of control authority of the throttles or inlet air temperature. A solution to the problem of control authority could be to use throttles optimized for the air flow in terms of throttle area, optimize the inlet manifold in terms of heat losses, flow profile and pulsations and minimize cylinder-to-cylinder variations in the combustion chamber to increase the bandwidth of the throttle control.

When control authority is increased it should be possible to identify the entire load and speed range of the engine and merge all data to one engine model. If the merged model does not correlate well with all the different test cases, two different controllers can be implemented as long as each model is good. The problem with the current controller for retarded CA50s is that it is based on the same model as the one used for advanced CA50s, but with a punishment on the actuator of 10 times that of the advanced controller to make it more conservative and thus stable.

Another difference between the other LQG CLCC controllers used in the literature [48,56,57,58] is that they have cycle-to-cycle control, while there is a time delay of approximately four engine cycles here. This could be decreased by fitting the throttles closer to the inlet ports and hence minimize the volume between inlet port and throttles. By having the throttle closer to the ports there is less air mass that is affected by the opposite air temperature due to backflow. This is not a problem as long as there is a reasonable flow through both hot and cold ports, but when the flow is low on the hot side cold air can mix up in the pipe and when flow is low on the cold side the air mass there is heated up by the piping due to heat transfer from the hot air mass. With the current throttles it could be a problem on the hot side to fit the throttle closer to the inlet port, since that throttle is placed up-stream from the heat exchanger to avoid the hot inlet air downstream the heat exchanger. However since it is only hot air of 200-300°C it should be no problem to find suitable throttles for that purpose and with an engine with less heat losses this temperature could be decreased with maintained CR. The heat transfer from the hot air to the cold can be decreased significantly by splitting the inlet manifold into two parts and having some kind of insulating material in between.

It is possible that an engine with less heat losses and a machined combustion chamber would be possible to operate at significantly lower CR, which could allow HCCI operation without any need for very powerful cylinder balancing. The need to balance the cylinder-to-cylinder variations on this engine is very large due to the extreme CR used to compensate for high heat losses. With a high CR cylinder-to-cylinder variations in casting in the combustion chamber have larger negative effects on CA50 variations as shown in Paper 7.

With the above optimizations on the FTM system it should be possible to run the engine with the two-throttle FTM₂ system and do small cylinder balancing using variable λ or use direct injection to introduce some minor stratification [24,25] of the charge in order to balance CA50. Spark assistance discussed in Paper 9 is also a viable cylinder balancing device.

The scaling approach shows that it is possible to improve fuel consumption on a 3.0L engine by 16% compared to an SI of the same size. This shows that for the American market with rather large engines it would be very beneficial to apply HCCI operation at the lower loads, where those large engines operate most of the time. The other approach to simulate a mode transfer to SI is more applicable for the European market with its smaller engines operating at higher loads.

By simulating a drive cycle with significantly lower FMEP an improvement in fuel consumption of 15% is achieved for the 3.0L engine and with the same FMEP optimization on the 1.6L engine substantially higher load levels can be reached. Higher load results in a larger part of the drive cycle operable in HCCI mode with an increased gain in fuel consumption and NO_x emissions both due to less FMEP and the fact that HCCI is superior in terms of fuel consumption and NO_x emissions.

With the high maximum geometric CR cold start in HCCI is possible, at least from 20°C ambient temperature, but it is not the recommended starting method. This is due to the very low exhaust gas temperature for HCCI, which results in a very long time before the catalyst reaches light-off and the heat exchanger is heated. If load is increased as quickly as possible the heat up time can be decreased, but the drive cycle consists of a fairly long time of low load and speed to start with. The suggested solution is to start in SI mode for approximately 10 to 15s [74] until the catalyst has reached light-off and thereafter do a mode transfer to HCCI mode. However it is possible that an HC trap [75] needs to be used since the major part of all HC is produced during cold start. It is likely that even if the HCCI engine would cover the drive cycle in terms of load that would not be considered sufficient, since acceleration is rather modest in the drive cycle and the top speed is only 120km/h. In real world driving mode transfer between HCCI and SI needs to be done anyway.

With a good controller at retarded CA50s it should be possible to use the steady state optimized maps for CA50 and CR and the simulated improvement in fuel consumption of 21% for the “ideal” 3.0L HCCI engine compared to the 3.0L SI is possible. The same holds for the improvement potentials for the emissions and if using a more suitable engine with low FMEP an improvement of 33% in fuel consumption is possible compared to the 3.0L SI. With lower heat losses it will only get better. Since it would allow lower CR, which result in lower CO emissions and fuel consumption.

5 Conclusions

It is shown that both variable compression ratio and the two-throttle fast thermal management are efficient actuators for combustion control, but some additional actuator is needed with these systems to get cylinder individual combustion phasing control. The variable λ proves effective, but has the disadvantage of increasing engine global COV_{IMEP} . Step changes in CA50 show a time constant of 14 engine cycles for the PID based closed-loop combustion control using variable compression ratio, while the PID based closed-loop combustion control using fast thermal management has a time constant of 8 engine cycles.

The six-throttle fast thermal management system is a cylinder individual combustion phasing actuator, requiring no additional active cylinder balancing. This system is used both with PID and state feedback controllers with similar time constants as the two-throttle closed-loop combustion controller. Systematic control design is applied by identifying an engine model as a black box model and using that model to create a type of state feedback controller called an LQG controller. The large benefit compared to a standard PID controller is the systematic design where merely three design parameters are needed to cover the entire load and speed range, while a PID controller would need to be gain scheduled for the same performance and hence has a lot more design parameters. The LQG controller is designed as a multi input single output controller, where combustion phasing error, compression ratio, load and engine speed are inputs and throttle command is output. An integrator is added in parallel to enable integral action, since integral action is not inherent in an LQG controller. Feed forward action is also included.

Retarded combustion phasings proved to be a problem during the system identification due to difficulties to disturb the system at retarded combustion phasings without combustion deterioration. This in combination with very small effect of the actuators, throttles, at low engine speeds resulted in a combination of one good controller used for normal combustion phasings and one very slow controller at retarded combustion phasings. These two controllers overlap each other and for combustion phasing between 5 and 9 crank angle degrees the controller outputs are weighted together linearly.

To improve controller bandwidth at low engine speeds the PID based closed-loop combustion control using variable compression ratio is applied below 1500 rpm. To avoid using variable λ for cylinder balancing, the six throttle system is used for slow cylinder balancing. Above 1500 rpm the state feedback based closed-loop combustion control is applied and compression ratio is set according to a predefined map.

A drive cycle test is run using the combined closed-loop combustion control to evaluate the controllers and especially the LQG controller. It is found that in terms of fuel economy the controller is good, but there is room for improvement especially when looking at the emissions. A fuel consumption of 9.8L/100km for an engine scaled to 3.0L is achieved, which is an improvement of 16% compared to the scaled 3.0L SI engine. When no scaling is done the fuel consumption is down to 6.8L/100km, which is an improvement of 13% compared to an 1.6L SI engine. The 1.6L approach consists of a transient HCCI operation up to 3 bar BMEP and simulated SI from mean steady state data above.

By simulating the drive cycle with a better engine in terms of friction losses, an improvement of an additional 15% is achieved compared to the ideal 3.0L HCCI with a perfect controller and would have a fuel consumption of 7.8L/100km. If anticipating the same improvement potential with a low friction engine for the 1.6L test a fair estimate would be a fuel consumption of 5.8L/100km during the drive cycle.

6 Future work

The current state feedback controller for $CLCC_{FTM6/LQG}$ needs to be optimized for retarded combustion phasing by identifying a suitable engine model. This can probably be done by applying slow integral action with the $CLCC_{CR/PID}$ while identifying the engine model.

Incorporate load control and CR control into the state feedback controller or create separate LQG controllers for load and CR. It is believed that the CR controller would benefit if it would work on a time base instead of crank angles as the current control program do. However it is not trivial to implement a time based control loop in the current control program and it would require an additional A/D and D/A-converter.

The mode transfer needs to be systemized by designing transition maps that probably consist of some kind of model for cylinder wall temperature. To allow SI operation with a three-way catalyst a broad band λ sensor and a fully functional λ controller are needed.

A more production based control system will probably consist of separate microprocessors for CA50 calculation where it is only necessary to send a scalar value to the main control module. This can be emulated with the current DAP A/D-converter, which can be set up to e.g. send the entire pressure trace to the hard drive for post processing, while a heat release can be made onboard the DAP. This is possible since the DAP is equipped with a standard 486 PC processor that can be programmed to make calculations online and send data to the control programs buffer. With this strategy it would be possible to use a standard engine control module used for SI engines.

Another controller like model predictive control could also be evaluated and perhaps some adaptivity.

References

1. J. B. Heywood, "Internal Combustion Engine Fundamentals", McGraw-Hill, 1988
2. S: Onishi, S. Hong Jo, K. Shoda, P Do Jo, S. Kato: "Active Thermo-Atmosphere Combustion (ATAC) – A New Combustion Process for Internal Combustion Engines", SAE790501
3. Y. Ishibashi, M. Asai: "Improving the Exhaust Emissions of Two-Stroke Engines by Applying the Activated Radical Combustion", SAE960742
4. P. Najt, D.E. Foster: "Compression-Ignited Homogeneous Charge Combustion", SAE830264
5. R.H. Thring: "Homogeneous-Charge Compression-Ignition (HCCI) Engines", SAE892068
6. A. Envall, A. Albinsson, "Smokey's omöjliga motor: Hälften så stor dubbelt så bra!—Del II I storyn om Smokey Yunick", BilSport 1984
7. H. Yunick, "Apparatus and operating method for an internal combustion engine", United States Patent 4,862,859, September 1989
8. M. Stockinger, H. Schäpertöns, P. Kuhlmann, Versuche an einem gemischsaugenden mit Selbstzündung, MTZ 53 (1992).
9. M. Christensen, P. Einewall, B. Johansson: "Homogeneous Charge Compression Ignition (HCCI) Using Isooctane, Ethanol and Natural Gas – A Comparison to Spark Ignition Operation", SAE972874
10. M. Christensen, B. Johansson, P. Amnéus, F. Mauss: "Supercharged Homogeneous Charge Compression Ignition", SAE 980787
11. M. Christensen, B. Johansson: "Influence of Mixture Quality on Homogeneous Charge Compression Ignition", SAE982454
12. M. Christensen, B. Johansson: "Homogeneous Charge Compression Ignition with Water Injection", SAE1999-01-0182
13. M. Christensen, A. Hultqvist, B. Johansson, "Demonstrating the Multi Fuel Capability for a Homogeneous Charge Compression ignition Engine with Variable Compression Ratio", SAE 1999-01-3679
14. M. Christensen, B. Johansson, "The Effect of In-Cylinder Flow and Turbulence on HCCI Operation", SAE 2002-01-2864
15. J. Lavy, J-C. Dabadie, C. Angelberger, P. Duret, J. Willand, A. Juretzka, J. Schäflein, T. Ma, Y. Lendresse, A. Satre, C. Shulz, H. Krämer, H. Zhao, L. Damiano, "Innovative Ultra-low NOx Controlled Auto-Ignition Combustion Process for Gasoline Engines: the 4-SPACE Project", SAE 2000-01-1837
16. H. Zhao, J. Li, T. Ma, N. Ladommatos, Performance and Analysis of a 4-Stroke Multi-Cylinder Gasoline Engine with CAI Combustion", SAE-2002-01-0420
17. J-O. Olsson, P. Tunestål, B. Johansson, "Closed-Loop Control of an HCCI Engine", SAE 2001-01-1031
18. J-O. Olsson, P. Tunestål, B. Johansson, S. Fiveland, R. Agama, M. Willi, D. Assanis, "Compression Ratio Influence on Maximum Load of a Natural Gas Fueled HCCI Engine" SAE 2002-01-0111
19. J. Willand, R-G. Nieberding, G. Vent, C. Enderle, "The Knocking Syndrome – Its Cure and Its Potential", SAE 982483
20. D. Law, D. Kemp, J. Allen, G. Kirkpatrick, T. Copland, "Controlled Combustion in an IC-Engine with a Fully Variable Valve Train" SAE 2001-01-0251
21. J. Li, H. Zhao, N. Ladommatos, T. Ma, "Research and development of controlled auto-ignition (CAI) combustion in a 4-stroke multi cylinder gasoline engine", SAE-2001-01-3608
22. H. Zhao, J. Li, T. Ma, N. Ladommatos, "Performance and Analysis of a 4-Stroke Multi-Cylinder Gasoline Engine with CAI Combustion" SAE-2002-01-0420
23. N. B. Kaahaaina, A. J. Simon, P. A. Caton, C. F. Edwards, "Use of Dynamic Valving to Achieve Residual-Affected Combustion", SAE 2001-01-0549

24. C. D. Marriott, R. D. Reitz, "Experimental Investigation of Direct Injection-Gasoline for Premixed Compression Ignited Combustion Phasing Control", SAE 2002-01-0418
25. T. Urushihara, K. Hiraya, A. Kakuhou, T. Itoh, "Expansion of HCCI Operating Region by the Combination of Direct Fuel Injection, Negative Valve Overlap and Internal Fuel Reformation" SAE 2003-01-0749
26. L. Koopmans, I. Denbratt, "A four Stroke Camless Engine, Operated in Homogeneous Charge Compression Ignition Mode with Commercial Gasoline", SAE 2001-01-3610
27. A. Fuerhapter, W. F. Piock, G. K. Fraidl, "CSI-Controlled Auto Ignition-the Best Solution for the Fuel Consumption-Versus Emissions Trade-Off?" SAE 2003-01-0754
28. H. Persson, M. Agrell, J-O. Olsson, B. Johansson, "The Effect of Intake Temperature on HCCI Operation Using Negative Valve Overlap", SAE 2004-01-0944
29. B. Johansson, "On Cycle to Cycle Variations in Spark Ignition Engines—The Effects of Fluid and Gas Composition in the Vicinity of the Spark Plug on Early Combustion" Doctoral thesis, ISRN LUTMDN/TMVK—1010-SE, Division of Combustion Engines, Department of Heat and Power Engineering, Lund Institute of Technology, Lund University, 1995
30. G. Fraidl, F. Piock, A. Fuerhapter, E. M. Unger, T. Kammerdiener, "Homogeneous Auto-Ignition – the Future of Gasoline Direct Injection?" MTZ 10/2002
31. A. Fuerhapter, E. Unger, W. F. Piock, G. K. Fraidl, "The new AVL CSI Engine-HCCI Operation on a Multi Cylinder Gasoline Engine" SAE 2004-01-0551
32. A. Fuerhapter, W. F. Piock, G. K. Fraidl, "The AVL CSI Engine with Controlled Autoignition an Application Example of HCCI", SAE HCCI Symposium, Berkeley, 2004
33. M. Hitomi, J. Sasaki, K. Hatamura, Y. Yano, "Mechanism of Improving Fuel Efficiency by Miller Cycle and Its Future Prospect" SAE-950974
34. J. Yang, T. Culp, T. Kenney, "Development of a Gasoline Engine System Using HCCI Technology – The Concept and the Test Results" SAE 2002-01-2832
35. O. Erlandsson, G. Lundholm, F. Söderberg, B. Johansson, V. W. Wong, "Demonstrating the Performance and Emission Characteristics of a Variable Compression Ratio Alvar- Cycle Engine", SAE 982682
36. C. Ashley, "Variable Compression Pistons", SAE 901539
37. M. Schwaderlapp, K. Haberman, K. I. Yapici, "Variable Compression Ratio-A Design Solution for Fuel Economy Concepts", SAE 2002-01-1103
38. W. H. Adams, H. G. Hinrich, F. F. Pischinger, P. Adamis, V. Schumacher, P. Walzer, "Analysis of the Combustion Process of a Spark Ignition Engine with a Variable Compression Ratio", SAE 870610
39. Alvar Engine, <http://www.dtek.chalmers.se/~hogra/alvar/index.htm> , 2003-01-16
40. W. A. Wallace, F. B. Lux, "A Variable Compression Ratio Engine Development", SAE 762A, 1963
41. C. Mandler, R. Gravel, "Variable Compression Ratio Engine", SAE 2002-01-1940
42. MCE-5 Development, <http://www.mce-5.com/> , 2003-02-05
43. K. Moteki, Nissan Motor Co., Ltd "VARIABLE COMPRESSION RATIO MECHANISM FOR RECIPROCATING INTERNAL COMBUSTION ENGINE", U.S. Patent No: 6,491,003 B2, Dec. 10, 2002
44. H. Drangel, L. Bergsten, "The new Saab SVC Engine - An Interaction of Variable Compression Ratio, High Pressure Supercharging and Downsizing for Considerably Reduced Fuel Consumption", 9. Aachener Kolloquium Fahrzeug- und Motorentechnik 2000
45. E. Olofsson, P. Alvestig, L. Bergsten, M. Ekenberg, A. Gawell, A. Larsén, R. Reinmann, "A High Dilution Stoichiometric Combustion Concept Using a Wide

- Variable Spark Gap and In-Cylinder Air Injection in Order to Meet Future CO2 Requirements on World Wide Emission Regulations” SAE 2001-01-0246
46. J. Martinez-Frias, S. Aceves, D. Flowers, J. R. Smith, R. Dibble, “HCCI Engine Control by Thermal Management” SAE 2000-01-2869
 47. J. O. Olsson, “Performance and Control of the Homogeneous Charge Compression Ignition (HCCI) Engine”, Thesis for the degree of Licentiate in Engineering, 2002, Department of Heat and Power Engineering
 48. P. Strand, J. Bengtsson, R. Johansson, P. Tunestål, B. Johansson, “Cycle-To-Cycle Control of a Dual-Fuel HCCI Engine”, SAE 2004-01-0941
 49. J. Bengtsson, “Closed-Loop Control of HCCI Engine Dynamics” Doctoral Thesis, ISSN 0280 5316, ISRN LUTFD2/TFRT—1070—SE, Department of Automatic Control, Lund Institute of Technology/Lund University, 2004
 50. J. Maciejowski, “Predictive Control with Constraints”, Prentice Hall, Pearson Education, England 2002
 51. J. S. Souder, “Closed-Loop Control of a Multi-Cylinder HCCI Engine”, SAE HCCI Symposium, Berkeley, 2004
 52. F. Agrell, H-E. Ångström, B. Eriksson, J. Wikander, J. Linderyd, “Integrated Simulation and Engine Test of Closed Loop HCCI Control by Aid of Variable Valve Timings”, SAE 2003-01-0748
 53. G. M. Rassweiler, L. Withrow, “Motion pictures of engine flames correlated with pressure cards”, SAE Transactions 38, 1938
 54. F. Agrell, H-E. Ångström, B. Eriksson, J. Wikander, J. Linderyd, “Transient Control of HCCI Through Combined Intake and Exhaust Valve Actuation”, SAE 2003-01-3172
 55. R. Sun, R. Thomas, C. L. Gray, “An HCCI Engine: Power Plant for a Hybrid Vehicle”, SAE 2004-01-0933
 56. G. M. Shaver, J. C. Gerdes, “Cycle-to-cycle control of HCCI Engines”, In the Proceeding of the 2003 ASME International Mechanical Engineering Congress and Exposition, IMECE2003-41966, Washington D.C.
 57. G. M. Shaver, J. C. Gerdes, M. Roelle, “Physics-Based Closed-Loop Control of Phasing, Peak Pressure and Work Output in HCCI Engines Utilizing Variable Valve Actuation”, In the Proceeding of the American Control Conference, 2004, Pages 150-155, Denver, Co.
 58. G. M. Shaver, J. C. Gerdes, Mail communication with PhD-Student G. M. Shaver, November 2004
 59. L. Koopmans, H. Ström, S. Lundgren, O. Backlund, I. Denbratt, “Demonstrating a SI-HCCI-SI Mode Change on a Volvo 5-Cylinder Electronic Valve Control Engine”, SAE 2003-01-0753
 60. M. Christensen, “HCCI Combustion Engine Operation and Emission Characteristics”, Doctoral Thesis, ISBN 91-628-5424-0, ISSN 0282-1990, ISRN LUTMDN/TMHP—02/1006—SE, Division of Combustion Engines, Department of Heat and Power Engineering, Lund Institute of Technology, Lund University, 2002
 61. K. E. Årzén, “Real-Time Control Systems” Department of Automatic Control, Lund Institute of Technology, Lund University, 2003
 62. P. L. Kelly-Zion, J. E. Dec, “A Computational Study of the Effect of Fuel-Type on Ignition Time in HCCI Engines”, Proceedings of the Combustion Institute, Vol 28, Part 1, pp. 1187-1194, 2000
 63. T. Aroonsrisopon, D. Foster, T. Morikawa, M. Lida, “Comparison of HCCI Operating Ranges for Combinations of Intake Temperature, Engine Speed and Fuel Composition”, SAE 2002-01-1924
 64. T. Aroonsrisopon, V. Sohm, P. Werner, D. E. Foster, T. Morikawa, M. Lida, “An Investigation Into the Effect of Fuel Composition on HCCI Combustion Characteristics”, SAE 2002-01-28
 65. K. Fieweger, R. Blumenthal, G. Adomeit, “Self-Ignition of S.I. Engine Models Fuels: A Shock Tube Investigation at High Pressure”, Combustion and Flame 109, pp 599-619, 1997

66. K. J. Åström, B. Wittenmark, "Adaptive control", Addison-Wessley Publishing Company, 1995
67. R. Pfeiffer, "Combustion control of the HCCI process--System identification and development of an LQG controller for the ignition phasing" Master Thesis, ISSN 0280-5316, ISRN LUTFD2/TFRT—5711—SE, Department of Automatic Control, Lund Institute of Technology, Lund University, 2003
68. J. G. Ziegler, N. B. Nichols, "Optimum settings for automatic controllers" ASME 1942
69. T. Glad, L. Ljung, "Reglerteknik Grundläggande Teori", ISBN 91-44-17892-1, 1997
70. O. Erlandsson, "Thermodynamic Simulation of HCCI Engine Systems", Doctoral Thesis, ISBN 91-628-5427-5, ISSN 0282-1990, ISRN LUTMDN/TMHP—02/1007—SE, Department of Heat and Power engineering, Division of Combustion Engines, Lund Institute of Technology, Lund University, 2002
71. Directive 98/69/EC of the European Parliament and of the Council of 13 October 1998
72. N. A. Henein, M. K. Tagomori, M. K. Yassine, T. W. Asmus, C. P. Thomas, P. G. Hartman, "Cycle-by Cycle Analysis of HC Emissions During Cold Start of Gasoline Engines", SAE 952402
73. F. T. Metzner, N. Becker, W. Demmelbauer-Ebner, R. Mueller, M. W. Bach, "The New 6-l-W12 Engine in the Audi A8" MTZ 4/2004
74. S. Zidat, M. Parmentier, "Exhaust Manifold Design to Minimize Catalyst Light-off Time" SAE 2003-01-0940
75. T. H. Ballinger, P. J. Andersen, "Vehicle Comparison of Advanced Three-Way Catalysts and Hydrocarbon Trap Catalysts", SAE-2002-01.0730

Summary of papers

Paper 1

A Turbo Charged Dual Fuel HCCI Engine

J-O. Olsson, P. Tunestål, G. Haraldsson, B. Johansson

SAE Technical paper 2001-01-1896

Presented by Jan-Ola Olsson at the International Spring Fuels & Lubricants Meeting, Orlando, May 2001

The possibility of running high load HCCI by using CLCC with a turbocharged dual fuel multi cylinder engine is presented. The fuels used are n-heptane and ethanol.

A load of 16 bar BMEP is shown with extremely low NO_x emissions. High exhaust backpressure due to turbo charging with low exhaust gas temperature is discussed. The engine is run without inlet air heating which severely deteriorates the combustion efficiency at low load and hence an extreme amount of CO is produced.

The author and first author jointly ran the experiments and evaluated data, while the first and second author wrote the paper.

Paper 2

HCCI Combustion Phasing in a Multi Cylinder Engine Using Variable Compression Ratio

G. Haraldsson, J. Hyvönen, P. Tunestål, B. Johansson

SAE Technical paper 2002-01-2858

Presented by the author at SAE Powertrain & Fluid Systems Conference & Exhibition, San Diego, CA, October 2002

The trade-off between inlet air temperature and CR is experimentally investigated together with the load and speed range of the SVC engine running in HCCI. Three different inlet air temperatures are run while scanning λ and keeping an approximate CA50 of 7 CAD ATDC by adjusting CR. The load and speed range are investigated for the SVC engine using VCR.

It is found that highest brake thermal efficiency and lowest NO_x emissions are achieved with as high CR as possible, with the drawback of higher CO emissions. A maximum load of 4.4 bar BMEP is reached at 2000 rpm. It decreases however as speed increase due to lack of diluent, which results in increased amounts of NO_x emissions. The maximum CR is found to be only 17 when the tests are evaluated, which partly explains the need for RON 60 to run the engine without excessive inlet air heating.

The author and the second author jointly wrote the paper and ran the experiments while the author processed the data except for the heat release, which the second author did. The author jointly wrote/rewrote the control PC software with the third author.

Paper 3

Operating range in a Multi Cylinder engine using Variable Compression Ratio

J. Hyvönen, G. Haraldsson, B. Johansson

JSAE Technical paper 20030178/ SAE 2003-01-1829

Presented by Jari Hyvönen at the JSAE/SAE Spring Fuels & Lubricants Meeting, Yokohama, Japan, May 2003

Load and speed range are investigated experimentally for a maximum CR of 21. The higher CR compared to the CR of 17 in Paper 2 is achieved by new pistons with less squish area and a new monohead with correct specs. The difference between the two pistons is investigated. The load and speed range for RON 92 and RON 60 is explored.

It is found to be no difference between the two pistons, while the load range with RON 60 is extended compared to Paper 2 since a higher maximum CR can be used, which results in lower inlet air temperature demand. The load range for RON 92 is however smaller than RON 60 due to a need for higher inlet air temperature, which results in thermal throttling.

The author and the first author ran the experiments jointly, while the first author wrote the paper and processed all data.

Paper 4

HCCI Combustion Phasing with Closed-Loop Combustion Control Using Variable Compression Ratio in a Multi Cylinder Engine

G. Haraldsson, J. Hyvönen, P. Tunestål, B. Johansson

JSAE Technical paper 20030126/SAE 2003-01-1830

Presented by the author at the JSAE/SAE Spring Fuels & Lubricants Meeting, Yokohama, Japan, May 2003

Performance of a CLCC of cascade coupled CA50 and CR controllers is experimentally investigated together with a strategy for cylinder balancing by using variable λ . Doing steps in set points of CA50, load and CR explores the performance of the controllers. The response to ramps in inlet air temperature and speed are explored. The maximum CR is 21 and RON 92 is used.

It is found that the CLCC using VCR performs well with the steps, while the ramps in inlet air temperature and speed are more demanding, especially the temperature ramp. The CLCC has a time constant of 14 engine cycles or 0.84s at 2000 rpm with a mean $dCA50/dt$ of 6.0 CAD/s. The cylinder balancing strategy with variable λ is shown to work, with the disadvantage of large deviation in IMEP net when no CA50 offset is used. The time from no cylinder balancing to a steady state value is 1.7s or 28 engine cycles at 2000 rpm.

The temperature measurement did not show the actual inlet air temperature, since the thermocouple response time was too slow.

The author and second author ran the experiments jointly, while the author wrote the paper and processed all data. The author and the third author jointly wrote/rewrote the control PC software. The second author invented and designed the two-throttle FTM, which was used manually but never mentioned in this paper.

Paper 5

Super Charging HCCI to extend the operating range in a Multi Cylinder VCR-HCCI engine

J. Hyvönen, G. Haraldsson, B. Johansson

SAE Technical paper 2003-01-3214

Presented by Jari Hyvönen at SAE Powertrain & Fluid Systems Conference & Exhibition, Pittsburgh, October 2003

The effect of advancing the combustion phasing and throttling the inlet air with respect to combustion efficiency at zero load is investigated. Together with the HCCI operation range with both mechanical supercharging and simulated turbocharger, which is compared to a naturally aspirated SI with gasoline as fuel.

It is found that the combustion efficiency increases drastically in both cases. The increase in the combustion efficiency overcomes the drawbacks of the early combustion phasing in the first case and the pumping losses in the second case. The operating range can be more than doubled with supercharging and higher brake efficiency than with a naturally aspirated SI is achieved at the same loads. Mechanical supercharging is however not an option with HCCI combustion, due to the high parasitic losses.

The first author ran the experiments, wrote the paper and processed the data. The author wrote/rewrote the control PC software.

Paper 6

HCCI Closed-Loop Combustion Control Using Fast Thermal Management

G. Haraldsson, J. Hyvönen, P. Tunestål, B. Johansson

SAE Technical paper 2004-01-0943

Presented by the author at SAE World Congress & Exhibition, Detroit, March 2004

In this paper CLCC using FTM is applied and step changes of set points for combustion phasing, CR, and load together with ramps of engine speed with either constant load, i.e. load control enabled, or constant fuel amount are investigated. Performances of the controllers are investigated by running the engine and comparing the result with CLCC using VCR in Paper 4.

Limitations to the speed ramps are further examined and it is found that choice of fuel and its low temperature reaction properties has a large impact on how the CLCC performs. The CLCC using FTM handles step changes in combustion phasing fairly well and has a time constant of 8 engine cycles, which is 57% faster than the CLCC using VCR even though it suffers from the large air volume between throttle and engine inlet.

The LTR effect is perhaps exaggerated in this paper, since the effect of throttle movement at low air flows is believed to be small for this design as well as in Paper 10.

The author ran the experiments, wrote the paper and processed the data. The author wrote/rewrote the control PC software and the second author served as feedback in discussions.

Paper 7

Balancing Cylinder-To-Cylinder Variations in a Multi-Cylinder VCR-HCCI Engine

J. Hyvönen, G. Haraldsson, B. Johansson

SAE Technical paper 2004-01-1897

Presented by Jari Hyvönen at SAE Fuels & Lubricants Meeting & Exhibition, Toulouse, June 2004

The cylinder-to-cylinder variations are investigated, and the effect it has on the engine performance. Different strategies to balance the cylinders are tested, i.e. static balancing of cylinder individual compression ratio and inlet air temperature, and closed loop control of cylinder individual combustion phasing using fuel offsets or inlet air temperature.

It is concluded that the best engine performance regarding fuel consumption, combustion stability and emissions are achieved with cylinder individual combustion phasing control using inlet air temperature, i.e. the six throttle system.

The first author ran the experiments, wrote the paper and processed the data. The author wrote/rewrote the control PC software. The Six throttle FTM was invented and designed by the first author while the author wrote the software to control it.

Paper 8

System Identification and LQG Control of Variable-Compression HCCI Engine Dynamics

R. Pfeiffer, G. Haraldsson, J-O. Olsson, P. Tunestål, R. Johansson, B. Johansson

CCA/ISIC/CACSD Technical Paper 688, Proceedings of the 2004 IEEE International Conference on Control Applications Taipei, Taiwan, pp 1442-1447, 2004

Presented by Roland Pfeiffer at Joint CCA, ISIC and CACSD, Taipei, Taiwan, September, 2004

This article attempts to describe a method for system identification of the HCCI process, and development of an effective LQG regulator for the combustion process, where Matlab and Simulink are used in computations and simulations.

A procedure for system identification on HCCI engines has been developed. The method is simple and produces good results.

It has been found that a low-order model is sufficient to describe the process dynamics. The process however is highly nonlinear in that it is much more sensitive to control action at a late timing than at an early timing. The process model obtained can be used to create an effective LQG controller, which in addition to being capable of suppressing disturbances and following a reference signal, also is capable of producing relatively smooth control signals under noisy conditions.

The first author and the author jointly ran the experiments. The author and the third author wrote/rewrote the control PC software. The first author, the author, third author and the fourth author jointly wrote the matlab scripts for controller synthesis, while the author processed the data and wrote the paper jointly with the first and third author. The fifth author served as feedback during controller synthesis.

Paper 9

Operating conditions using spark assisted HCCI combustion during combustion mode transfer to SI in a Multi-Cylinder VCR-HCCI engine

J. Hyvönen, G. Haraldsson, B. Johansson

SAE Technical paper 2005-01-0109

Accepted for publication at SAE World Congress & Exhibition, Detroit, April 2005

The mixed combustion region and the operating conditions are investigated in this paper from lean SI limit to pure HCCI without SI assistance. Parameters as compression ratio, inlet air pressure, inlet air temperature, and λ are used for controlling the mixed combustion mode. A strategy for closed-loop combustion mode transfer is discussed.

It is found that spark assistance can be used for controlling the combustion phasing during a mode change between HCCI and SI combustion. However, the combustion fluctuations are large in the intermediate combustion region where some cycles have both spark ignited flame propagation and auto ignition, but some cycles have only partially burnt flame propagation. The partially burnt cycles increase COV_{IMEP} and produce much unburned hydrocarbon emissions in the exhaust. The auto-ignited cycles have also high audible noise due to the decreasing amount of dilution in the intermediate combustion region.

The first author ran the experiments, wrote the paper and processed the data. The author wrote/rewrote the control PC software.

Paper 10

Transient Control of a Multi Cylinder HCCI Engine during a Drive Cycle

G. Haraldsson, J. Hyvönen, P. Tunestål, B. Johansson

SAE Technical paper 2005-01-0153

Accepted for publication at SAE World Congress & Exhibition, Detroit, April 2005

CLCC using FTM_6 is applied as a main parameter to control the combustion phasing during a drive cycle. Above 1500 rpm the FTM's bandwidth is broadened by using the VCR feature of this engine according to a predefined map which is a function of load and engine speed. Below 1500 rpm the CLCC using VCR is used instead of the FTM while slow cylinder balancing is applied by the FTM. Desired combustion phasing depending on load and speed are taken from a map. The main issue of this drive cycle test is to show performance of the state feedback controllers used during predefined transients.

It is found that the state feedback controller used for combustion phasing above 1500 rpm, handles most tasks well but has some problem with retarded combustion phasings, where the controller is outside of its design range. A mean fuel mileage of 6.8 L/100km is achieved, which is an improvement of 13% compared to the SI SVC.

The author ran the experiments, wrote the paper, processed the data and wrote/rewrote the control PC software, while the other authors served as feedback during the experiments and analysis. The HCCI steady state data were collected by the second author and the SI steady state data were jointly collected by the author and the second author, while the second author partly compiled those data.